LATTICE DEFECTS AND SPECIFIC HEATS

A Thesis Submitted for the Degree

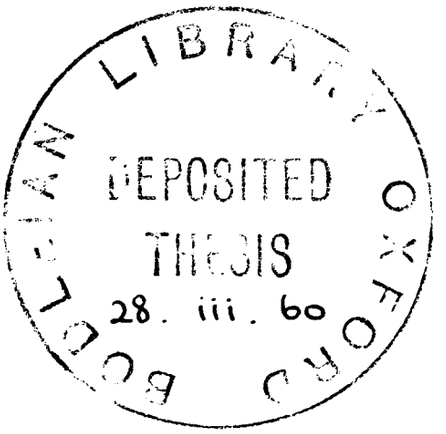
of Doctor of Philosophy

in the University of Oxford

by

C.A. BAILEY

St. Peter's Hall



Clarendon Laboratory,

Oxford.

October, 1959.

ABSTRACT.

The subject of this thesis is the measurement and interpretation of specific heats at low temperatures. The measurements fall into two main groups, those on magnetic salts described in Chapters II and III and those on alloys described in Chapters V and VII. The purpose of the former measurements was to obtain information about the energy states of the magnetic ions and the interactions between them and of the latter to investigate the band structure of copper.

A review of the theory of the lattice contribution to the specific heat is given in Chapter I. It is shown that the present state of the theory enables the lattice contribution to be distinguished from any other contribution at the lowest temperatures. However the theoretical calculation of the lattice contribution can still only be carried out to a semiquantitative degree but the general trend of these calculations is towards greater agreement with experimental results.

The apparatus existing when this research was commenced is described in Chapter II. The cryostat consists of an expansion liquefier (Simon, 1932) which carries a vacuum tight radiation shield enclosing the experimental chamber. A calorimeter similar to that described by Wolcott and Smith (1956) is suspended in this experimental chamber.

The only determination of a pure lattice specific heat was

carried out on Cerium Magnesium Nitrate. This salt is widely used in obtaining temperatures below $1^{o}K$ by the method of adiabatic demagnetisation and in measuring those temperatures. Unlike most salts used for demagnetisation experiments, cerium magnesium nitrate has an extremely small magnetic specific heat so that a knowledge of the lattice specific heat is required for a complete understanding of the properties of the salt around $1^{o}K$. This was obtained by extrapolation from measurements made in the liquid helium range of temperatures where the magnetic specific heat is negligible compared with the lattice specific heat. It was found that above $3^{o}K$ the lattice specific heat could not be represented by a single Debye term but below this temperature it is given by $C_L = 1.13 \times 10^{-3} RT^3$.

Chapter III is devoted to the study of specific heat anomalies of the Schottky and co-operative types. The results of measurements on a powdered specimen of uranium tetrafluoride which exhibit a Schottky anomaly are given. The lattice specific heat was assumed to be the same as the specific heat of the diamagnetic salt Thorium Tetrafluoride for which specific heat values were available down to $5^{o}K$. The maximum of the anomalous specific heat occurs at $6.8^{o}K$ and its value is 0.245 calories per mole per degree. By a mathematical analysis of the results using a scheme of levels proposed by Bleaney and Wolf (1957) and taking into consideration the investigation of the crystal structure by Burbank (1951) a tentative explanation of the anomalous specific heat

is obtained. It is proposed that the observed anomalous specific heat is made up of two simple Schottky anomalies with splittings of the doublet lowest in energy of 14°K and 28.3°K. The present results taken in conjunction with those of Burns, Osborne and Westrum (1958) confirm that there is a difference between the anomalous specific heat of powder and granular specimens of uranium tetrafluoride. It is shown that the anomalous specific heat of the granular specimen can also be accounted for by the same two simple Schottky anomalies the only difference between the granular and powder specimens being the relative number of uranium ions with each energy splitting.

Paramagnetic resonance experiments carried out in this laboratory on dilute and semi-dilute crystals with iridium ions replacing platinum ions in ammonium and potassium chloro-platinates had indicated that there might be antiferromagnetic transitions in the pure chloroiridate salts in the liquid helium range of temperatures. Antiferromagnetic transitions are an example of an order-disorder transition and are therefore accompanied by a λ type anomaly in the specific heat and the presence of such an anomaly provides the most distinct evidence that there is such a transition. The results of measurements of the specific heats of ammonium, potassium and sodium chloroiridates are given which show that an anomaly of the expected λ type occurs at 2.15°K for the ammonium salt, 3.05°K for the potassium salt and 3.95°K for the sodium salt. It was found that these temperatures for the

ammonium and potassium chloroiridates correspond to the temperatures at which the susceptibilities show the greatest rate of decrease with temperature. The anomalous entropy of all three salts was found to be of the order of R $\log_e 2$ as was to be expected for a system with spin 1/2. The shape of the specific heat curve for the sodium salt indicated that the transition for this salt might be more complex than for the ammonium and potassium salts.

The theory of the electronic specific heat of metals is reviewed in Chapter IV and this is followed by a review of both the theory and experimental evidence regarding the electronic band structure of copper. Excluding evidence from specific heat measurements it is concluded that the Fermi surface in copper must be assumed to be nearly spherical and contain approximately one free electron per atom. It must also be assumed that the surface is distorted in the (111) directions and almost certainly makes contact with the first Brillouin zone boundaries in those directions.

Methods of investigating the shape of an electronic band are considered especially the method of altering the position of the Fermi level in one element by alloying with another element. The underlying assumption in this method is that the addition of atoms of another metal does not alter the band structure of the solvent metal but only alters the position of its Fermi level.

The results of measurements of the electronic specific heat of

copper-zinc alloys which were made to study the shape of the s band in copper are given in Chapter V. The publication by Rayne (1957) of similar measurements on a series of α brasses showed differences between the results of the two researches which lay completely outside the combined limits of accuracy. Repeated measurements of the heat capacity of the same specimen showed that results obtained with the Simon bomb apparatus were not always reproducible and this could be only attributable to helium absorbed by both specimen and calorimeter. It was therefore decided to construct a new apparatus in which the use of helium exchange gas in the calorimeter would be avoided and in which cooling would not be carried out by direct contact with liquid helium.

The new apparatus is described in Chapter VI and may be briefly described as a free helium cryostat containing a vacuum calorimeter which embodies a mechanical heat switch. Its construction, evolution and operation are described in detail. Experimental results obtained with the new apparatus on pure copper and dilute copper-zinc alloys are given in Chapter VII.

The specific heat of pure copper was determined with the dual purpose of testing the apparatus and acting as a reference from which the changes in the electronic and lattice terms could be evaluated. The resulting values of γ and θ were:

$$\gamma = (0.698 \pm 0.002) \times 10^{-3} \text{ joules per mole per degree}^2$$

$$\theta = 341.3 \pm 1.1^{\circ}\text{K}.$$

These values are compared with other experimental values and values calculated from theory. The results are then given for a series of α brasses none of them containing more than 5% of zinc by weight. The initial rise of γ from that for pure copper is shown to be much more steep than indicated by Rayne's results, (1957). There is also evidence of an initial 1% increase in Θ on the introduction of zinc atoms into pure copper. The initial rise in γ is inexplicable from the free electron point of view and it must be assumed that the Fermi surface departs appreciably from sphericity. Contrary to the bulk of evidence discussed in Chapter IV it would appear that the Fermi surface makes contact with the zone boundaries at a zinc concentration of about 1%.

The band model proposed by Cohen and Heine (1958) to reconcile this conflicting evidence is then described. These authors propose that the zone boundary effect observed in the specific heat of the α brasses at low zinc concentrations is not the Fermi surface touching the zone boundaries but pulling away from them. Further evidence for the breakdown of the rigid band model is given and it is concluded that it must be rejected. Whereas a few years ago the abandonment of the rigid band model would have left an uneasy vacuum, the experimental results can now be explained qualitatively with the use of the model of Cohen and Heine until such time as the non-periodic potential problem is finally solved.

REFERENCES.

Bleaney, B. and Wolf, W.P., 1957, Private communication.

Burbank, R.D., 1951, A.E.C.D. - 3216 (Unpublished).

Burns, J., Osborne, D.W. and Westrum, E.F., Jr., 1958, Private communication.

Cohen, M.H. and Heine, V., 1958, Advances in Physics, 7, 395.

Rayne, J.A., 1957, Phys. Rev., 108, 22.

Simon, F.E., 1932, Z. ges. Kälte Ind., 39, 89.

Smith, P.L. and Wolcott, N.M., 1956, Phil. Mag. Ser. 8, 1, 854.

ACKNOWLEDGEMENTS.

The author is indebted to the late Professor Lord Cherwell, K.C.B., F.R.S., to the late Professor Sir Francis Simon, F.R.S., and to Professor B. Bleaney, F.R.S. for extending to him the facilities of the Clarendon Laboratory.

The research described in this thesis was supervised at its commencement by Professor Sir Francis Simon and latterly by Dr. R.W. Hill. I wish to record my gratitude to them both for their encouragement and advice.

I am indebted to Dr. P.L. Smith now at the National Physical Laboratory for teaching me the techniques of low temperature physics and for his assistance in the early part of this research. I am also indebted to Dr. H. Montgomery for the preparation of the copper-zinc alloys; to Mr. A. Le Claire, Dr. H. Montgomery and other members of the staff of the Metallurgy Division, A.E.R.E., Harwell, for many useful discussions.

I would like to thank the workshop staff for their friendly assistance in technical problems and in particular Mr. L. Waine who constructed the major part of the new heat-switch apparatus.

I am most grateful to the Extra-mural Research Department of A.E.R.E., Harwell who supported this research in its entirety.

C.A. Bailey.

October, 1959.

CONTENTS.

Abstract		ii
Acknowledgements		ix
Introduction		xiii
CHAPTER I	The Lattice Specific Heat	1
	References	10
CHAPTER II	1. Simon Bomb Apparatus	
	(a) The Cryostat and Calorimeter	11
	(b) Electrical Circuits	12
	(c) The Thermometers	13
	(d) Experimental Procedure	15
	(e) Heat Capacity of the Empty Calorimeter	17
	(f) Errors	17
	2. The Specific Heat of Cerium Magnesium Nitrate	
	(a) Introduction	24
	(b) The Specimen	25
	(c) Experimental Results	26
	(d) Discussion	27
	(e) Errors	28
	References	29

CHAPTER III	Specific Heat Anomalies	
	1. Introduction	30
	2. The Specific Heat of Uranium Tetrafluoride	
	(a) Introduction	31
	(b) Calculation of the expected Anomaly	33
	(c) The Specimen	34
	(d) Experimental Results	35
	(e) Discussion	39
	3. The Specific Heats of Ammonium, Potassium and Sodium Chloroiridates	
	(a) Introduction	45
	(b) The Specimen	47
	(c) Experimental Results	47
	(d) Discussion	47
	References	50
CHAPTER IV	1. The Electronic Specific Heat of Metals	51
	2. The Electronic Band Structure of Copper	59
	References	66
CHAPTER V	The Heat Capacity of Copper-Zinc Alloys	
	1. Introduction	68
	2. Specimens	71
	3. Results	71
	4. Discussion	73
	References	78

CHAPTER VI The Heat Switch Apparatus

1. Introduction 79

2. The Apparatus 79

3. The Heat Switch 81

4. The Heater and Thermometer Assembly 86

5. Electrical Circuits 87

6. Experimental Procedure 88

7. Experimental Accuracy 91

8. Experimental Technique 92

References 94

CHAPTER VII Experimental Results with the Heat Switch Apparatus

1. The Heat Capacity of the Thermometer and Heater Assembly 95

2. The Heat Capacity of Copper-Zinc Alloys

(a) The Specimens 96

(b) Experimental Results 99

(c) Discussion :

i. The Lattice Specific Heat 106

ii. The Electronic Specific Heat 110

References 116

Appendix Specific Heat Tables 118

INTRODUCTION.

The original scope of this research was intended to be the study of the effect of lattice defects on the specific heat of metals. It was hoped to obtain information about the electronic band structure resulting from an imperfect lattice. The problem of a periodic lattice has already been solved by theoretical studies and results are in semi-quantitative agreement with experimental studies. However the problem of a non-periodic lattice is yet to be solved theoretically and therefore the only source of information can be from experiment.

Any defect in the lattice structure should theoretically influence the internal energy and if the resulting change in internal energy is a function of temperature then a change in the specific heat would be expected. The principal defects which can occur in a lattice are:

(1) Impurity atoms either as interstitials or occupying lattice sites.

(2) Vacant lattice sites and interstitial atoms.

(3) Dislocations.

Experiments with the existing Simon bomb apparatus showed that the results were not of sufficient accuracy or reproducibility to investigate the small changes in the specific heat which it was desired to detect. Due to the time spent developing a new apparatus, incorporating a mechanical heat switch only the effect of the first type of defect was

investigated.

Also included in this dissertation are measurements on several magnetic salts. These salts were the subject of other investigations being carried out in this laboratory and the specific heat measurements could provide much helpful information. The nature of the information will be dealt with in the relevant chapters.

CHAPTER I.

The Lattice Specific Heat.

A monatomic crystalline solid can be considered as a three dimensional lattice of similar point masses which can vibrate about their equilibrium positions. For temperatures well below the melting point of the solid the vibrations will be small in amplitude and can be assumed to be simple harmonic.

On the classical equipartition of energy theory each atom would have a mean energy 3kT where k is Boltzmann's constant and T is the absolute temperature. Thus one mole of a monatomic solid should have a specific heat at constant volume of 3R (where R is the gas constant), which accounts for Dulong and Petit's law. With a few exceptions most simple solids obey this law at room temperature but at low temperatures the specific heat decreases approaching zero as the temperature approaches absolute zero.

Einstein (1907, 1911) was able to explain this decrease in the specific heat at low temperatures by introducing quantum ideas to the problem. He again represented a solid of N atoms by a system of 3N linear harmonic oscillators, but, assumed that each oscillator has a series of quantised non degenerate energy states. The jth energy

state of the ith oscillator is then

$$e_{ji} = jh\nu_i$$

where h is Planck's constant and ν_i is the frequency of vibration of the ith oscillator. The average energy of the ith oscillator at a temperature T is obtained from Boltzmann's theorem

$$\bar{e}_i = \frac{\sum_{j=0}^{j=\infty} jh\nu_i e^{-jh\nu_i/kT}}{\sum_{j=0}^{j=\infty} e^{-jh\nu_i/kT}} = \frac{h\nu_i}{(e^{h\nu_i/kT} - 1)}$$

Therefore the internal energy of one mole of the solid is given by

$$E = \sum_{i=1}^{i=3N} \frac{h\nu_i}{(e^{h\nu_i/kT} - 1)}$$

where N is now Avogadro's number, and the specific heat at constant volume, C_V

$$C_V = \left(\frac{\partial E}{\partial T}\right)_V = k \sum_{i=1}^{i=3N} \frac{(h\nu_i/kT)^2 \, e^{h\nu_i/kT}}{(e^{h\nu_i/kT} - 1)^2} \qquad (1)$$

Without considering the possible value(s) of ν_i it can be seen that

$$C_V \longrightarrow 0 \quad \text{as} \quad T \longrightarrow 0$$

$$C_V \longrightarrow 3R \quad \text{as} \quad T \longrightarrow \infty$$

Einstein further assumed that all the oscillators had the same frequency ν_E for any particular solid, therefore

$$C_V = 3R(h\nu_E/kT)^2 . \frac{e^{h\nu_E/kT}}{(e^{h\nu_E/kT} - 1)^2} \qquad (2)$$

The value of ν_E was chosen to fit the experimental specific heat data and usually corresponds to a frequency in the infra-red part of the spectrum.

At the lowest temperatures the Einstein values of the specific heat fall off too rapidly and to rectify this Nernst and Lindemann (1911) proposed that the frequency spectrum consists of two lines ν and $\nu/2$ of equal probability. With suitable choice of ν the calculated values of C_V can be made to fit the experimental data reasonably well. However there were still discrepancies at very low temperatures so there must be modes of frequency lower than $\nu/2$ which are the principal ones excited at these temperatures.

If $f(\nu)d\nu$ is the number of modes with frequencies between ν and $\nu + d\nu$ a plot of $f(\nu)$ against ν gives a representation of the frequency spectrum of the solid. Debye (1912) showed that if the solid is treated as an isotropic continuous elastic medium then the frequency distribution $f(\nu)$ is given by

$$f(\nu) = 4\pi V \left(\frac{1}{c_L^3} + \frac{2}{c_T^3} \right) . \nu^2 \qquad (3)$$

where V is the molar volume, c_L and c_T are the velocities of the longitudinal and transverse waves respectively. Debye assumed that this proportionality of $f(\nu)$ to ν^2 was valid for even the shortest wavelengths (highest frequencies) that are present in the frequency spectrum of the solid. The highest frequency, ν_D, permitted was chosen so that the total number of modes is 3N.

Thus
$$\int_0^{\nu_D} f(\nu)d\nu = 3N$$

and
$$f(\nu) = \frac{9N\nu^2}{\nu_D^3} \quad \text{where} \quad 0 < \nu < \nu_D . \tag{4}$$

Equation (1) can be rewritten in integral form:

$$C_V = k \int_0^{\nu_D} \frac{(h\nu/kT)^2 . e^{h\nu/kT} . f(\nu)d\nu}{(e^{h\nu/kT} - 1)^2} \tag{5}$$

substituting for $f(\nu)$ from equation (4) and putting $\theta_D = h\nu_D/k$ and $x = h\nu/kT$ equation (5) becomes

$$C_V = 9R \left(\frac{T}{\theta_D}\right)^3 . \int_0^{\frac{\theta_D}{T}} \frac{x^4 e^x}{(e^x - 1)^2} . dx$$

Thus Debye's formula like its predecessors has only one parameter in this case θ_D. The value of θ_D can be determined from ν_D and

therefore from the elastic constants of the solid (see equation (3)). Again it can be seen that

$$C_V \longrightarrow 0 \qquad \text{as} \qquad T \longrightarrow 0$$

$$C_V \longrightarrow 3R \qquad \text{as} \qquad T \longrightarrow \infty$$

The most interesting feature of the formula is the prediction of the way in which C_V approaches zero. As T approaches zero

$$C_V \approx 9R \left(\frac{T}{\theta_D}\right)^3 \frac{4\pi^4}{15}$$

$$= 464.5 \left(\frac{T}{\theta_D}\right)^3 \text{ calories per mole per degree.}$$

This T^3 dependence of the specific heat should be reached at about $\theta_D/12$, but in actual fact many substances that have been investigated have not reached this region at $\theta_D/12$ and some not even at a temperature of $\theta_D/100$. Since the crystal lattice behaves as a continuum for the very long wavelengths C_V must eventually obey a T^3 law as a temperature must be reached where these wavelengths form the major contribution to the frequency spectrum.

Born and von Karman (1912) made the first attempt to calculate the normal modes of an atomic lattice from crystal dynamics. They derived the approximate spectrum of a simple cubic lattice by analogy with the spectrum of a linear chain of atoms. The expression found for the frequency distribution was

$$f(\nu) = \frac{72N}{\pi^3 \nu_o} \frac{(\sin^{-1}\nu/\nu_o)^2}{(1-(\nu/\nu_o)^2)^{1/2}}$$

Because the calculation of C_V using this frequency spectrum is very difficult and the agreement with experimental results is no better than that given by Debye theory, their result aroused little interest. For low frequencies the frequency distribution is proportional to ν^2 and therefore agrees with Debye's result. The upper frequency limit was derived more naturally from consideration of the dispersion of lattice waves.

Between 1912 and 1935 more and more accurate specific heat measurements were made and it became increasingly obvious that the specific heat of any one solid could not be fitted to a single Debye curve characterised by a single value of Θ_D. Blackman (1935) decided to investigate the limits of the Debye theory and calculated a Θ_D to fit each observed point on a C_V versus T curve for a given solid. A plot of these Θ_D values versus T differed markedly from a straight line especially at low temperatures. Thus these curves gave direct evidence of the discrepancies between the vibrational spectrum of Debye's continuum and that of an actual atomic lattice. Using an extension of Born's lattice dynamics Blackman (1937) calculated an approximate spectrum for an ideal simple cubic lattice taking into account interactions between nearest and next-nearest neighbours.

From this spectrum he constructed a θ_D versus T curve for such a lattice which showed a resemblance to the experimental curves he had derived.

The shape of Blackman's spectrum with its two peaks showed immediately why the formula of Nernst and Lindemann gave such good results. At the origin there is a true ν^2 distribution but as soon as the continuum region is passed the distribution function increases faster than ν^2, thus C_V/T^3 increases and therefore the value of θ_D will decrease. Blackman estimated that the true T^3 law does not hold until temperatures of the order of $\theta/50$ or even $\theta/100$ are reached. He also pointed out that due to the maximum or minimum in many θ versus T curves there is the possibility of finding false T^3 regions at higher temperatures.

Similar calculations of frequency spectra were first carried out by Fine (1939) for a body centred cubic lattice, Leighton (1948) for a face centred cubic lattice and Slutsky (1958) for an hexagonal close packed lattice. These are the three most common lattice structures that are met with in the field of metals and alloys. The frequency spectra of graphite, diamond and the alkyl halides have also received considerable attention. Comprehensive reviews of the application of lattice theory to the calculation of specific heats have been given by Blackman (1956) and de Launay (1956). The main difficulty apart from the length of the calculation is the selection of the force constants between atoms for substitution in the secular

equations. The force constants must in general allow for two types of forces; firstly the simple quasi-elastic central forces which act along the line joining two neighbouring atoms and obey Hooke's law, and secondly the non-central forces arising from the change in angle between a pair of bonds. In metals there is yet a third force known as a volume force due to the presence of electrons which behave as though they have a bulk modulus but cannot support a shear stress. The majority of calculations consider only the elastic central forces and these only between nearest and next-nearest neighbours and also assume that there is no mutual interaction between the lattice waves. Despite these assumptions by suitable choice of the force constants very good agreement can be obtained with experimental results in certain cases, but such a procedure is necessarily not a very satisfactory one. Anharmonic forces which account for thermal expansion and thermal equilibrium should obviously be taken into account although this leads to a mathematical wilderness where modern computors are the only sign of salvation.

The converse problem of calculating the vibrational spectrum from experimental specific heat data has also been investigated. Montroll (1942), Grayson-Smith and Stanley (1950), Kroll (1952) and Taylor (1956) have all considered this problem. The main result of this work has been to show how relatively insensitive the specific heat is to the finer details of the frequency spectrum.

Details of the frequency spectrum can be obtained from scattering experiments using either x rays or neutrons.

The present state of the theory of the lattice specific heat allows the lattice contribution to be distinguished from any other contribution at the lowest temperatures. However, the calculation of this lattice contribution can still only be carried out to a semi-quantitative degree but the general trend of these calculations is towards greater agreement with experimental results.

REFERENCES : Chapter I.

Blackman, M., 1935, Proc. Roy. Soc., A 148, 365.

1937, Proc. Roy. Soc., A 159, 416.

1956, Handbuck der Physik, 7, Pt. 1, 325.

Born, M. and von Karman, T., 1912, Phys. Zeits., 13, 297.

Debye, P., 1912, Ann. d. Physik, 39, 789.

Einstein, A., 1907, Ann. d. Physik, 22, 180, 800.

1911, Ann. d. Physik, 34, 170.

Fine, P.C., 1939, Phys. Rev., 56, 355.

Grayson-Smith, H. and Stanley, J.P., 1950, J. Chem. Phys., 18, 136.

Kroll, W., 1952, Progr. Theor. Phys., Japan, 8, 457.

de Launay, J., 1956, Solid State Physics, 2, 220.

Leighton, R.B., 1948, Rev. Mod. Phys., 20, 165.

Montroll, E., 1942, J. Chem. Phys., 10, 218.

Nernst, W. and Lindemann, F.A., 1911, Zeits. f. Electrochemie, 17, 817.

Slutsky, L.J., J. Chem. Phys., 29, 1191.

Taylor, W.J., 1956, J. Chem. Phys., 25, 721.

CHAPTER II.

1. The Simon Bomb Apparatus.

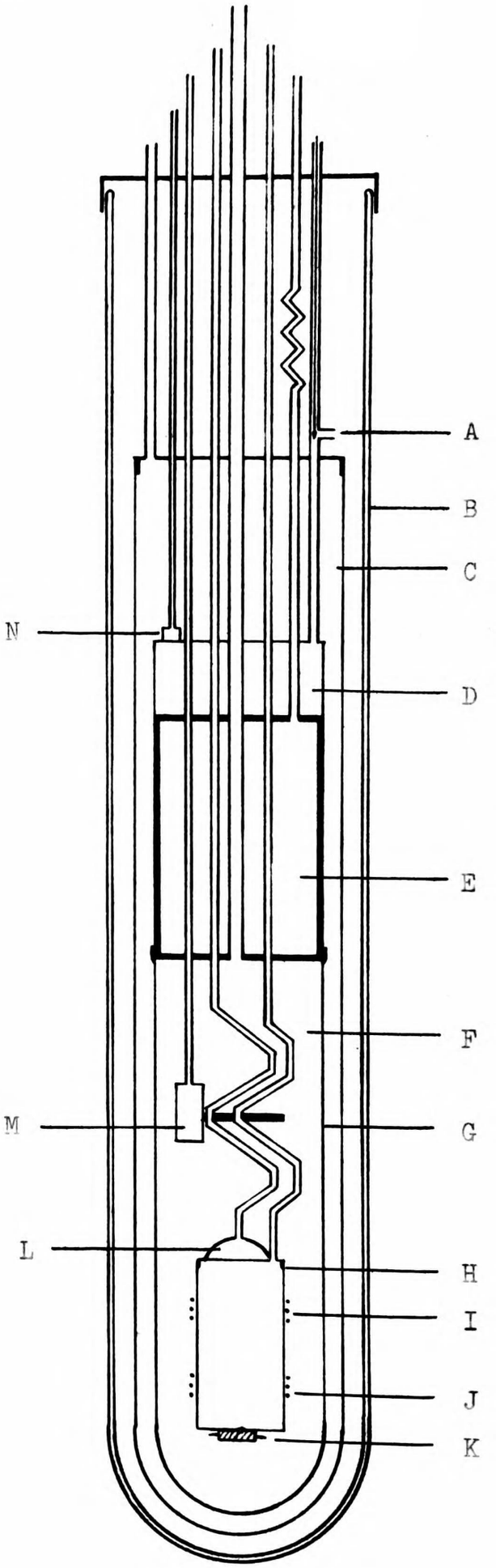
(a) The Cryostat and Calorimeter.

The apparatus for measuring specific heats of solids below 20°K which existed at the time when these researches were commenced is shown in Fig. 2.1. The cryostat consists of a Simon expansion liquefier (Simon, 1932), which carries a vacuum tight radiation shield enclosing the experimental chamber. About 80 cc. of liquid helium can be produced in the helium bomb and this is enough to last for three to four hours under normal experimental conditions. In the absence of liquid helium the experimental chamber can be maintained at about 10°K by pumping on solid hydrogen in the upper compartment of the Simon bomb.

The calorimeter is similar to that described by Wolcott and Smith (1956), and is suspended in the experimental chamber by two 1 mm. german silver tubes which give access to its two sections. The main part of the calorimeter is a cylindrical copper vessel 7 cm. in length, 2.5 cm. in diameter and 6 thousandths of an inch thickness, on top of this is a vessel of about 1 cc. capacity into which helium can be condensed. A heater of 42 S.W.G. constantan wire with room

THE SIMON BOMB APPARATUS.

A	Needle Valve
B	Glass Dewar Vessel
C	Outer Vacuum Space
D	Hydrogen Cap
E	Helium 'Bomb'
F	Inner Vacuum Space
G	Radiation Shield
H	Calorimeter
I	Heater
J	Constantan Thermometer
K	Carbon Thermometer
L	Helium Vessel
M	Heat Sink
N	Gas Thermometer



temperature resistance of approximately 1000 ohms is wound directly on the outside wall of the calorimeter, 'Araldite' surface coating resin 985 E being used as adhesive. A constantan resistance thermometer is also wound on the outside wall of the calorimeter and a carbon resistance thermometer is fixed to the base of the calorimeter.

A 2 cc. vessel into which helium can be condensed is suspended in the experimental chamber below the helium bomb. The vessel is connected by a piece of thick copper braid to the midpoint of the two german silver tubes leading to the calorimeter and acts as a heat 'sink'.

(b) The Electrical Circuits.

(i) The Heater. The current passing through the heater is determined using a Pye potentiometer and a standard 100 ohm resistance. The resistance of the heater as a function of temperature is measured with a Wheatstone bridge using a three lead system. The leads of approximately equal resistance are thermally anchored at the base of the Simon bomb. The resistance of one lead from the thermal anchor to the heater is also measured and this resistance is added to the resistance of the heater to correct for the heat generated in the two heater leads. In order to determine the heat supplied to the calorimeter the micro-switch for the current is mechanically coupled to a stop-watch. The stop-watch can be read to the nearest 1/10 of

a second and the heating periods used are normally of 30 seconds duration.

(ii) The Thermometers. The resistances of the thermometers are measured using a Wheatstone bridge in conjunction with a galvanometer amplifier (MacDonald, 1947). The bridge can be read to 1/10 ohm directly and interpolated by means of the galvanometer scale. Each thermometer has three leads of approximately equal resistance and these are thermally anchored at the base of the Simon bomb.

(c) The Thermometers.

The calorimeter is provided with two thermometers, a constantan resistance thermometer for the temperature range 20°K to 4°K and a carbon resistance thermometer for temperatures below 4°K where the constantan thermometer develops too much heat.

The wire for the constantan thermometer is taken from a special reel which has a sensitivity constant to within 1% between 20°K and 10°K with a value of $1/R \times dR/dT$ of 1.36×10^{-3} at the hydrogen triple point. The sensitivities between 10°K and 4°K are calculated from data on this wire obtained by D.H. Parkinson. The constantan thermometer is carefully calibrated against the vapour pressure of hydrogen in the temperature range 20°K to 10°K and against the vapour pressure of helium at 4°K during each experiment.

For temperature measurements below 4°K various types of commercial

radio resistors were tried as carbon resistance thermometers. It was found that a 47 ohm L.A.B. resistor gave the most satisfactory variation of resistance with temperature in the range required. This resistor has a value of dp/dT, (where p = 1/R, R being the resistance), which is approximately constant between 4.0°K and 2.5°K, below 2.5°K the value of dp/dT decreases rapidly with decreasing temperature.

The carbon thermometer has to be carefully calibrated against the vapour pressure of helium during each experiment as the calibration shifts between experiments. It was found that the shift could be decreased, but not eliminated, by removing the leads of the resistor, copper plating its ends, and then soldering fresh leads onto the copper plating. The resistor is coated with araldite and wound with a spiral of enamelled copper wire. The copper wire has a flat surface filed on it, is tinned and soldered to the base of the calorimeter thus ensuring good thermal contact between the thermometer and the calorimeter. The carbon resistor also exhibits an ageing process, the shift in calibration between successive experiments becoming less with time. The shift Δp is not temperature independent for each experiment and therefore a new sensitivity curve as well as a new calibration curve has to be drawn for each experiment.

(d) Experimental Procedure.

The calorimeter is surrounded with helium exchange gas to keep it in thermal contact with the Simon bomb while the latter's temperature is reduced to 10°K. The exchange gas is then removed and an expansion is carried out. The calorimeter is then cooled from 10°K to 4°K by oscillating cold helium gas in and out of the small vessel on the lid of the calorimeter. If the exchange gas is not removed until after the expansion the vacuum obtained after prolonged pumping is not nearly as good and there is also a loss of valuable experimental time at 4°K.

A quantity of helium is condensed in the small vessel on the calorimeter lid and by pumping away the vapour above the liquid helium the temperature of the calorimeter is reduced to about 1.2°K. As soon as this helium evaporates the temperature of the calorimeter begins to rise due to heat influx down the german silver tubes and electrical leads. Condensed helium in the heat sink can be pumped by means of a rotary pump to about 1.2°K and this considerably reduces the heat influx to the calorimeter, the calorimeter temperature drifts in fact become negative at about 2.5°K.

Once the helium liquid in the small vessel on the lid of the calorimeter has evaporated the thermometer resistance is read every fifteen seconds to record the temperature drift of the calorimeter and its contents. When it is seen that the drift is regular a current is passed through the heater for approximately thirty seconds. The

current has previously been adjusted so that the heat supplied will raise the temperature of the calorimeter and its contents through a reasonable temperature interval. For most specimens the interval is between 1/10 and 1/5 of a degree in the liquid helium range with somewhat larger intervals in the liquid hydrogen temperature range. The size of the interval is determined by the temperature variation of the heat capacity being measured. The heater current is measured with the potentiometer and standard resistance and the heating period recorded from the stop-watch coupled to the heater switch. When the temperature drift of the calorimeter and its contents shows a regular behaviour again sufficient readings of the thermometer resistance are taken to enable the drift to be extrapolated back to the middle of the heating period and then a further heating is carried out. This sequence of events is repeated throughout the whole of the temperature range which is being investigated.

In order to provide good thermal contact between specimens and the calorimeter it is found necessary to leave a small pressure of helium gas in the calorimeter. For most specimens a pressure of 0.3 mm. of mercury at 20°K was found sufficient to give good thermal contact though how much gas was adsorbed in producing this pressure is different for each specimen and uncertain.

(e) The Heat Capacity of the Empty Calorimeter.

The heat capacity of the empty calorimeter must be measured in order to determine the specific heat of any specimen it may contain. The heat capacity is measured in a separate experiment before and after each series of experiments with a particular specimen. The experimental points from one such experiment are given in Table 2.1.

Below $2^{\circ}K$ the heat capacity of the calorimeter is very small and the temperature drift of the calorimeter is too large for experimental points to be obtained. Fortunately an analysis of the points from $2^{\circ}K$ to $4^{\circ}K$ on a C/T against T^2 plot shows that the heat capacity can be separated into a cubic and a linear term in T (Fig. 2.2). Thus, values for the heat capacity of the empty calorimeter below $2^{\circ}K$ can be predicted with reasonable confidence.

The heat capacity of the calorimeter below $4^{\circ}K$ is given by:

$$C = (0.062T^3 + 0.745T) \times 10^{-4} \text{ calories per degree.}$$

$$= (0.259T^3 + 3.12T) \times 10^{-4} \text{ joules per degree.}$$

(f) Errors.

The main errors in calculating the heat capacities of specimens from the experimental data arise from an inaccurate knowledge of the temperature heating interval and the change of thermometer resistance with temperature. There are quite a large number of other smaller sources of error and an investigation of all the probable sources of

Empty Calorimeter.

$C = (0.259\ T^3 + 3.12\ T) \times 10^{-4}$ joules per degree.

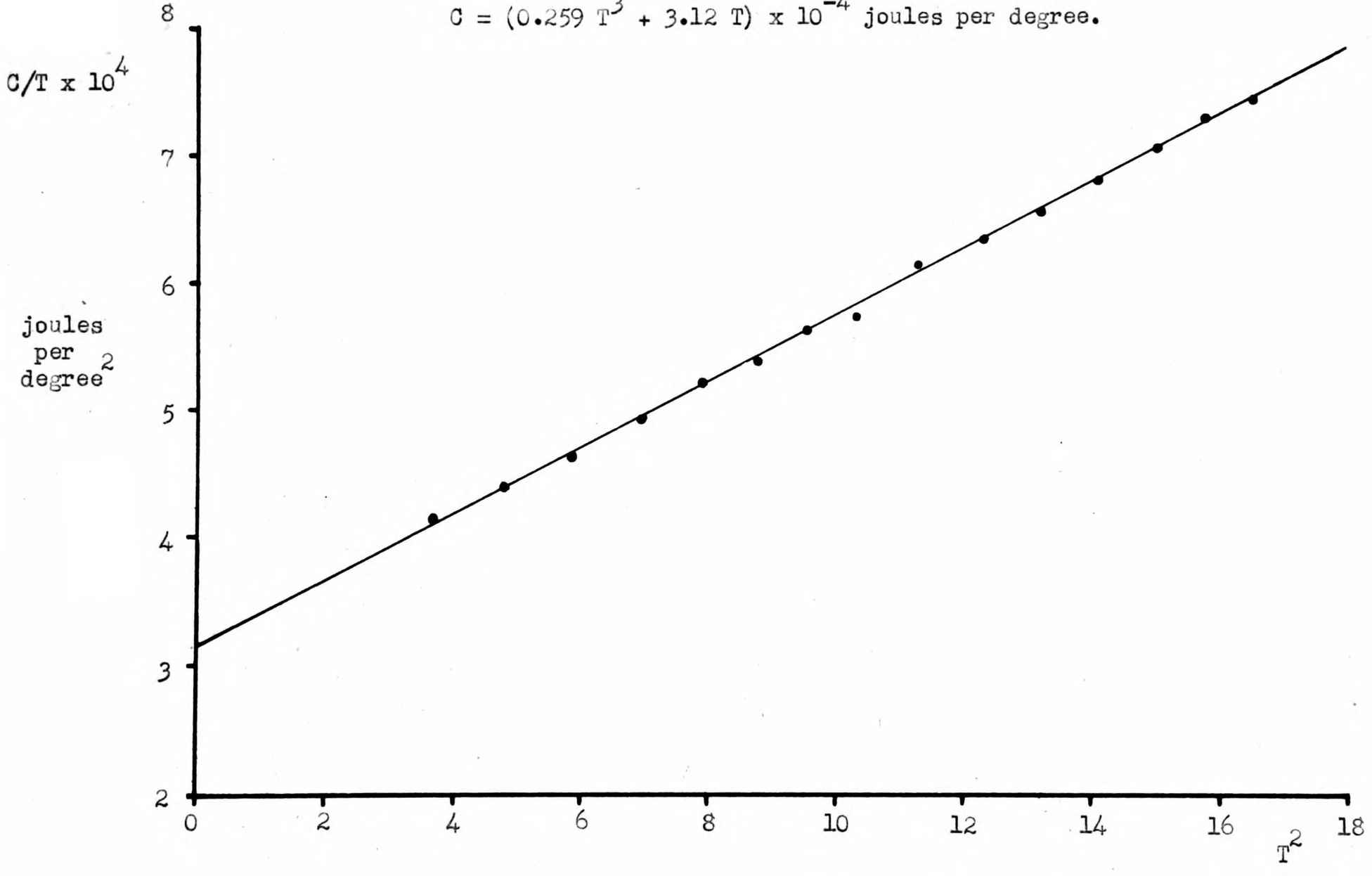


Fig. 2.2

error will be carried out in this section. Since most of the errors are temperature dependent the total error will be displayed on an error versus temperature graph (see Fig. 2.3). Some of the errors depend on the magnitude of the heat capacity of the specimen being measured so that only a typical graph will be given here and specific heat measurements in this and the following chapters will contain a note of the magnitude of their respective total errors. The figures given in this section refer to an experiment in which the specimen was 2.5 moles of pure copper.

Each experimental point for a specimen is quoted as a temperature with its associated value for the specific heat, so there are two quantities to be investigated

(i) Error in the Temperature. The error in the temperature of each point depends only on the accuracy with which the temperature drifts before and after heating can be extrapolated to the midpoint of the heating period and the accuracy with which the resistance of the thermometer can be converted into temperatures.

The temperature drift before the heating period has only to be extrapolated for a further 15 seconds giving an error in the resistance for the helium range of ± 0.03% at 1.5°K decreasing to virtually zero at 2.5°K (where the drifts become zero), and increasing to ± 0.02% at 4.0°K. After the heating period the Wheatstone bridge has to be balanced but with practice this can be done in 30 seconds so that the error introduced

Systematic Errors in the Heat Capacity Measurements.

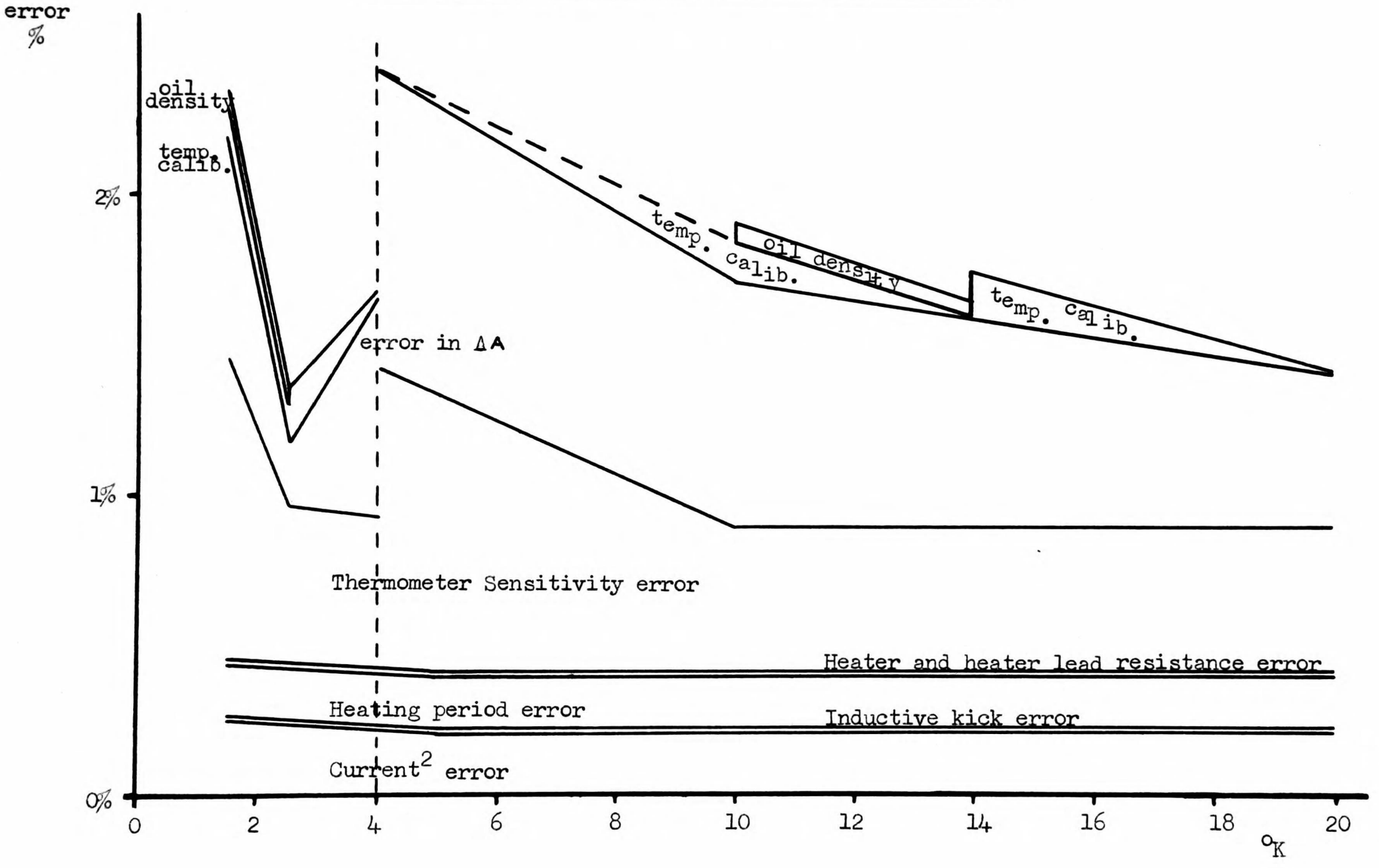


Fig. 2.3

by the extrapolation is double that for the drift before the heating period. Between 4°K and 20°K the error due to extrapolation of the resistance of the constantan thermometer to the midpoint of the heating period is never more than ± 0.0005%.

The error introduced in calibrating the thermometers depends on the accuracy with which the resistance of the thermometers can be read and also the accuracy with which the manometers can be read. The error in reading the resistance of the constantan thermometer is ± 0.0002% and the error in reading the resistance of the carbon thermometer is ± 0.01%, so that no appreciable error arises from this source. The manometers give readings of the vapour pressure to the nearest half millimetre thus the resultant error in the temperature will vary with temperature and will suffer abrupt changes when the readings are transferred from the mercury manometer to the oil manometer. The resultant error is ± 0.1% at 1.5°K decreasing to ± 0.01% at 2.4°K where it changes abruptly to 0.15% decreasing to ± 0.01% at 4.0°K. In the hydrogen range the error is ± 0.15% at 10°K decreasing to ± 0.01% at 14°K where it changes abruptly to ± 0.15% decreasing to ± 0.02% at 20°K. The conversion of vapour pressure readings taken on the oil manometer to millimetres of mercury requires a knowledge of the density of the oil and this introduces a further source of error in some parts of the temperature range. The uncertainty in the value of the density and hence in the pressure is ± 0.3%; in the helium range this gives an error in the temperature of ± 0.03% at

2.4°K increasing to ± 0.04% at 1.5°K and in the hydrogen range an error of ± 0.04% at 14°K increasing to ± 0.05% at 10°K. The helium vapour pressures were converted to temperatures on the T_{55E} scale (Clement, Logan and Gaffney, 1955). This scale may be expected to give temperatures to within two millidegrees of the true thermodynamic temperature.

Therefore throughout the temperature range 1.5°K to 20°K the temperatures of the experimental heat capacity measurements should be known to an accuracy better than ± 0.2%.

(ii) Error in the Heat Capacity. The experimental heat capacities are subject to many more sources of error than their respective temperatures. The heat capacities are calculated from the formula:

$$C = \frac{I^2 R t.(dA/dT)}{\Delta A}$$

where I is the current passed for time t through the heater of resistance R and A is the resistance of the constantan thermometer and the reciprocal of the resistance of the carbon thermometer.

The current is determined by measuring the potential drop across a standard 100 ohm manganin resistance. The value of the standard resistance is correct to ± 0.02%; the standard cell has an e.m.f. correct to ± 0.001% and its value does not vary by more than 0.1% between 10°C and 40°C. The potentiometer can be read to 0.0001ma.

in the range required and interpolated by means of the galvanometer scale to 0.00002 ma. According to the manufacturer each of the readings can be relied upon to within ± 0.1%. At 1.5°K the current is approximately 0.1 ma. so that the error is ± 0.12%, at 4.0°K the current is approximately 0.2 ma. giving an error of ± 0.11% and from 4°K to 20°K the error is virtually constant and equal to ± 0.1%. These errors must be doubled as the current appears as a squared term in the expression for the heat capacity.

The heating coil had not been wound non-inductively and initially the currents rose to a value greater than the steady value read with the potentiometer. The maximum value of the current was 0.5% higher than the steady current which was reached after 2 seconds. Assuming this peak in the current to be triangular in shape the error in the power dissipated in the heater is + 0.025% throughout the whole temperature range.

The heater has a resistance of approximately 900 ohms constant to within 1% throughout the whole temperature range and as its resistance is measured to 0.1 of an ohm during calibration, the error in the value of the heater resistance is ± 0.01% at all temperatures in the range 1.5°K to 20°K. To allow for the heat dissipated in the heater leads which reaches the calorimeter by conduction down the leads, the resistance of one lead is added to the resistance of the heater. The resistance of one lead is approximately 15 ohms and this resistance is

measured to 0.1 of an ohm, thus the error in the lead resistance is ± 0.67% but the lead has only 1/60th of the resistance of the heater so the resultant additional error in the heater resistance is ± 0.01%.

The length of the heating period is measured by a stop-watch which can be read to the nearest 1/10th of a second so that with a heating period of 30 seconds the error should be ± 0.17% throughout the whole temperature range. The synchronisation of the heater micro-switch with the stop-watch and also the accuracy of the stop-watch were tested by making the micro-switch start and stop an electronic timing device instead of the heater current. Over a large number of 30 second periods the electronic counter and stop-watch always agreed to the nearest 1/10th of a second and the actual error was never greater than ± 0.17%.

The temperature heating interval, represented by ΔA in the formula for the heat capacity is much more sensitive to the temperature drift errors than was the temperature of the midpoint of the heating period. With the heating intervals normally used the error in ΔA is about ± 0.75% at 1.5°K, decreasing to ± 0.2% at 2.4°K and then increasing to ± 0.75% at 4.0°K; on changing over to the constantan thermometer the error in ΔA at 4°K is ± 1% decreasing to ± 0.5% at 20°K.

The value of dA/dT at any temperature is deduced jointly from the calibration graph for the thermometer and from the actual calibration points. It is subject to both the thermometer calibration

errors listed in (i) above and also the error in the derived dA/dT versus T graph. Between 20°K and 10°K dA/dT is known to ± 0.5%, the error increasing below 10°K to probably ± 1% at 4°K; on changing over to the carbon thermometer the error becomes ± 0.5% in the range 4.0°K to 2.5°K, below 2.5°K dA/dT falls off rapidly with temperature and the error increases to ± 1% at 1.5°K.

A graph of all these errors is shown in Fig. 2.3. Now, the total heat capacity measured is the sum of the heat capacity of the specimen and the heat capacity of the calorimeter. The measurement of the heat capacity of the empty calorimeter is subject to approximately the same total error and so the error in the molar heat capacity of a specimen depends on the relative magnitudes of the heat capacities of the calorimeter and specimen. For most specimens the heat capacity of the calorimeter is only 10% of the total heat capacity measured and so to obtain the total error in the molar heat capacity of a specimen the error shown in Fig. 2.3 must be increased by approximately 1/10th of its value at any temperature.

It would appear from the graph that greater accuracy could be attained in the temperature range 4°K to 10°K by using the carbon resistance thermometer instead of the constantan resistance thermometer. Unfortunately the carbon thermometer is much less reproducible than the constantan and would require calibration against a gas thermometer during each experiment and this is not possible. Apart from the errors

introduced from thermometry the total error amounts to only ± 1/2% throughout the whole temperature range so that the need for more reliable thermometers is very apparent.

The calculated heat capacities are actually the average heat capacity between the temperature limits of the heating period. Since small temperature heating intervals are used the average heat capacity is essentially the same as the true heat capacity except in the region of a λ-type anomaly.

2. The Specific Heat of Cerium Magnesium Nitrate.

(a) Introduction.

Cerium magnesium nitrate is widely used in obtaining temperatures below $1^{o}K$ by the method of adiabatic demagnetisation and in measuring those temperatures. The magnetic specific heat, which is extremely small, has been measured by Cooke, Duffus and Wolf (1953) in the helium range and is given by:

$$C_I = 7.5 \times 10^{-6} R/T^2.$$

Daniels and Robinson (1953) showed that the susceptibility of the salt obeys Curie's law to within an accuracy of 2% down to a temperature of six millidegrees. This combination of properties makes it an ideal substance for a magnetic thermometer. The smallness of the magnetic specific heat also implies that the salt can readily be cooled to very low temperatures using only moderate fields. The maximum in the

magnetic specific heat occurs at a temperature of about three millidegrees and is extremely pronounced. Thus most of the anomalous entropy is contained in a small temperature interval and if sufficiently large demagnetisation fields have been applied a nearly constant temperature of three millidegrees can be maintained for some time. Therefore it is also a very good coolant.

The majority of salts used for demagnetisation experiments have a lattice specific heat which is negligible compared with the magnetic specific heat at $1^{o}K$. In the case of cerium magnesium nitrate with its extremely small magnetic specific heat this is not so. Observations by Cooke, Duffus and Wolf (1953) on the rate of warming of specimens cooled below $1^{o}K$ indicated that the magnetic specific heat only became comparable with the lattice specific heat at about $0.5^{o}K$. For a complete understanding of the properties of the salt around $1^{o}K$ a knowledge of the lattice specific heat is therefore required. This can best be obtained by extrapolation from measurements made in the liquid helium range of temperatures where the magnetic specific heat is negligible compared with the lattice specific heat. The measurements were undertaken as there was no available data on the lattice specific heat.

(b) Specimen.

Cerium magnesium nitrate is one of the isomorphous series of rare earth double nitrates which have the formula $A_2B_3(NO_3)_{12}.24H_2O$, where A

is the trivalent rare earth ion and B is a divalent metal. The salt is very soluble in water from which it crystallises readily in thick plates of trigonal symmetry. The crystals were prepared by mixing solutions of cerium nitrate and magnesium nitrate in the correct proportions and then seeding the resultant saturated solution and allowing the crystals to grow slowly at a constant temperature. It is very difficult to prevent the inclusion of water in the crystals. The density was measured by weighing the crystals in air, benzene and carbon tetrachloride and crystals with the maximum density of 2.02 grms. per cc. were selected from those available. The only density measurements available are those by Jantzsch (1912) who gives a value of 2.002 grms. per cc.

(c) Experimental Results.

Measurements of the specific heat of the cerium magnesium nitrate crystals were carried out in the temperature range 1.5°K to 10°K (Bailey, 1959). The crystals were placed directly in the calorimeter and a small amount of helium gas was introduced to ensure good thermal contact between the crystals and the calorimeter.

The experimental specific heat values are given in Table 2.2 and smoothed specific heat values in half degree intervals up to 4°K then in one degree intervals up to 10°K are given in Table 2.3.

(d) Discussion.

Above $3^{\circ}K$ the lattice specific heat cannot be represented by a single Debye term, but, below this temperature it was found to be given by:

$$C_L = 1.13 \times 10^{-3} RT^3.$$

Figure 2.4 shows both the extrapolated lattice specific heat and the magnetic specific heat below $1^{\circ}K$. It will be seen that the two are of equal magnitude at a temperature of $0.37^{\circ}K$. Although the lattice specific heat at $1^{\circ}K$ is 150 times the magnetic specific heat the lattice entropy is only 1/2000th of the magnetic entropy of $R \log_e 2$.

The variation of the effective θ per gram mole with temperature is shown in figure 2.5. The shallow minimum in this curve centred at $8^{\circ}K$ gives an almost pseudo T^3 region in the specific heat between $6^{\circ}K$ and $10^{\circ}K$. The similarity between the curve shown in figure 2.5 and the θ versus T relation derived by Blackman for an idealised three-dimensional cubic lattice is somewhat surprising considering the complicated nature of the cerium magnesium nitrate lattice. However, the lattice although a rhombohedral (trigonal) system has a unit cell specification a=b=c with an interaxial angle of 79 $1/2^{\circ}$, so that it may not be very different from a simple cubic system.

Variation of Lattice and Magnetic Specific Heats of Cerium Magnesium Nitrate with Temperature below 1°K.

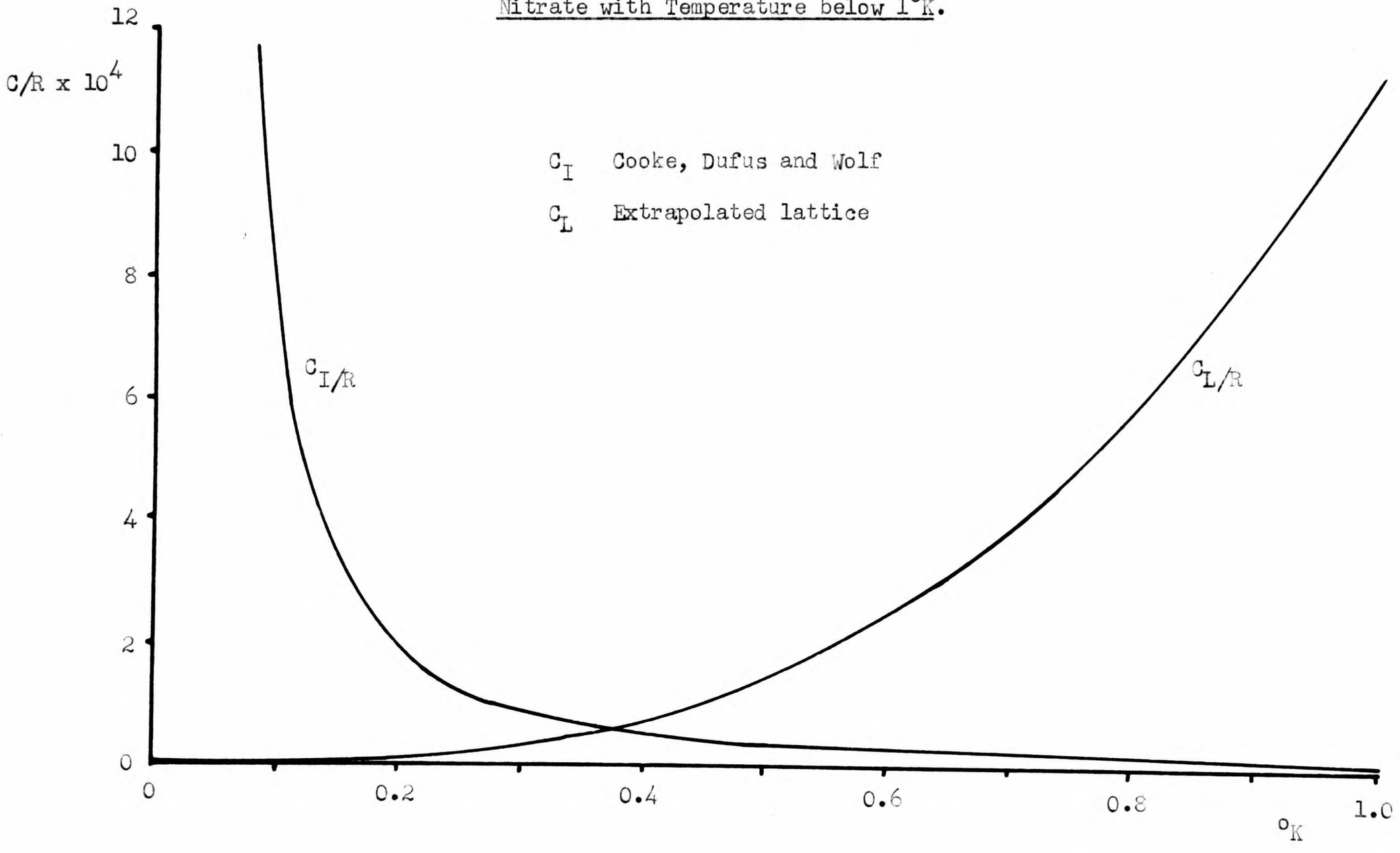


Fig. 2.4

Variation of the Debye θ of Cerium Magnesium Nitrate with Temperature.

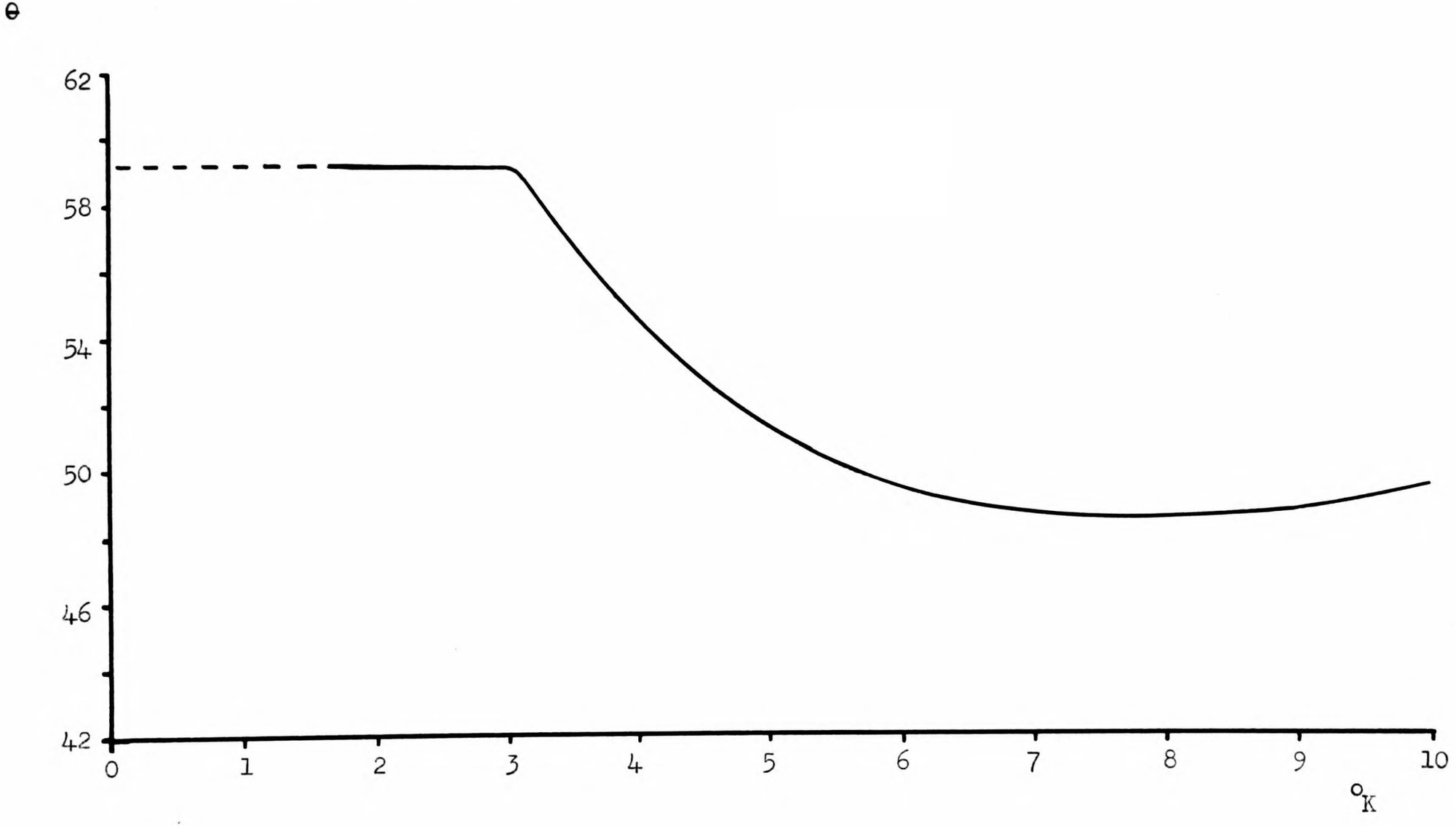


Fig. 2.5

(e) Errors.

Approximately 40 grms. of cerium magnesium nitrate crystals were placed in the calorimeter but although this only represents 1/40th of a mole its heat capacity between $10^{\circ}K$ and $4^{\circ}K$ is of the same order as 2.5 moles of pure copper. Below $4^{\circ}K$ however the heat capacity of the crystals decreased more rapidly because of the absence of any electron contribution and therefore the temperature drifts were larger than those considered in paragraph 1(f) of this chapter.

Taking account of the above fact the total error at $10^{\circ}K$ should be ± 2% increasing to ± 2 1/2% at $4^{\circ}K$ where the change of thermometer reduces the total probable error to ± 2% increasing to ± 3% at $1.5^{\circ}K$.

REFERENCES : Chapter II.

Bailey, C.A., 1959, Phil. Mag. Ser. 8, 4, 833.

Clement, J.R., Logan, J.K. and Gaffney, J., 1955, Phys. Rev., 100, 743.

Cooke, A.H., Duffus, H.J. and Wolf, W.P., 1953, Phil. Mag., 44, 623.

Daniels, J.M. and Robinson, F.N.H., 1953, Phil. Mag., 44, 630.

Jantzsch, H., 1912, Z. anorg. Chem., 76, 303.

MacDonald, D.K.C., 1947, J. Sci. Instrum., 24, 232.

Simon, F.E., 1932, Z. ges. Kalte Ind., 39, 89.

Smith, P.L. and Wolcott, N.M., 1956, Phil. Mag. Ser. 8, 1, 854.

CHAPTER III.

Specific Heat Anomalies.

1. Introduction.

Many substances have anomalies in their specific heats at low temperatures and measurements of these anomalies give much valuable and significant information about the solid state. The most interesting anomalies are those for which the excess specific heat covers only a limited range of temperature. There are two main groups of anomalies of this type:

(a) Co-operative anomalies.

(b) Schottky anomalies.

Co-operative anomalies occur when a substance undergoes an order-disorder transition which may be either spatial or magnetic. The state of order at any temperature depends on the state of order already existing and this gives rise to a sharp λ-shaped peak in the specific heat which characterises this type of anomaly. Such anomalies occur in ferromagnetic and antiferromagnetic salts, liquid helium, certain alloys (for example β-brass), and at the onset of superconductivity in some metals.

Schottky anomalies are due to atomic or molecular excitations.

In the theories of the lattice specific heat it is assumed that the atoms or molecules are all in their lowest energy states but if this is not so we have an extra contribution to the internal energy which varies with temperature. The excess specific heat again shows a maximum at a definite temperature but falls away gradually on either side. Such anomalies occur in the specific heats of paramagnetic salts.

Examples of both groups of anomalies will be given in this chapter.

2. The Specific Heat of Uranium Tetrafluoride.

(a) Introduction.

Measurements on the magnetic susceptibility of Uranium Tetrafluoride had been carried out at the Clarendon Laboratory by Wolf and Park (1957). They found that above 77°K the susceptibility obeyed a Curie-Weiss law,

$$X = C/(T-\theta) \qquad \text{with } C = 1.33 \text{ and } \theta = -116^{\circ}K$$

but, below 77°K the susceptibility depended on the temperature in a more complicated way. At the lowest temperature the susceptibility seems to be approaching a maximum value, or a value independent of temperature.

These results were tentatively interpreted by Bleaney and Wolf (1957) on the basis of a simple scheme of three energy levels.

The scheme was based on the fact that a $5f^2$ system, for which the free ion state is $^3H_4$, will be split by a crystalline electric field of cubic symmetry into two triplet levels, a doublet, and a singlet (Hutchison and Candella, 1957). If the sign of the field is such that one of the triplets lies lowest in energy, it will behave very like a system having S = 1, g = 2, giving a Curie constant at high temperatures of 1.0, close to the observed value at high temperatures (T = 77°K). It is then assumed that the triplet is split by a distortion of the field from cubic symmetry to give states characterised by the effective component of S, S_Z, along the axis of distortion, giving a singlet state $S_Z = 0$ and a doublet $S_Z = \pm 1$. To account for the trend towards temperature independent susceptibility at very low temperatures, it is further assumed that the doublet is split by a distortion of rhombic symmetry, giving a singlet ground state. To fit the observed susceptibility curve requires a splitting of the doublet of about 15°K, with the $S_z = 0$ state at about 180°K higher in energy.

For a simple known scheme of energy levels it is not too difficult to calculate the form of the resulting specific heat anomaly. Therefore measurement of the specific heat in the region of the anomaly was undertaken at the request of Dr. Wolf to test the correctness of the proposed scheme of energy levels.

(b) Calculation of the expected Anomaly.

It will be assumed that there is no appreciable interaction between the paramagnetic ions, which is equivalent to saying that the partition function of an assembly of N ions is simply the Nth product of the partition function for a single ion. Also since the $S_Z = 0$ state has an energy separation from the doublet $S_Z = \pm 1$ which is twelve times the splitting of the doublet only the doublet will be considered in the calculation.

Let the degeneracies of the two energy levels forming the doublet be g_1 and g_2 and let the energy separation be $k\theta$. The distribution of energy between these two levels will be given by the partition function, Z.

$$Z = g_1 + g_2 e^{-\theta/T}$$

The resultant total energy, U, of an assembly of N ions is given by:

$$U = \frac{-\partial \log Z}{\partial (1/KT)}$$

$$= Nk\theta g_2/(g_1 e^{\theta/T} + g_2)$$

and the specific heat, C_v is given by:

$$C_v = dU/dT$$

$$= \frac{\alpha R(\theta/T)^2 e^{-\theta/T}}{(1 + \alpha e^{-\theta/T})^2} \qquad \text{where } \alpha = g_2/g_1$$

The condition for a maximum in C_v is obtained by differentiating the above expression, and is a transcendental equation which can be solved graphically. The equation is:

$$e^{-\theta/T} = \frac{\theta/T - 2}{\alpha(\theta/T + 2)}$$

Using the proposed energy scheme for Uranium Tetrafluoride, $\theta = 15^{\circ}K$ and $\alpha = 1$ an anomaly of maximum value 0.871 cals/mole deg. at $6.2^{\circ}K$ would be expected in the specific heat.

Also the entropy associated with the anomaly should be $R \log_e(1+\alpha)$; that is $R \log_e 2$.

(c) Specimen.

The specimen used for the specific heat measurements was from the same batch as that used by Park and Wolf for susceptibility measurements. The material was supplied by the Chemistry Division of A.E.R.E., Harwell and the analysis sent with it was:

Total U	75.3%
Tetravalent U	74.7%
UO_2F_2	0.4%
Fe	45 p.p.m.
Cr	20 p.p.m.
Ni	8 p.p.m.

The material was in the form of a very finely divided green powder.

(d) Experimental results.

The chief difficulty of making measurements on such a finely divided powder is that if helium gas is used to provide thermal contact between the powder and the calorimeter, inaccuracies arise at low temperatures owing to the desorption of helium by the powder on heating. To minimise this effect the specimen was compressed into a thin walled copper container fitted with eight internal copper vanes to assist thermal contact. The copper container was then placed in the calorimeter and the measurements were carried out with a very low pressure of helium gas in the calorimeter. The heat capacity of the container was corrected for by determining its mass and using the measured value for the specific heat of pure copper. Satisfactory results were obtained in the temperature range 1.8°K to 7.5°K and these are given in table 3.1 but above 7.5°K the results were irreproducible. It is fairly safe to assume that the divergences between experiments were due to the desorption of helium gas from the powder but the possibility of the salt being affected by its thermal history must not be altogether excluded. Figure 3.1 shows the measured specific heat points from 1.8°K to 8°K after correction for the thermal capacity of the container and calorimeter. The graph also shows measurements from 5°K to 20°K by Osborne, Westrum and Lohr (1955), also at 20°K the lowest point from the smoothed curve of results by Brickwedde, Hoge and Scott (1948). In order to study the anomalous contribution to the specific

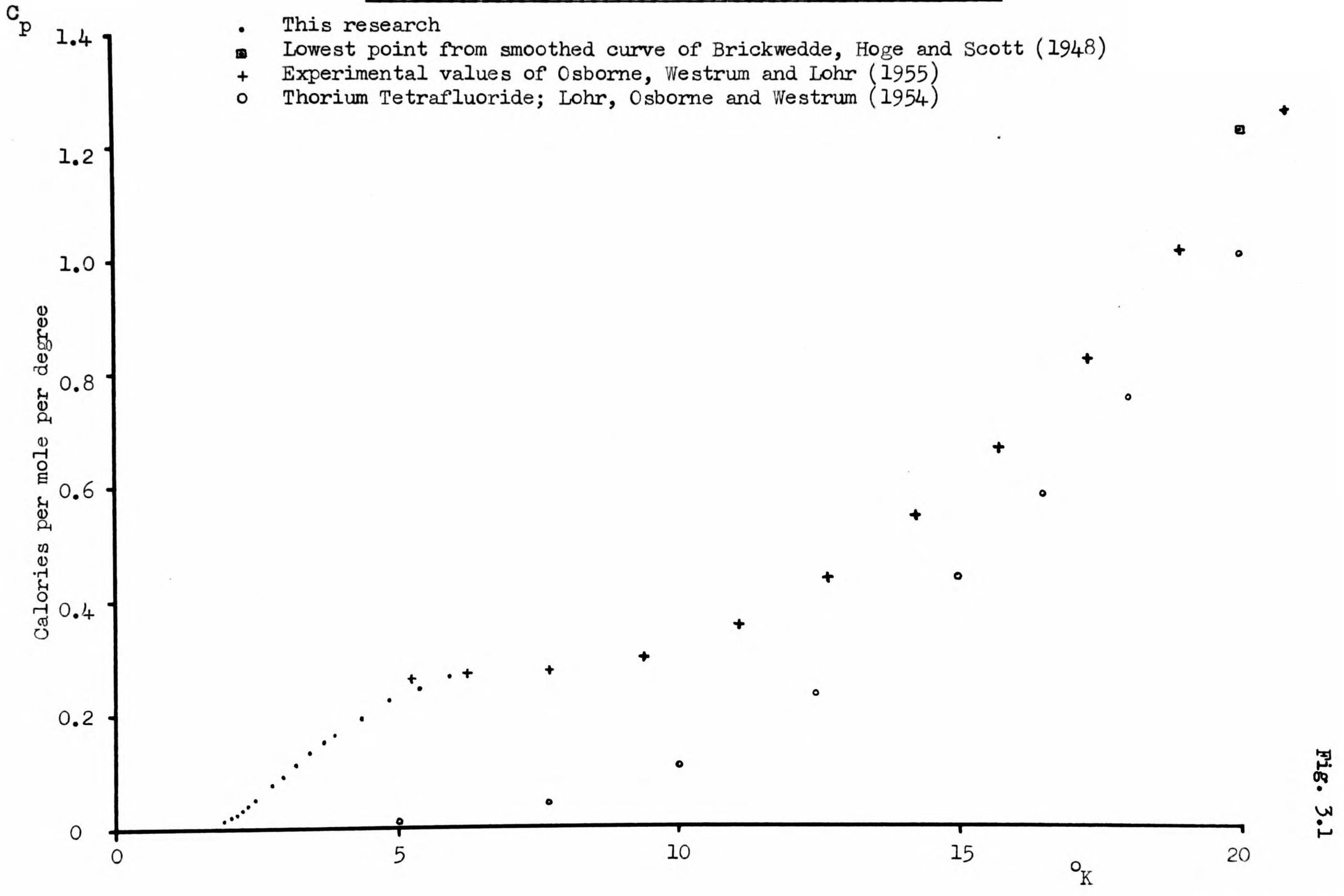

The Specific Heat of Uranium Tetrafluoride below 20°K.
C_p
This research
Lowest point from smoothed curve of Brickwedde, Hoge and Scott (1948)
Experimental values of Osborne, Westrum and Lohr (1955)
Thorium Tetrafluoride; Lohr, Osborne and Westrum (1954)
Calories per mole per degree
1.4
1.2
1.0
0.8
0.6
0.4
0.2
0
0
5
10
15
20
°K

Fig. 3.1

heat a knowledge of the normal lattice contribution is required. There are usually two alternative ways of obtaining the lattice specific heat. One method is to make use of the fact that at temperatures well above the maximum the anomalous specific heat decreases as $1/T^2$. If it can be assumed that the lattice specific heat obeys the Debye T^3 law then the total specific heat of the salt can be represented by the following expression

$$C = A/T^2 + BT^3$$

and by plotting CT^2 against T^5 it is possible to estimate A and B. Unfortunately in this case no reliable results for C were available at temperatures well above the maximum of the anomaly. The alternative method of assuming the lattice specific heat to be the same as the total specific heat of a similar diamagnetic salt had to be employed. The salt chosen was Thorium Tetrafluoride for which specific heat values were available down to $5^{\circ}K$ (Lohr, Osborne and Westrum, 1954). Thorium tetrafluoride has the same crystal structure as uranium tetrafluoride, the difference in the lattice dimensions is only about 2.5% (Zachariasen, 1949) and the masses of the thorium and uranium ions only differ by 2.6%. The available data showed that the specific heat of thorium tetrafluoride had not at $5^{\circ}K$ reached a true T^3 dependence but the deviations from a single Debye function were quite small. Below $5^{\circ}K$ the lattice was therefore taken to be represented by

$$C_L = (0.91 \times 10^{-4})T^3 \text{ calories per mole per degree.}$$

Figure 3.2 shows the variation of the anomalous specific heat of the Uranium Tetrafluoride with temperature. The maximum of the anomaly occurs at 6.8°K instead of at 6.2°K as required by the provisional scheme of energy levels. On the other hand, the maximum value of the anomalous specific heat is only 0.245 calories per mole per degree instead of 0.871 calories per mole per degree. Combining the present measurements below 6°K with the measurements of Osborne, Westrum and Lohr (1955) above 6°K an estimate of the total entropy associated with the anomaly was made. The entropy change due to the anomaly only amounted to 0.41 calories per mole per degree or approximately $R \log_e 1.25$ instead of $R \log_e 2$. The simplest scheme of levels which could give this change of entropy is four degenerate levels separated from a single higher level. Using this value of 1/4 for α and the value 6.8°K for the temperature of the maximum in the transcendental equation which is a condition for the maximum a value of 14.8°K is obtained for θ.

The energy separation, θ, can also be obtained by considering the exponential rise before the maximum of the anomaly is reached.

$$C/R = \frac{\alpha(\theta/T)^2 e^{-\theta/T}}{(1 + \alpha e^{-\theta/T})2}$$

now if T is very much less than θ

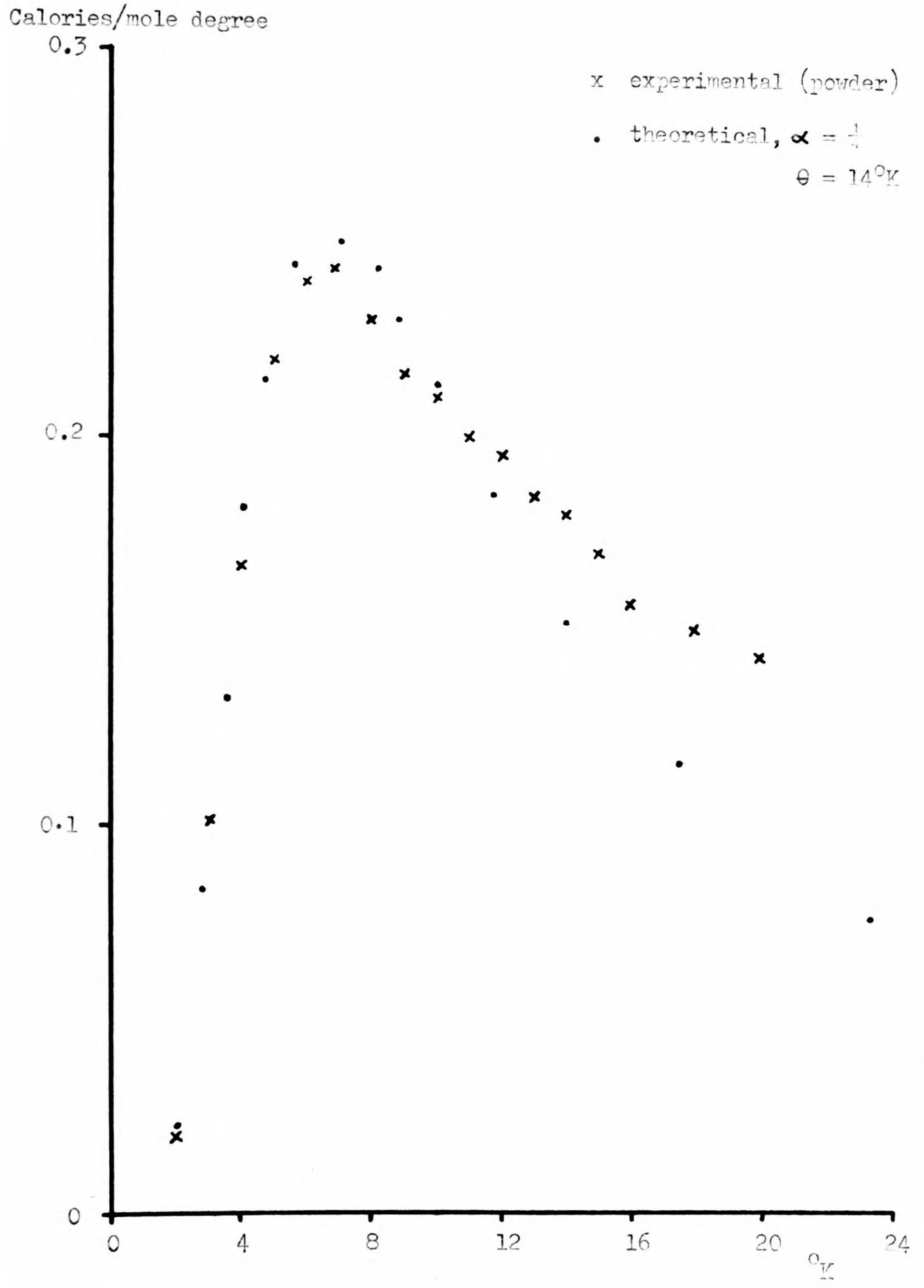
$$C/R = \alpha(\theta/T)^2 e^{-\theta/T}$$

therefore

$$\log_e CT^2/R = \mathrm{Log}_e \alpha\theta^2 - \frac{\theta}{T}$$

Fig. 3.2

The Anomalous Specific Heat of Uranium Tetrafluoride.



Thus a plot of $\log_e CT^2/R$ against 1/T should be a straight line of slope θ so by this means a value for θ is obtained without assigning a value to α. The results in the helium range were treated in this way and fitted very closely a straight line of slope 14.0. This value of 14.0°K for θ should be much more accurate than that obtained using the value for α derived from the rather uncertain total entropy of the anomaly. From the intercept on the 1/T axis using θ = 14.0°K a value for α between 1/4 and 1/5 was found.

Figure 3.2 shows the form of a Schottky anomaly corresponding to four degenerate levels separated by an energy difference of 14.0°K from a single higher level. It will be seen that such an anomaly fits the experimental curve rather closely. However this scheme of levels could not be reconciled with the results of the susceptibility measurements. For the susceptibility to become independent of temperature at low temperatures the scheme of levels must have a singlet ground state.

At this juncture further specific heat measurements by Burns, Osborne and Westrum (1958) became available. They had made measurements on a granular sample of Uranium Tetrafluoride in the temperature range 1.3°K to 20°K and on a powdered sample in the temperature range 4.5°K to 20°K. Below 4.5°K they had lost thermal contact with the powdered sample and above this temperature they had encountered no trouble from the desorption of helium despite the fact that their sample had been

sealed into its calorimeter at room temperature with an atmosphere of helium as exchange gas. Their results below 10°K are shown in Figure 3.3 together with the results of this research.

(e) Discussion.

The present results agree closely with the results of Burns, Osborne and Westrum (1958) on their granular specimen up to 3°K, above this temperature there is an increasing divergence which amounts to 6% at the temperature of the maximum in the anomaly. However, the results on their powdered specimen are a further 2% lower at this temperature, so it would seem that there is a difference between the specific heats of the powder and the granular specimens and possibly a difference between the two powdered specimens. The fact that up to 9°K the granular specific heat is larger than the powder specific heat suggests that the difference cannot be due to exchange gas effects.

Analysis of the exponential rise of the anomalous specific heat of the granular specimen yielded a value for Θ of 14.1°K compared with Θ = 14.0°K for the powder. The temperature of the maximum had shifted from 6.8°K for the powder to 6.2°K, the temperature expected from the scheme of levels proposed to account for the susceptibility measurements but the maximum value of the anomalous specific heat although greater than for the powdered specimen was still only 0.26 calories per mole per degree. If it is assumed that the same scheme of levels applies

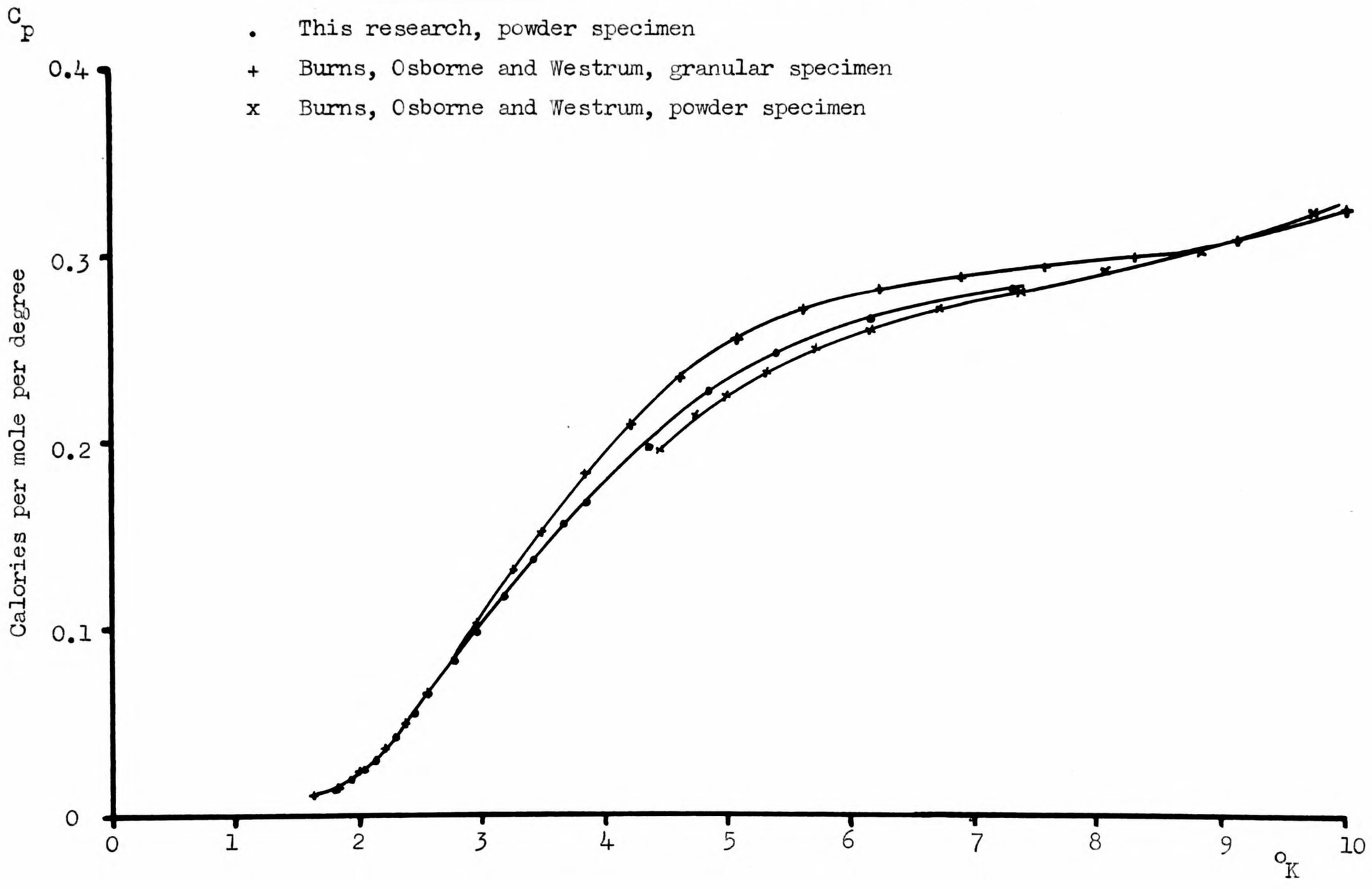

The Specific Heat of Uranium Tetrafluoride below 10°K.
C_p
. This research, powder specimen
+ Burns, Osborne and Westrum, granular specimen
x Burns, Osborne and Westrum, powder specimen
Calories per mole per degree
0.4
0.3
0.2
0.1
0
0
1
2
3
4
5
6
7
8
9
10
°K

Fig. 3.3

to both the powdered and the granular specimens then it is to be expected that the temperature of the maximum would be proportional to θ since θ/T must be a constant. So the observed shift in temperature of the maximum is in the opposite direction to that which would be expected from the change in θ.

There is also a change in height of the anomaly to be accounted for. Now the height of the anomaly depends on the way in which the energy levels are arranged and not on the splitting so it would seem that this arrangement must be different for the two specimens. The results of Burns, Osborne and Westrum (1958) for the granular specimen confirm that the entropy associated with the specific heat anomaly is approximately $R \log_e 1.25$ indicating $\alpha = 1/4$ a result untenable as far as the magnetic measurements are concerned.

Wolf (1958) proposed that only one third of the uranium ions were contributing to the observed effect. Thus the entropy associated with the anomaly, 0.41 calories per mole per degree is almost exactly one third of $R \log_e 2$ and the height of the anomaly is nearly one third of 0.871 calories, the value calculated for $\alpha = 1$. An unpublished report by R.D. Burbank (1951) on the structure of uranium tetrafluoride gave weight to this idea. He found that there were twelve uranium ions per unit cell and four of these had a different environment to the other eight. Now if the environment of the four uranium ions is such that they contribute to the Schottky anomaly and the other eight uranium

ions do not it would seem possible to reconcile the scheme of levels proposed initially with the observed specific heat anomaly. However it can be seen from Figure 3.4 that an anomaly with $\alpha = 1$, $\theta = 14^{\circ}K$ and one third of the uranium ions taking part does not fit the observed anomaly for either the powder or the granules very well, in fact the anomaly with $\alpha = 1/4$, $\theta = 14^{\circ}K$ and all the uranium ions taking part is a much better fit.

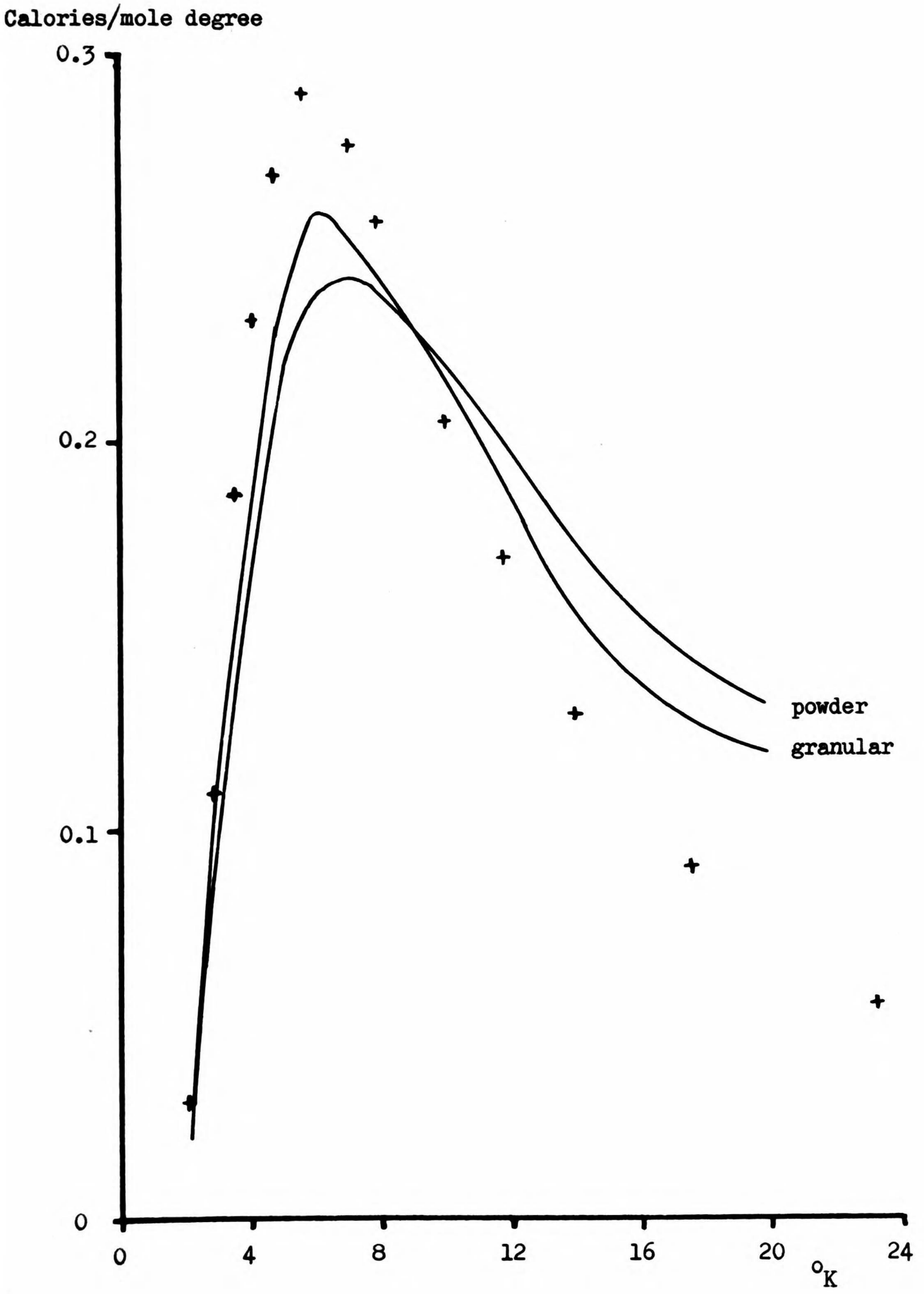
Now, if it is believed that only one third of the uranium ions are taking part in the anomaly and that the proposed scheme of levels is correct there is no logical reason why the observed and calculated anomalous specific heats should differ by more than the experimental error. It might be argued that the assumption that the lattice specific heat of uranium tetrafluoride is the same as the specific heat of thorium tetrafluoride is at fault, but in order to increase the maximum in the anomalous specific heat of either the powder or the granules to the expected value would require uranium tetrafluoride to have a negative lattice specific heat at that temperature! Some other explanation must be found and so it was decided to re-investigate the exponential rise of the anomalous specific heat.

If it is assumed that only a fraction x of the uranium ions contribute to the anomaly then the expression for the specific heat associated with the anomaly becomes

$$C = \frac{x\alpha R(\theta/T)^2 e^{-\theta/T}}{(1+\alpha e^{-\theta/T})^2}$$

The Anomalous Specific Heat of Uranium Tetrafluoride.

\+ theoretical anomaly with only 1/3 of the uranium ions taking part, $\alpha = 1$ and $\theta = 14^{\circ}K$.



and when T is very small compared with θ

$$C/R = x\alpha(\theta/T)^2 e^{-\theta/T}$$

thus

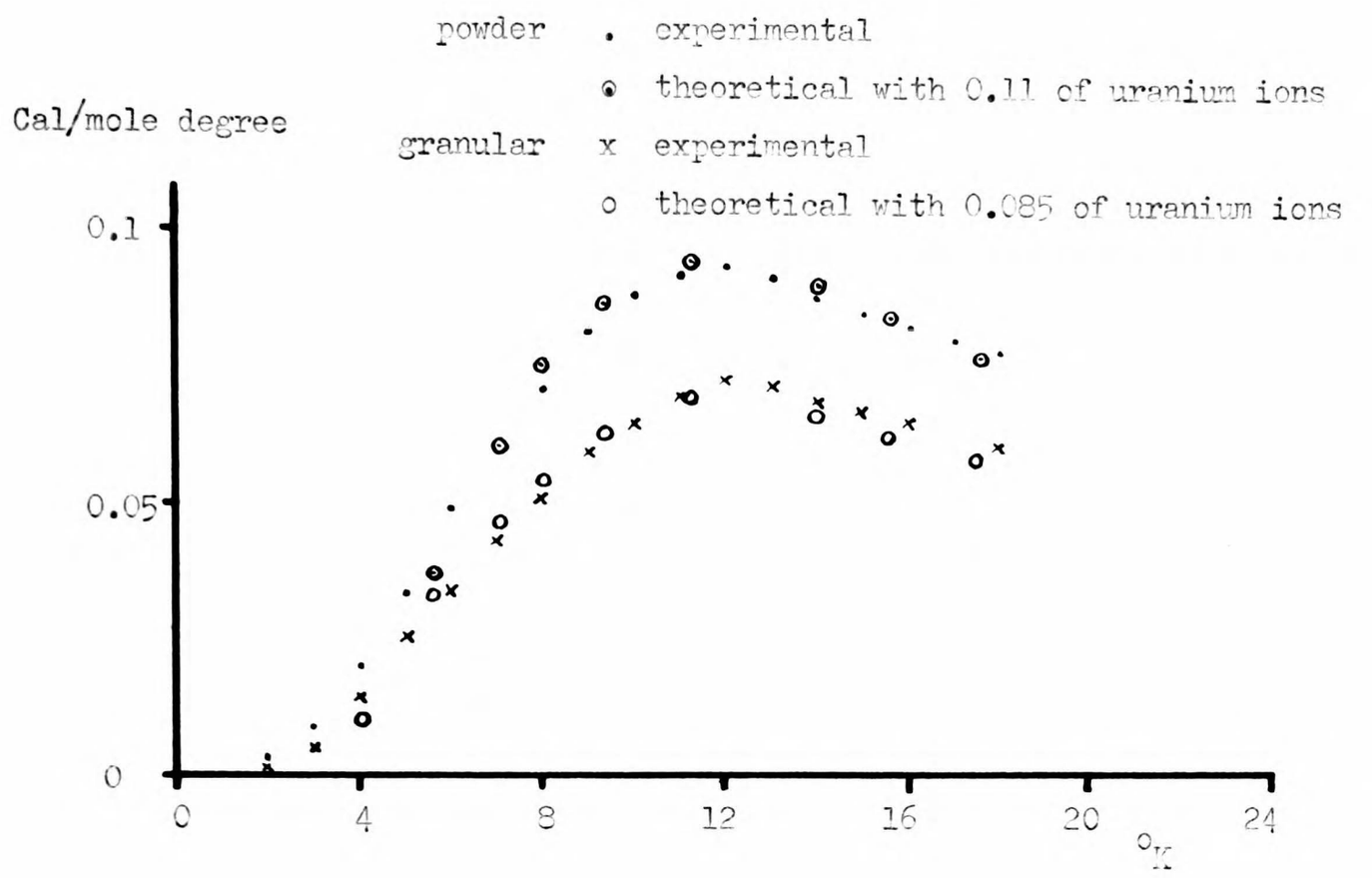
$$\log_e CT^2/R = \log_e x\alpha\theta^2 - \theta/T$$

Therefore the analysis of the exponential rise still gives a value for θ independent of the value of α and now also independent of x. If it is assumed that $\alpha = 1$ an estimate of x can be obtained. For the granular specimen $x = 0.25$ although from the height of the maximum a value of 0.30 is required. For the powder $x = 0.22$ compared with a value of 0.28 from the height of the maximum. Thus for the granular specimen there would seem to be slightly more uranium ions with $\theta = 14^{\circ}K$ than for the powder but in neither case is this the total number contributing to the anomaly. There must also be a small number of uranium ions in each case with a value of θ which is greater than $14^{\circ}K$ giving an anomaly with its maximum at a higher temperature. If the second anomaly is sufficiently higher in temperature and there is a smaller number taking part it should not interfere appreciably with the exponential rise of the lower anomaly.

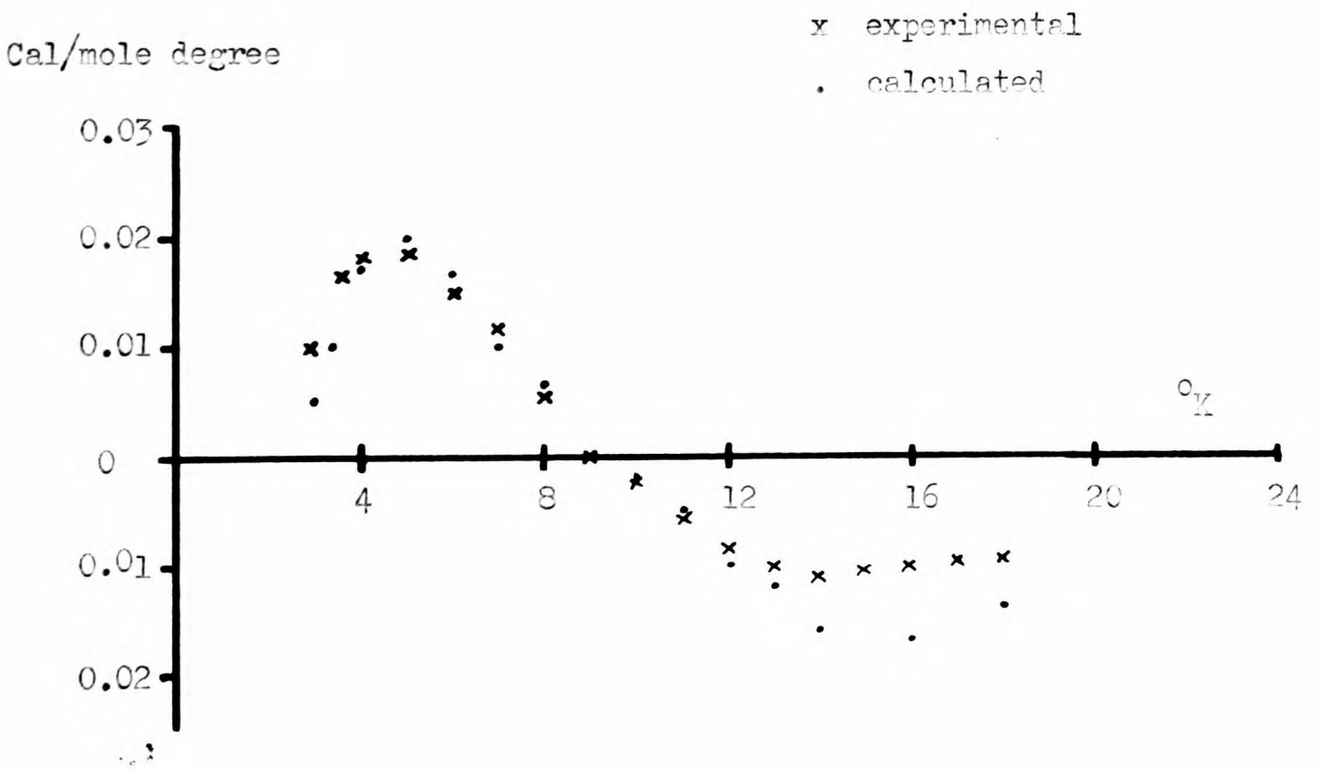
Figure 3.5a shows the result of subtracting fractions 0.25 and 0.22 of an anomaly with $\alpha = 1$, $\theta = 14^{\circ}K$ from the observed anomalies in the granular and powder specimens respectively. Two further Schottky anomalies are obtained with maxima at $11.8^{\circ}K$, the one for the powder being now larger than that for the granular. If it is assumed that the same

Fig. 3.5

(a) Anomalies with $\Theta = 28.3^{\circ}K$.



(b) Difference between the Specific Heats of the Granular and Powder Specimens.



scheme of levels applies to this second anomaly, i.e. $\alpha = 1$ then the required splitting of the lowest doublet is $\theta = 28.3^{\circ}K$. Thus the required splitting for the second anomaly is double that for the first.

The most interesting feature of the second anomalies is the heights of their maxima. The height for the granular specimen is 0.085 times and the height for the powder is 0.11 times the height of an anomaly with $\alpha = 1$. Taking these respective fractions of an anomaly with $\alpha = 1$ and $\theta = 28.3$ two anomalies are obtained which fit the anomalies found by subtraction very well (see Figure 3.5a). The fit is such that it can be assumed that a single anomaly is now being dealt with and therefore the fractions 0.085 and 0.11 are also the fractions of uranium ions taking part in the anomalies for the granular and powder specimens respectively. Thus the total fraction of uranium ions taking part in the two anomalies for the granular specimen is $(0.25 + 0.085) = 0.335$ and the total fraction for the powder specimen is $(0.22 + 0.11) = 0.33$. Hence for both specimens there are now one third of the uranium ions taking part in the anomalous specific heat. The only difference between the granular and the powder specimens being the relative number of ions with $\theta = 14^{\circ}K$ and $\theta = 28.3^{\circ}K$, 3 to 1 for the granular and 2 to 1 for the powder.

Susceptibility measurements have now been carried out on the granular specimen of Burns, Osborne and Westrum by Leask, Osborne and Wolf (1959) and at low temperatures these are slightly different from

those obtained with the powdered specimen. Preliminary calculations show that results obtained above from the analysis of the specific heat anomalies can account for this difference qualitatively and possibly quantitatively. However there is no theoretical reason why some of the four seemingly similar uranium ions per unit cell should behave differently from the others and also why the number so behaving should differ from the granular specimen to the powder specimen. It must be emphasised that the proposed analysis is not the only possible explanation of the observed results but the simplest one. Also the assumption has been made that there is no appreciable interaction between the paramagnetic ions and the possibility of such interactions must not be forgotten. Now Uranium dioxide exhibits an antiferromagnetic transition so there must be exchange interaction between uranium ions. However in uranium tetrafluoride Burbank has shown that each uranium ion that takes part in the specific heat anomaly is surrounded by eight that do not. Thus each magnetic uranium ion is screened from its magnetic neighbours and it seems reasonable to assume that there will be no appreciable interaction.

Lastly as a test of the accuracy with which the derived expression fits the experimental results and one which requires no assumption of the magnitude of the lattice specific heat of uranium tetrafluoride, consider the difference between the total specific heats of the granular and powder specimens. This has the form:

$$C_{diff.} = C_{granular} - C_{powder}$$

$$= (C_L + 0.25C_1 + 0.085C_2) - (C_L + 0.22C_1 + 0.11C_2)$$

$$= 0.03C_1 - 0.025C_2$$

where C_1 is the expression for the anomalous specific heat of the lower anomaly and C_2 that for the upper anomaly, C_L being the lattice specific heat. Figure 3.5b shows a plot of this expression together with the experimental $C_{diff.}$, the agreement is quite pleasing considering that at no time does $C_{diff.}$ exceed 6% of the measured total specific heat.

3. The Specific Heats of Ammonium, Potassium and Sodium Chloroiridates.

(a) Introduction.

Extensive investigations of the magnetic properties of chloroiridate salts have been made in this laboratory during the past few years. Griffiths and Owen (1954) carried out paramagnetic resonance experiments on iridium ions present in low concentration in ammonium chloroplatinate. Each iridium ion was therefore so far from any other iridium ion that it could be assumed that there were no exchange interactions. It was found that the Iridium ions behave as magnetic carriers, each iridium ion having one unpaired electron with spin, s = 1/2. It was also deduced from the hyperfine structure of the paramagnetic resonance spectrum that there is appreciable charge

transfer between the central iridium ion and its surrounding chlorine ions. Experiments on semi-dilute crystals with iridium ions replacing platinum ions in ammonium and potassium chloroplatinates have been made by Griffiths, Owen, Park and Partridge (1957, 1959). In a semidilute crystal there is an appreciable chance of pairs of iridium ions occupying nearest-neighbour positions in the lattice. There is then an overlap of the two unpaired electrons via their transfer onto the intervening chlorine ions and an exchange coupled pair of iridium ions results. Investigation of the paramagnetic resonance spectrum showed that the main contribution to the exchange interaction is isotropic and the sign of the isotropic exchange parameter is such that an antiparallel alignment of the spins is preferred. Thus the paramagnetic resonance experiments indicated that there might be antiferromagnetic transitions in the pure chloroiridate salts in the liquid helium range of temperatures.

Confirmation of an antiferromagnetic transition can be provided by both susceptibility and specific heat measurements. The susceptibility measurements were made by Cooke, Lazenby, McKim, Owen and Wolf (1959) and the specific heat measurements by Bailey and Smith (1959).

Antiferromagnetic transitions are an example of an order-disorder transition and are therefore accompanied by a λ-type anomaly in the specific heat and the presence of such an anomaly provides the most distinct evidence that there is such a transition.

(b) Specimens.

The salts were prepared by Messrs. Johnson Matthey of London and were classified as high purity material. They were all fine powders but not nearly as fine as the uranium tetrafluoride specimen referred to earlier in this chapter.

The ammonium and potassium salts both have the formula M_2IrCl_6, where M is the monovalent ion and the lattice structure is face-centred cubic. The sodium salt has the formula $Na_2IrCl_6.6H_2O$ and its lattice structure is triclinic.

(c) Experimental Results.

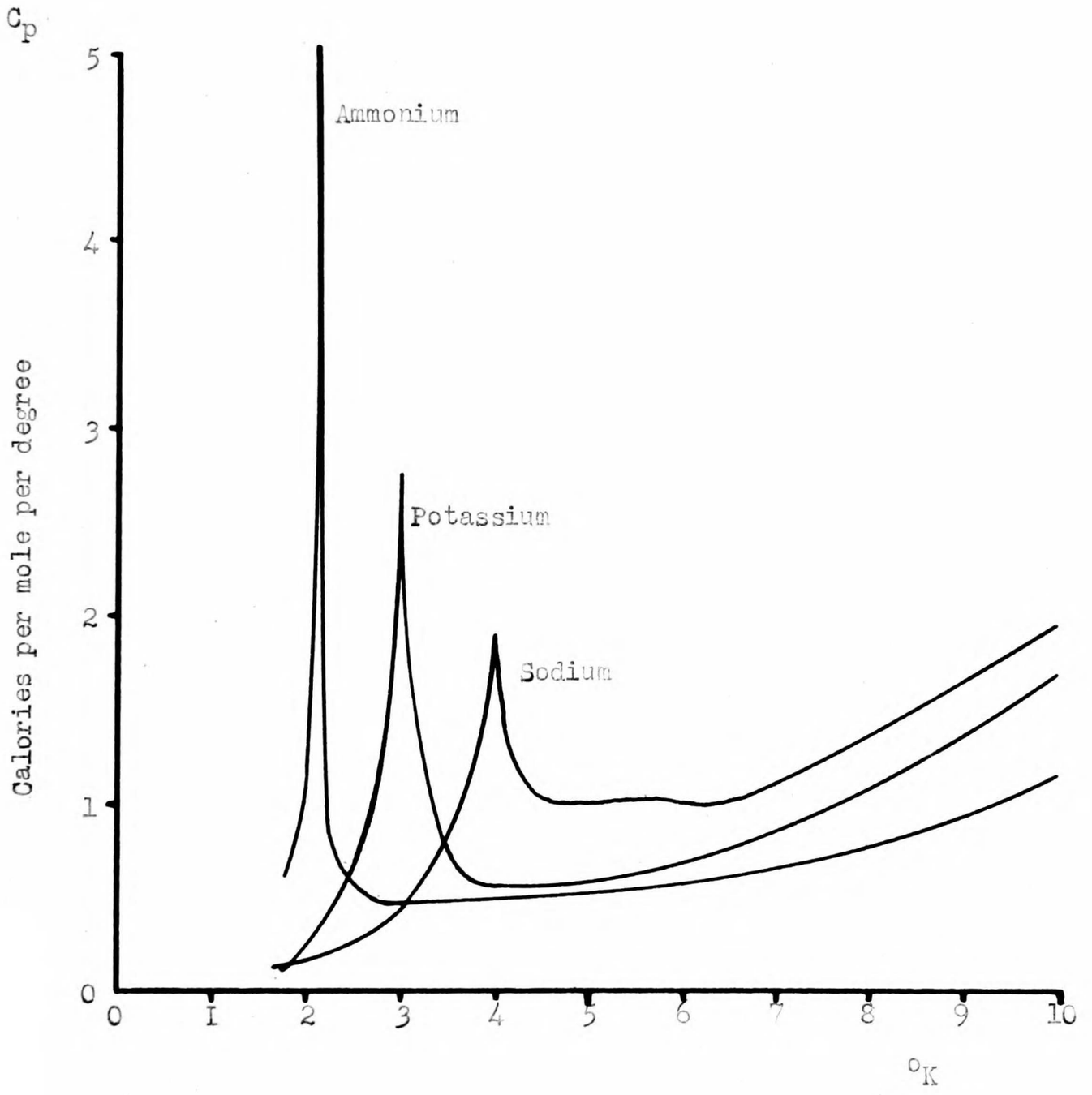
The specimens were again compressed into a thin-walled copper container fitted with eight internal copper vanes to assist thermal contact. The copper container was then placed in the calorimeter and the measurements carried out with a very low pressure of helium gas in the calorimeter. Measurements were carried out on all three salts in the temperature range 1.5°K to 20°K and no noticeable trouble was encountered from the use of helium as exchange gas.

The specific heat measurements are listed in Tables 3.2, 3.3 and 3.4; the specific heat curves for all three salts below 10°K are shown in Fig. 3.6.

(d) Discussion.

The results show quite clearly that an order-disorder transition

The Specific Heats of Ammonium, Potassium and Sodium Chloroiridates.



takes place in each of the three salts in the liquid helium temperature range. An anomaly of the expected λ-type in the specific heat occurs at 2.15°K for the ammonium salt, 3.05°K for the potassium salt and 3.95°K for the sodium salt. However, the specific heat measurements unlike the susceptibility measurements cannot give any information as to the nature of the order-disorder transition. The transition temperatures can be defined as the temperature of the peaks in the specific heat curves. It was found that these temperatures for the ammonium and potassium chloroiridates correspond to the temperatures at which the susceptibilities show the greatest rate of decrease with temperature (2.16°K for the ammonium salt and 3.08°K for the potassium salt). Figure 3.7 shows the susceptibility measurements of Cooke, Lazenby, McKim, Owen and Wolf (1959) on ammonium and potassium chloroiridates below 20°K. The temperatures of the maxima of the specific heat anomalies are indicated by arrows. Thus the temperature at which the entropy is changing the most rapidly is also that at which the susceptibility changes most rapidly.

The anomalous entropy was found to be of the order of $R \log_e 2$ for each salt as was to be expected for a system with spin 1/2. These approximate results were found by attempting to fit those parts of the specific heat curves lying well above the maxima to equations of the form:

$$C = C_{lattice} + C_{anomaly}$$

assuming that $C_{lattice} = AT^3$ and $C_{anomaly}$ B/T^2.

Variation of the Molar Magnetic Susceptibility of Ammonium and Potassium Chloroiridates with Temperature below 20°K.

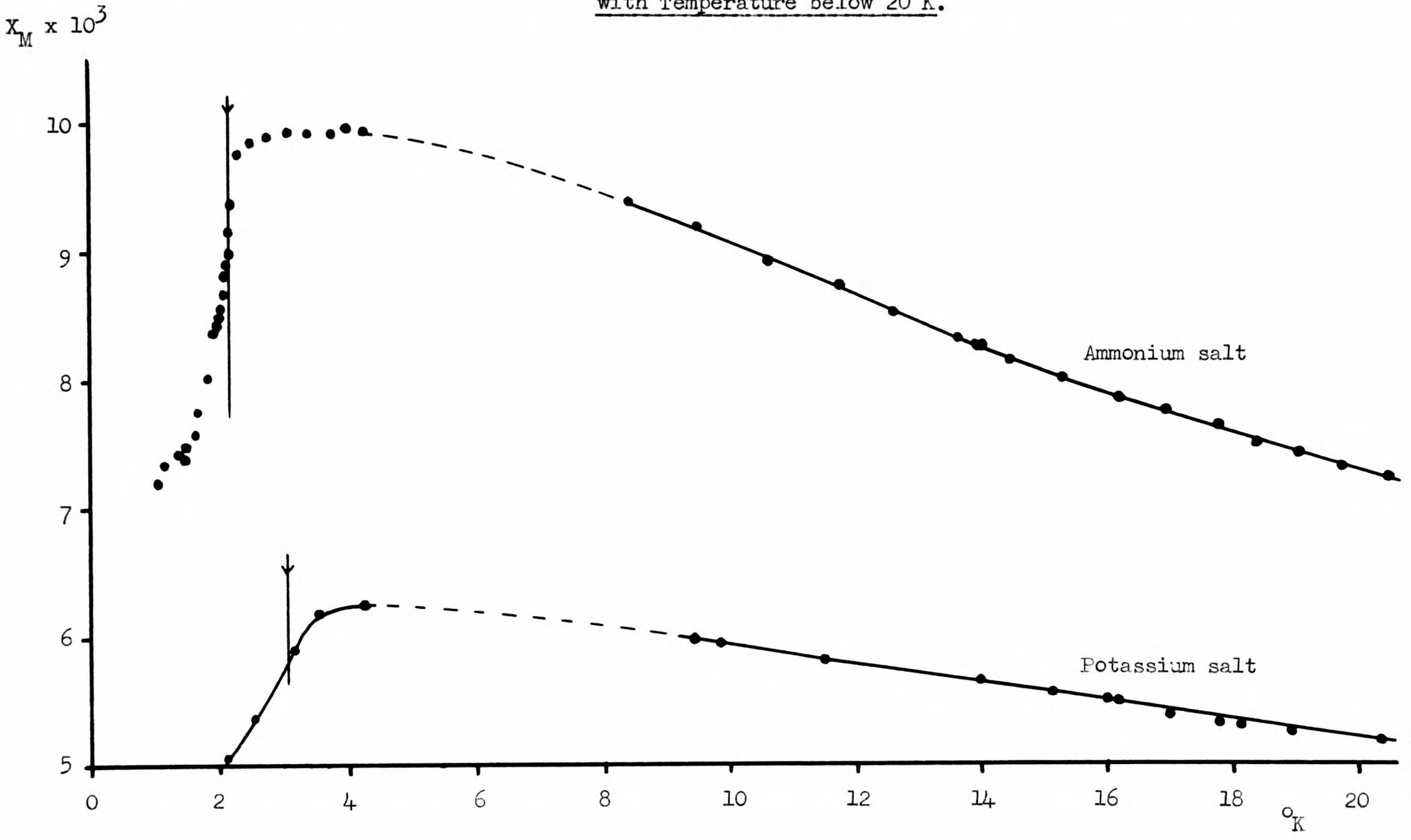


Fig. 3.7

In fact the experimental results did not fit closely a curve of this form for any of the salts. This is really not surprising in view of the assumptions made; for the anomalous specific heat to vary as $1/T^2$ the temperature must be well above the transition temperature and here the lattice specific heats are unlikely to still obey a Debye T^3 law.

Measurements on the diamagnetic ammonium, potassium and sodium chloroplatinates are however to be made in the near future, since the specific heats of these salts should represent very closely the corresponding lattice terms of the chloroiridates and enable the anomalous contributions to be evaluated more accurately.

One curious feature of the results is the shape of the specific heat curve for the sodium salt. It would appear that there is a second less distinct anomaly immediately following the λ-type anomaly, its appearance being almost that of a Schottky anomaly. If it is simply a smeared out λ anomaly then it would indicate that the ordering process takes place in two stages instead of one as for the ammonium and potassium salts. Such a difference in behavious could possibly be explained by the difference in lattice structure.

It will have become evident that far less information is forthcoming from a λ-type anomaly than from a Schottky anomaly.

REFERENCES : Chapter III.

Bailey, C.A. and Smith, P.L., 1959, Phys. Rev., 114, 1010.

Bleaney, B. and Wolf, W.P., 1957, Private communication.

Brickwedde, F.G., Hoge, H.J. and Scott, R.B., 1948, J. Chem. Phys., 16, 429.

Burns, J., Osborne, D.W. and Westrum, E.F., Jr., Private communication.

Burbank, R.D., 1951, A. E. C. D. - 3216 (unpublished).

Cooke, A.H., Lazenby, R., McKim, F.R., Owen, J. and Wolf, W.P., 1959, Proc. Roy. Soc. A, 250, 97.

Griffiths, J.H.E. and Owen, J., 1954, Proc. Roy. Soc. A, 226, 96.

Griffiths, J.H.E., Owen, J., Park, J.G. and Partridge, M.F., 1959, Proc. Roy. Soc. A, 250, 84.

Hutchison, C.A., Jr. and Candela, G.A., 1957, J. Chem. Phys., 27, 207.

Leask, M., Osborne, D.W. and Wolf, W.P., 1959, Verbal communication.

Lohr, H.R., Osborne, D.W. and Westrum, E.F., Jr., 1954, J. Amer. Chem. Soc., 76, 3837.

Park, G. and Wolf, W.P., 1957, Private communication.

Osborne, D.W., Westrum, E.F., Jr. and Lohr, H.R., 1955, J. Amer. Chem. Soc., 77, 2737.

Wolf, W.P., 1958, Verbal communication.

Zachariasen, W.H., 1949, Acta. Cryst., 2, 388.

CHAPTER IV.

1. The Electronic Specific Heat of Metals.

The classical Drude-Lorentz theory of metals assumes that some of the electrons in a metal are free to move from atom to atom and obey laws of classical dynamics. Most of the characteristic properties of metals can be explained on this basis but the existence of a free electron gas inside a metal implied a contribution of $3R/2$ per mole of electrons to the specific heat for which there was no experimental evidence.

Sommerfeld (1928) using Fermi-Dirac statistics instead of the classical Maxwell-Boltzmann statistics was able to solve the problem qualitatively. He disregarded the periodic potential variations that must be associated with any lattice of charged ions and assumed that the potential within a metal was constant. This does not entirely rule out electron-lattice interaction as any part of it which results in no net field is effectively included. Also any electron-electron interaction which can be represented by a time average is included if it produces no net field in the metal.

The potential along a line through a metal will thus appear as a flat-bottomed well with very steep sides at the surface of the metal.

This well will contain a large number of closely spaced energy levels each of which according to the Pauli Exclusion Principle can only hold two electrons of opposite spin. At absolute zero all the levels up to a certain energy E_o will contain two electrons. If N(E)dE is defined as the number of energy levels per unit volume having energies between E and E + dE, then E_o is given by

$$2\int_0^{E_o} N(E)dE = n \tag{1}$$

where n is the total number of free electrons per unit volume.

At any temperature above absolute zero, some of the electrons will be excited to energy levels above E_o. The probability that a level of energy E is occupied at a temperature T is given by the Fermi-Dirac distribution function

$$f(E) = \frac{1}{e^{(E-E_1)/kT} + 1} \tag{2}$$

where E_1 is the thermodynamic potential per electron and can be determined by the requirement that:

$$2\int N(E)f(E)dE = n \tag{3}$$

the integral being evaluated for all energies for which N(E) is finite. Although E_1 is slightly temperature dependent it is found to be approximately equal to E_o except at extremely high temperatures. For most metals E_o is of the order of several electron volts and hence

$E_1 >> kT$ for all temperatures up to the melting point of most metals, and the electron gas is said to be degenerate. The degeneracy temperature T_o is defined as $T_o = E_1/k$ and is the temperature above which the electron gas behaves classically.

The total energy per unit volume of the electron gas at any temperature above absolute zero is given by

$$U = 2\int_0^\infty N(E)f(E)EdE \tag{4}$$

Evaluating this integral Sommerfeld found that

$$U = 2\int_0^{E_o} N(E)EdE + 1/3(\pi kT)^2 N(E_o) \tag{5}$$

and hence the specific heat per unit volume at constant volume is

$$C_v = (dU/dT)_v = 2/3\ \pi^2 k^2 T\ N(E_o) \tag{6}$$

In deriving this expression no assumptions have been made as to the form of the density of energy states and this part of the calculation is quite general and forms the basis of all other more refined theories. In order to evaluate the specific heat it is necessary to assume a certain field within the metal and calculate the resulting form of the density of states.

Sommerfeld considered the case of free electrons in a constant negative potential well for which the permitted energies are

$$E = -W + \frac{h^2}{8\pi^2 m}(k_1^2 + k_2^2 + k_3^2) \tag{7}$$

where k_1, k_2, k_3 are the components of the electronic wave number vector which have discrete values.

Now N(E)dE was defined as the number of energy levels per unit volume lying in the range E to E + dE, hence

$$N(E)dE = 1/8\pi^3 \iiint dk_1 dk_2 dk_3 \qquad (8)$$

The factor $8\pi^3$ occurs because when the integral is taken through the fundamental cube $-\pi/a \leqslant k_1, k_2, k_3 \leqslant \pi/a$ the number of energy levels per unit volume must be equal to the number of atoms per unit volume, namely, $1/a^3$. For perfectly free electrons the energy contours are concentric spheres and the volume between those of radii k and k+dk is $4\pi k^2 dk$, so that

$$N(E)dE = (1/2\pi^2)k^2 dk \qquad (9)$$

Also if -W equals zero then equation (7) becomes

$$E = \frac{h^2k^2}{8\pi^2 m} \quad \text{giving} \quad k = \frac{2\pi}{h}(2mE)^{1/2}$$

Eliminating k from equation (9)

$$N(E) = \frac{2\pi(2m)^{3/2} \cdot E^{1/2}}{h^3}$$

Equation (1) can now be evaluated:

$$n = 2\int_0^{E_o} N(E)dE \quad \text{giving} \quad E_o = (3n/\pi)^{2/3} \frac{h^2}{8m}$$

and the density of states at the Fermi level becomes

$$N(E_o) = \frac{2\pi m}{h^2} (3n/\pi)^{1/3} \qquad (10)$$

Thus the specific heat contribution due to the free electron gas within the metal is given by

$$C_v = \frac{4\pi^3 mk^2}{3h^2} (3n/\pi)^{1/3}. T \qquad (11)$$

It must be remembered that this equation only applies at temperatures much lower than the degeneracy temperature, T_o, but this is of the order of 10^4°K for most metals. The observed linear term in the total C_v is generally larger than that predicted when a reasonable choice of the number of free electrons per atom is taken, but the fact that it is linear in temperature shows that some of the electrons do behave as a degenerate Fermi-Dirac gas.

The first improvement in the theory is obviously to replace the constant internal potential with a varying potential which takes into account the periodic nature of the lattice through which the electrons move. The motion of electrons in an idealised three-dimensional periodic potential has been investigated by Bloch (1928). The energy E is found to be no longer a continuous function of the wave number k and there are regions of forbidden energies. These forbidden ranges divide the energy spectrum into bands, when displayed in k-space the allowed 'bands' are known as Brillouin zones. The zone or band theory

of solids is of the greatest importance in understanding the structure and properties of solids. The distinction between metals, insulators and semi-conductors emerges quite readily.

Of direct interest to the problem of electronic specific heats is the way the energy levels within a band are distributed, i.e., the density of states. Since within a band the motion of an electron is very similar to that of a free electron it has been found possible to make use of formula derived on the basis of free electrons with the substitution of a so-called effective electronic mass m^* for the real mass. The problem has been investigated by Wilson (1936) and Mott and Jones (1936) and they find for the lower portion of a band that the energy of moderately bound electrons may be represented by

$$E = \frac{h}{8\pi^2 m^*}(k_1^2 + k_2^2 + k_3^2)$$

and the density of states is given by

$$N(E) = \frac{2\pi(2m^*)^{3/2}}{h^3} \quad E^{1/2}$$

Thus the density of states still depends on E in the same way but is usually increased in value since m^* is usually larger than the free electron mass m.

For the upper portion of a band the same authors find that:

$$E = A - \frac{h}{8\pi^2 m^*}(k_1^2 + k_2^2 + k_3^2)$$

where A is the maximum energy of the band and k_1, k_2 and k_3 are measured from the position of the maximum. Also m^* is the effective mass of the holes at the top of the band. In many cases the calculation is complicated by bands overlapping. The N(E) of the combined band in the region of overlap will then be the sum of two expressions with different m^*'s. Unfortunately no simple expressions are available to describe the variation of N(E) with E in the middle of a band but calculations have been carried out numerically for some specific structures. The surfaces of constant energy in K space have first to be found and then the states between successive shells dE apart are summed. A number of methods have been devised for dealing with the various solid models that have to be adopted, and these have been reviewed by Reitz (1955). For even a simple metal however it must be admitted that the calculations are only qualitatively informative. The failure as in the case of the lattice specific heat is mainly due to limited computational facilities but there is now every reason to believe that this can be overcome.

The theory does however relate the observed electronic specific heat to the structure of the bands. The ratio of the observed to the free electron specific heat gives the ratio m^*/m but its value will only be significant if the Fermi surface lies near the top or bottom of a single band. Values for m^*/m can be compared with results obtained for this ratio from other properties but here again the

specific heat data is not very useful for these measurements give only a mean effective mass of electrons at the Fermi surface. Of much greater value are the directional values for m^* which can be obtained from cyclotron resonance and anomalous skin effect measurements. In fact Pippard (1957) from a study of the anomalous skin effect in copper has not only mapped out the Fermi surface but has been able to calculate a value for the electronic specific heat in good agreement with direct experiment.

So far no mention has been made of any possible mutual interaction of the electrons in a metal yet it would seem that the inclusion of exchange interactions, which are so important in the theories of ferromagnetism, should improve the agreement between theory and experiment. However, Bardeen (1936) and Wohlfarth (1950) found that in actual fact agreement was worse. Wohlfarth found that he was able to restore agreement if he replaced the Coulomb potential by a screened potential for which Landsberg (1948) had set up a precedent in his x-ray calculations. The problem was put on a sound theoretical footing by Bohm and Pines (1951, 1952, 1953) who included the long range Coulomb interactions and the correlated motions of the electrons in their calculation of the motions of the electrons in a metal. They found that the short range interactions are equivalent to those of free particles interacting with a screened potential and that the long range interactions can be neglected.

2. Electronic Band Structure of Copper.

Of the monovalent metals the noble ones have received a great deal of attention because theoretical predictions could be tested experimently with relative ease. With only one free electron per atom the first Brillouin zone is half filled and the Sommerfeld model should be a reasonable approximation. However these metals have ions which occupy a large proportion of the atomic volume and the repulsion between closed shells of electrons must be taken into account in any comprehensive calculation of the relation between the energy and the wave vector. This has been done for copper by Jones (1937) who calculated a value for y of 0.69×10^{-3} joules per mole per degree^2. Much study has been devoted to the electronic band structure of the noble metals and in particular to the position and shape of the Fermi surface. Only the material concerning copper will be dealt with here and the problem of the position and shape of the Fermi surface will first receive attention.

Regarding copper as very nearly a free electron metal with a spherical Fermi surface it is difficult to explain the electrical and thermal conductivities. Jones and Mott (1937) were forced to consider that the Fermi surface must touch the first Brillouin zone despite the fact that the available evidence pointed to the effective number of free electrons being less than one per atom. More recently Klemens (1954) considering the same properties has not only suggested

that the Fermi surface touches the first Brillouin zone but also that the Fermi surface must be considerably distorted. The sign for the thermo-electric is incorrect from the standpoint of the free electron model but Jones (1955) does not believe that it is necessary to assume contact, only that the Fermi surface lies very close to the first Brillouin zone. Chambers (1956) considers that both the magnitude of the Hall effect and the absence of saturation of the transverse magneto-resistance could indicate that the Fermi surface touches the Brillouin zone. Jones (1957) considered the case of the Fermi surface lying very close to the first Brillouin zone and showed that the consequent electron-phonon interaction should give an additional term in the low temperature specific heat linear in temperature. (This paper will be dealt with more fully in Chapter V when the results of specific heat measurements on a series of copper-zinc alloys are considered.)

One of the most reliable pieces of evidence has come from measurements of the anomalous skin effect in copper by Pippard (1957). The surface resistance is related to the geometric shape of the Fermi surface and a surface was determined which had the correct shape to account for the experimental variation of the anomalous skin resistance with crystal orientation. The surface determined in this way did not quite fit into the first Brillouin zone overlapping in the (111) directions where the zone boundary is closest to the origin. It was therefore concluded that contact over small areas around these points

was extremely likely. Apart from the extension to the zone boundaries in the (111) directions the derived Fermi surface is approximately spherical. From electron resonance measurements with copper, Morse, Bohm and Gavenda (1958) have estimated the average electron momentum at the Fermi surface. Their result gives 1.02 for the number of conduction electrons per atom. Cohen (1958) has shown from theoretical considerations that the ratio of the optical and thermal effective masses depends on the shape of the Fermi surface. Using the experimental values for the optical constants and the electronic specific heat he finds that not only is the Fermi surface in copper not spherical but that contact with the first Brillouin zone should be appreciable.

Recently, Shoenberg (1959) has observed the De Haas-Van Alphen effect in copper for the first time. The whisker was orientated with the (111) axis along the field and the period observed was close to the value for a free electron sphere of one electron per atom and not inconsistent with the Fermi surface proposed by Pippard. From the temperature variation of the effect Shoenberg estimates the effective electron mass to be about 1.3 times the free electron mass. Although no effect was observed with whiskers orientated along the (100) and (110) axes it is hoped that with more sensitive apparatus it will be possible to carry out a detailed investigation of the position and shape of the Fermi surface in copper.

Considering all the evidence outlined above which excludes

evidence from specific heat measurements (see Chapters V and VII), the Fermi surface in copper must be assumed to be nearly spherical and contain approximately one free electron per atom. The surface is distorted in the (111) directions and almost certainly makes contact with the first Brillouin zone boundaries in those directions.

Detailed calculations of the electronic band structure of copper have been carried out by Krutter (1935) and Slater (1936), which allowed a curve of density of states against energy to be plotted. The shape of the unfilled portion of the band system can be explored by determining the X-ray absorption limit and the experimental results of Beeman and Friedmann (1939) gave reasonable confirmation of the theoretical curve. The problem of the filled portion of the band system can be divided into two, namely the shape of the completely filled d band and the shape of the partially filled s band. The specific heats of the transition metals provide one method of examining the d band if it is accepted that the general shape of the band should be similar in both cases. Unlike copper, the transition metals have a filled s band but an incomplete d band. The density of states in the d band is very much higher than in the s band so that although the d and s bands overlap, the density of states at the Fermi level is determined mainly by the number of electrons in the d band. Therefore measurements of the electronic specific heats of the transition metals should enable the shape of

the d band to be investigated. Wolcott (1955) using both his own results and those of other investigators compared the shape of the 3d, 4d and 5d bands of the transition elements. Neglecting the abnormally high electronic specific heat of α-manganese all three bands have the same shape which is reasonably close to that derived by Krutter for copper, considering the elements do not have the same crystal structures.

Another method of investigating the shape of a band is to alter the position of the Fermi level in one element by alloying with another element. It is at once obvious that elements of near atomic number and similar atomic radii must be used so that small quantities of the one have a negligible effect on the crystal structure of the other. Copper and Nickel form a suitable solid solution and it would appear that measurements of the electronic specific heat of a series of copper-nickel alloys should give an outline of the d band in nickel and the supposedly similar d band in copper. The underlying assumption in this method is that the addition of atoms of another metal does not alter the band structure of the solvent metal but only alters the position of its Fermi level. This so-called rigid band theory of alloys was questioned by Mott (1936) even at the time that it was formulated by Hume-Rothery and Jones (1936). Measurements of the electronic heat capacities of copper-nickel alloys have been made by Keesom and Kurrelmeyer (1940) and more recently by Guthrie, Friedberg

and Goldman (1959). The fact that the linear relation between copper concentration and low temperature spontaneous magnetisation in copper-nickel alloys could be explained by the simple filling up of the d band had caused these alloys to be cited in favour of the rigid band theory. Despite the added complication of the magnetic effects the electronic specific heats suggested by the experimental measurements do not agree with the density of states curve calculated by Krutter and Slater. In particular, at 60% copper the d band should be full and for higher concentrations of copper the electronic specific heat should be smaller because of the lower density of states in the s band but the experimental results show no such decrease. This, together with the fact that these alloys are strongly paramagnetic suggests that the d band is still not full which in turn implies that the bands themselves must be altering contrary to the basic assumption. However, measurements by Hoare and Yates (1957) on the very similar alloy system of palladium and silver confirms the collective electron treatment. The electronic specific heat of palladium falls off rapidly as silver is added up to 60 atomic % and then remains small for higher concentrations.

It would also seem possible to study the shape of the s band in copper by carrying out measurements of the electronic specific heat of copper-zinc alloys providing it is assumed that each zinc atom contributes one additional valence electron to the s band without altering its shape. Although the structure of the alloys changes

from that of pure copper at approximately 35% zinc, it was decided to carry out measurements on alloys with up to 70% zinc content and the results of these measurements are given in the next chapter.

REFERENCES : Chapter IV.

Bardeen, J., 1936, Phys. Rev., 50, 1098.

Beeman, W.W. and Friedmann, H., 1939, Phys. Rev., 56, 392.

Bloch, F., 1928, Zeits. f. Physik, 52, 555.

Bohm, D. and Pines, D., 1951, Phys. Rev., 82, 625.

1952, Phys. Rev., 85, 338.

1953, Phys. Rev., 92, 609.

Chambers, R.G., 1956, Proc. Roy. Soc. A, 238, 344.

Cohen, M.H., 1958, Phil. Mag. Ser. 8, 3, 762.

Guthrie, G.L., Friedberg, S.A. and Goldman, J.E., 1959, Phys. Rev., 113, 45.

Hoare, F.E. and Yates, B., 1957, Proc. Roy. Soc. A, 240, 42.

Jones, H., 1937, Proc. Phys. Soc., 49, 250.

1955, Proc. Phys. Soc. A, 68, 1191.

1957, Proc. Roy. Soc. A, 240, 321.

Keesom, W.H. and Kurrelmeyer, B., 1940, Physica, 7, 1003.

Klemens, P.G., 1954, Aust. J. Phys., 7, 70.

Krutter, H.M., 1935, Phys. Rev., 48, 664.

Landsberg, P.T., 1948, Proc. Phys. Soc. A, 62, 806.

Morse, R.W., Bohm, H.V. and Gavenda, J.D., 1958, Phys. Rev., 109, 1394.

Mott, N.F., 1936, Proc. Cambridge Phil. Soc., 32, 281.

Mott, N.F., and Jones, H., 1937, Proc. Roy. Soc. A, 162, 49.

Mott, N.F. and Jones, H., 1936, The Theory of the Properties of Metals and Alloys, O. U. P., 81, 171.

Pippard, A.B., 1957, Phil. Trans. A, 250, 325.

Reitz, J.R., 1955, Solid State Physics, 1, 1.

Shoenberg, D., 1959, Nature (London), 183, 171.

Slater, J.C., 1936, Phys. Rev., 49, 537.

Sommerfeld, A., 1928, Zeits. f. Physik, 47, 1.

Wilson, A.H., 1936, The Theory of Metals, C. U. P., 53.

Wohlfarth, E.P., 1950, Phil. Mag., 41, 534.

Wolcott, N.M., 1955, Conference de Physique des Basses Températures, (Paris : Inst. Int. du Froid), 286.

CHAPTER V.

The Heat Capacities of Copper-Zinc Alloys.

I. Introduction.

There are two main types of alloys, those in which the solute atoms occupy interstitial positions and those in which the solute atoms occupy positions which are normally occupied by atoms of the solvent. The former type is known as an interstitial solid solution and an example of this type of alloy is austentite, which is an interstitial alloy of carbon in γ-iron. The latter type is known as a substitutional solid solution and the experimental work described in this chapter relates to one of this type, namely the solution of zinc in copper.

Substitutional solid solutions of two metals can only occur over limited ranges of composition and the structure changes from range to range. If zinc is added to copper, which has a face-centred cubic lattice structure, a solid solution is obtained with zinc atoms replacing some of the copper atoms. With concentrations up to approximately 35% the solid solution has a face-centred cubic structure and this phase is known as the α phase. The β phase is stable only over

a very narrow range of concentration at about 50% zinc and this phase has a body-centred cubic structure. In the vicinity of 60% zinc there is a complicated cubic structure containing 52 atoms per unit cell known as the γ phase and in the vicinity of 80% zinc there is an hexagonal close-packed structure known as the ε phase. These phases are separated from each other by regions where there is a mixture of the two neighbouring phases.

Many alloys show a similar sequence of phases with the same structures but the compositions at which they occur are different from those given above for the brass system. However, Hume-Rothery showed that the electron to atom ratio is approximately the same for a given phase of different alloys. The explanation for this change in structure with increasing electron to atom ratio was found in terms of the band theory of metals by Jones (1934). As the electron to atom ratio is increased the total energy of the system increases due to the kinetic energy of the additional conduction electrons. Jones showed that at certain ratios it would be advantageous for the lattice to change its structure in order to reduce the total energy of the system and these ratios are approximately those found by Hume-Rothery. The theory does not take into account the difference in size of the constituent atoms or the electro-chemical difference between them. Jones assumed that in any particular phase the solute contributes its valence electrons to the collective valence band, thereby altering the

extent to which the band is filled but without altering the shape of the band. Now, if a foreign atom is introduced into a pure metal there will be a break in the periodicity of the field at the point occupied by the foreign atom, and Mott (1936) raised the question of whether it is still possible to speak of zones for a disordered alloy. Jones' explanation of the Hume-Rothery rule was taken as evidence that the band structure is not affected very much by the break in periodicity.

Recently Friedel (1953) has argued that in dilute alloys the density of states at the Fermi level must be the same as in the pure metals since the additional electrons contributed by the solute atoms are localised to screen out the additional nuclear charge of the solute atoms. Since the screening radius is only of the order of $1^{o}A$ the majority of the copper atoms see the same potential as in the pure metal. Friedel (1954) has developed a theory in which the density of states curve for the alloy is to a first order approximation the same shape as in the pure solvent but suffers a shift towards lower energies. The additional levels at the bottom of the band may be subtracted from the band to form the bound states screening the solute atoms. If the position of the Fermi level is altered by an amount ΔE_o then he obtains for the density of states in the alloy the expression

$$N'(E_o + \Delta E_o) = N(E_o + \frac{CZ}{vN(E_o)})$$

where C is the concentration of the solute and Z is the valence of

solute relative to solvent and v the atomic volume.

As this is exactly the same result as that obtained by assuming that the Fermi level alters by an amount corresponding to the change in electron concentration experimental determinations of the electronic specific heat of copper-zinc alloys should still enable the shape of the s band in pure copper to be investigated.

2. Specimens.

The specimens were prepared from high purity copper and zinc by the Metallurgy Division of the Atomic Energy Research Establishment at Harwell, and care was taken to make them as homogeneous as possible. The copper content of the specimens was determined independently by A.E.R.E. and the Chemical Inspectorate at Chatham. The analyses agreed in all cases to within 0.5% and in most cases to within 0.2%. Each specimen weighed approximately 150 grammes.

The specimens were cut into half centimeter cubes and placed in the calorimeter. The calorimeter was then sealed off with about 0.3 mm. of mercury pressure of helium exchange gas at 20°K.

3. Results.

Heat capacity measurements were made on each specimen in the temperature range 1.5° to 4.2°K. At sufficiently low temperatures

the specific heat of a metal is of the form

$$C = \gamma T + A(T/\theta)^3$$

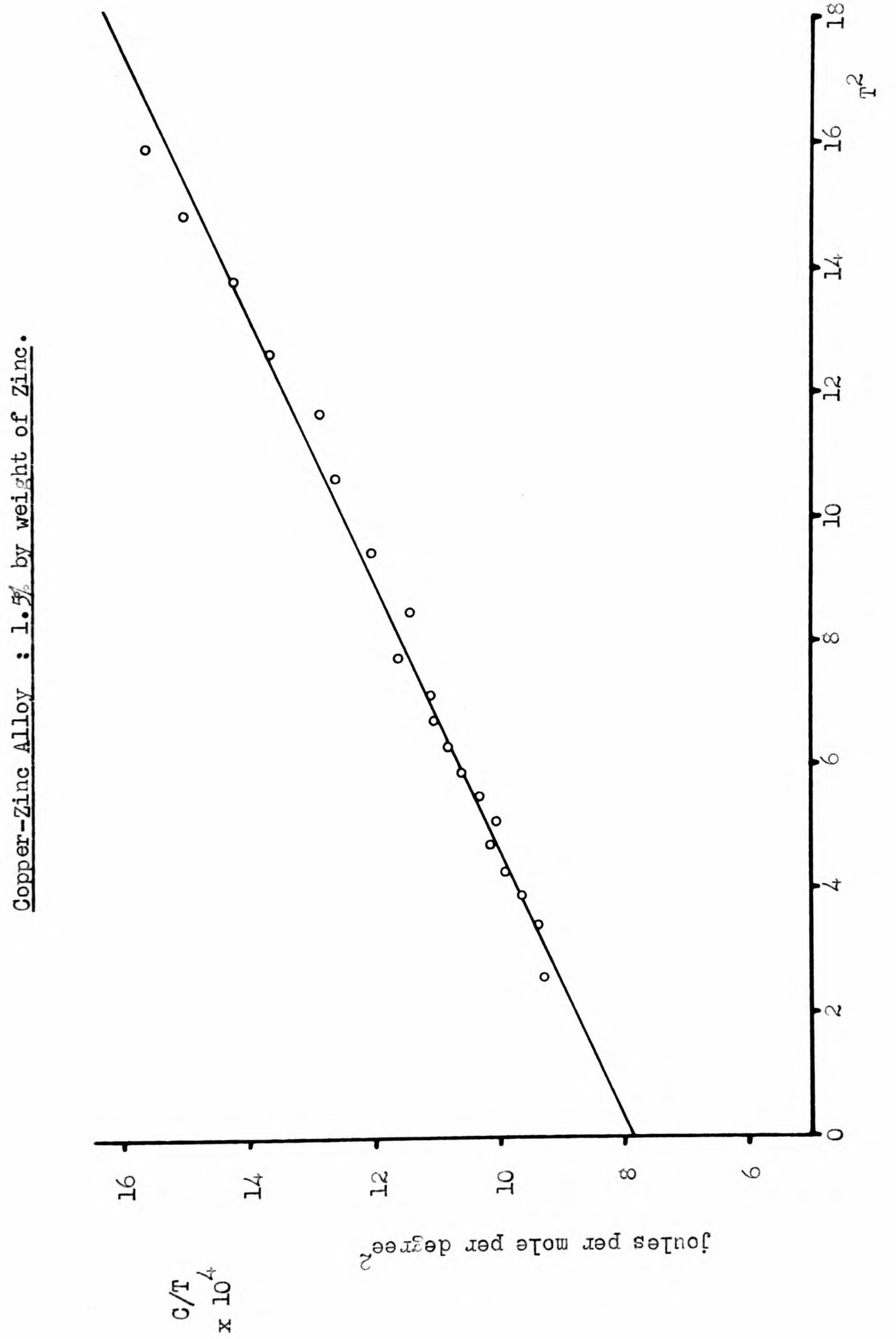
where $A = 12\pi^4 R/5$, R being the gas constant per mole,

and $\gamma = (1/3)\pi^2 k^2 N(E_o)$, (see Chapters I and IV).

Therefore a graph of C/T against T^2 should be a straight line with slope A/θ^3 and intercept on the C/T axis of γ. The specific heat measurements for each specimen when plotted in this form fitted fairly closely a straight line (Figs. 5.1 - 5.16), the maximum deviation of any point from its respective line being 4%. Values of γ and θ for each specimen were obtained from a least-square analysis of the results and these are given in Tables 5.1 - 5.8 together with the experimental points. The variation of γ and θ with zinc concentration is shown in Figs. 5.17 and 5.18 respectively. Also shown in these two figures are the results of Rayne (1957) on a series of α brasses with compositions ranging up to thirty-four weight percent of zinc. These results were published six months after the series of measurements described here were completed.

The experimental conditions for each specimen were very similar to those described in section 1.f of Chapter II for a specimen of 2 1/2 moles of pure copper. Therefore the experimental error associated with each set of measurements is that given in Fig. 2.5 of Chapter II. The probable error derived from the scatter of points

Fig. 5.1


Copper-Zinc Alloy : 1.5% by weight of Zinc.
C/T x 10^4
joules per mole per degree^2
T^2
0
2
4
6
8
10
12
14
16
18
6
8
10
12
14
16

Copper-Zinc Alloy : 2.2% by weight of Zinc.

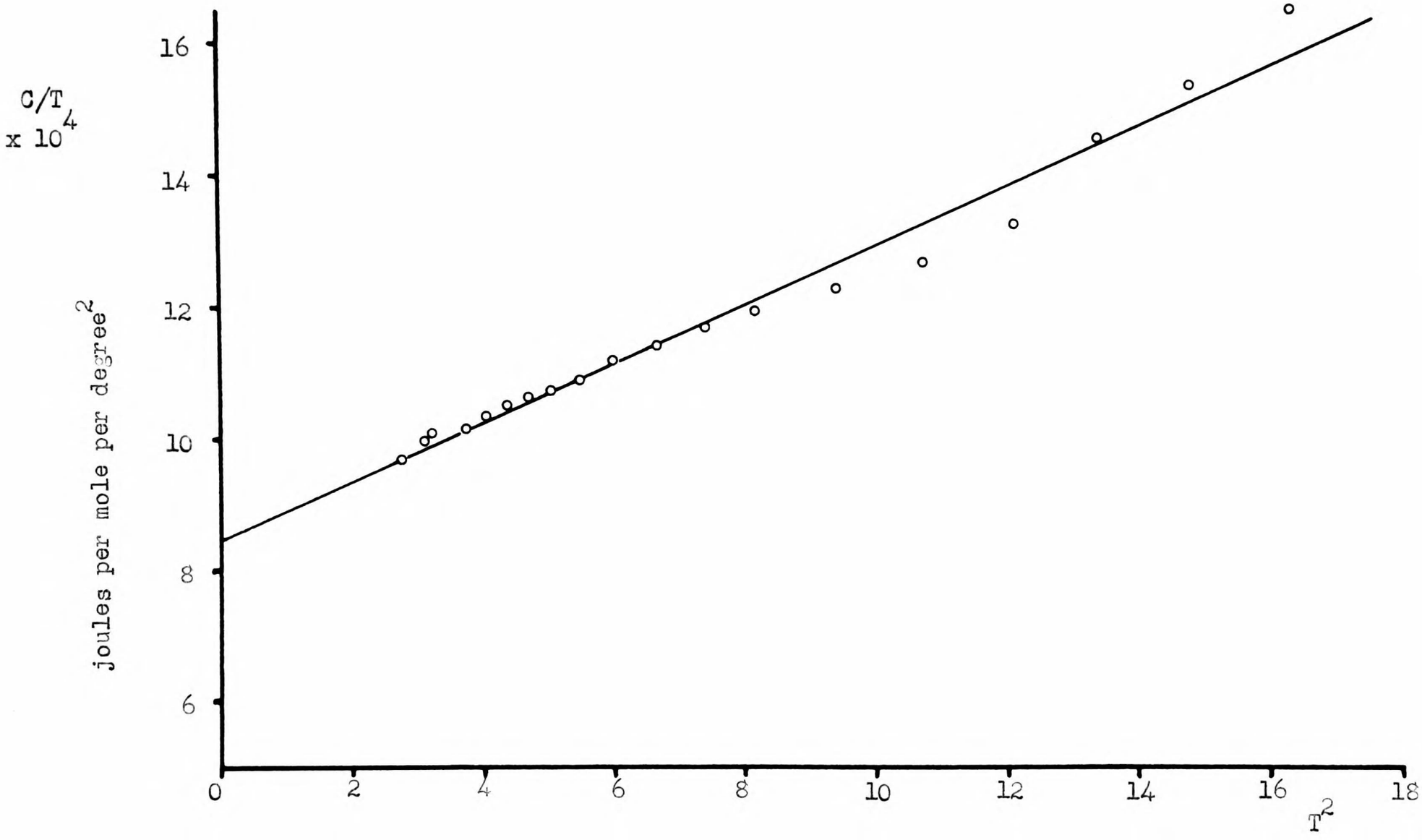


Fig. 5.2

Fig. 5.3

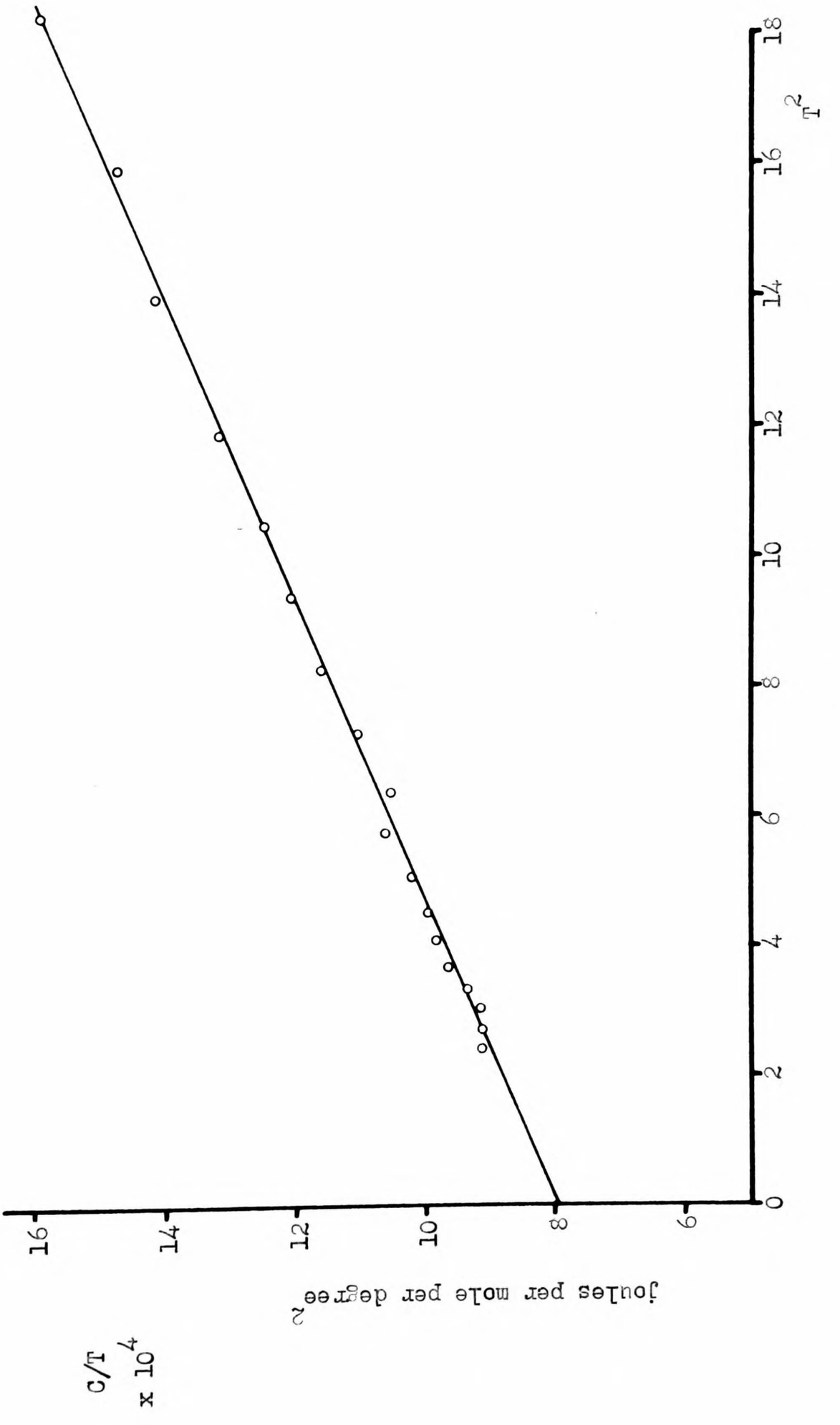
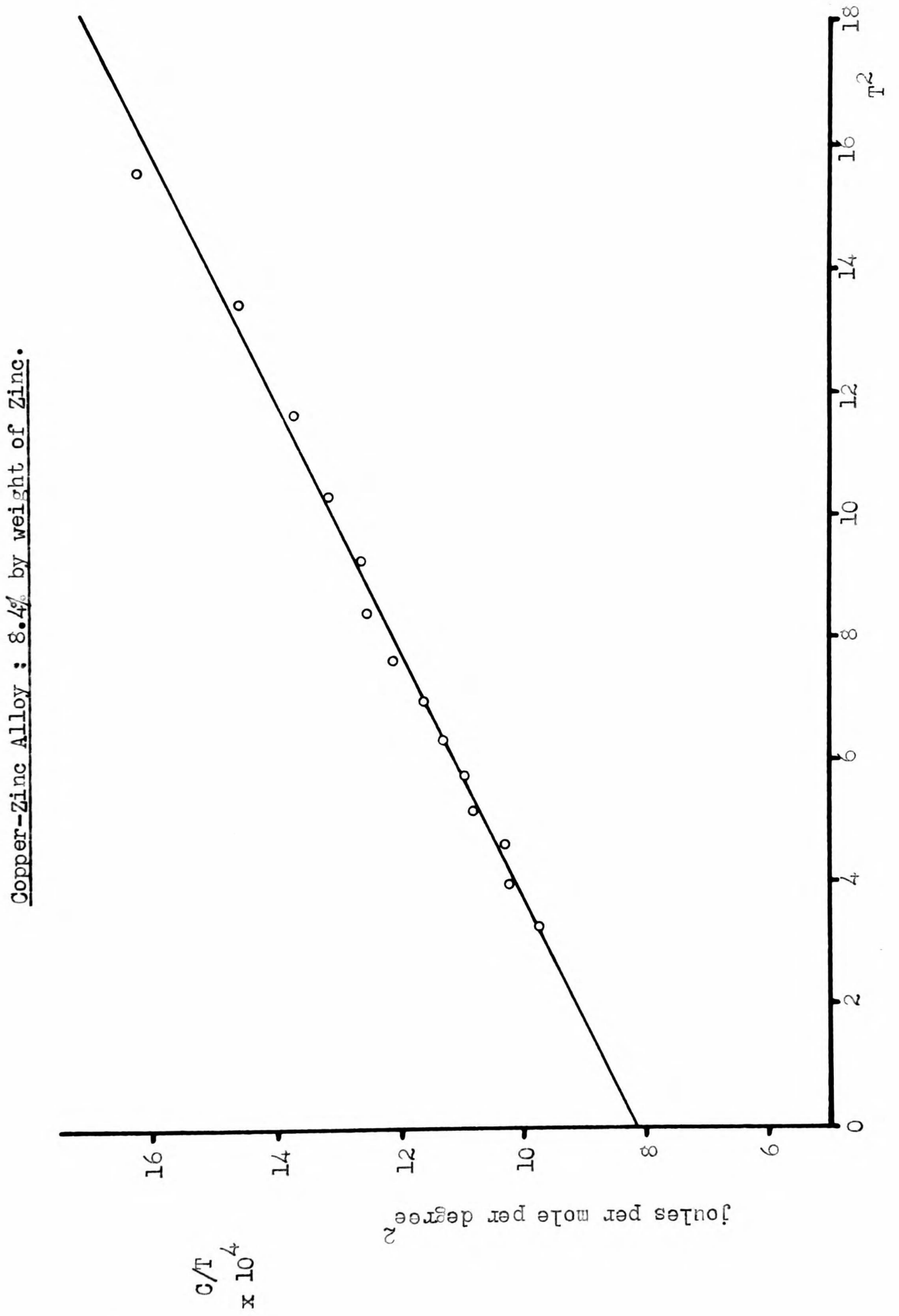

Copper-Zinc Alloy : 5.0% by weight of Zinc.
C/T
x 10^4
joules per mole per degree^2
T^2
0
2
4
6
8
10
12
14
16
18
6
8
10
12
14
16

Fig. 5.4


Copper-Zinc Alloy : 8.4% by weight of Zinc.
C/T x 10^4
joules per mole per degree^2
T^2
0
2
4
6
8
10
12
14
16
18

Copper-Zinc Alloy : 9.3% by weight of Zinc.

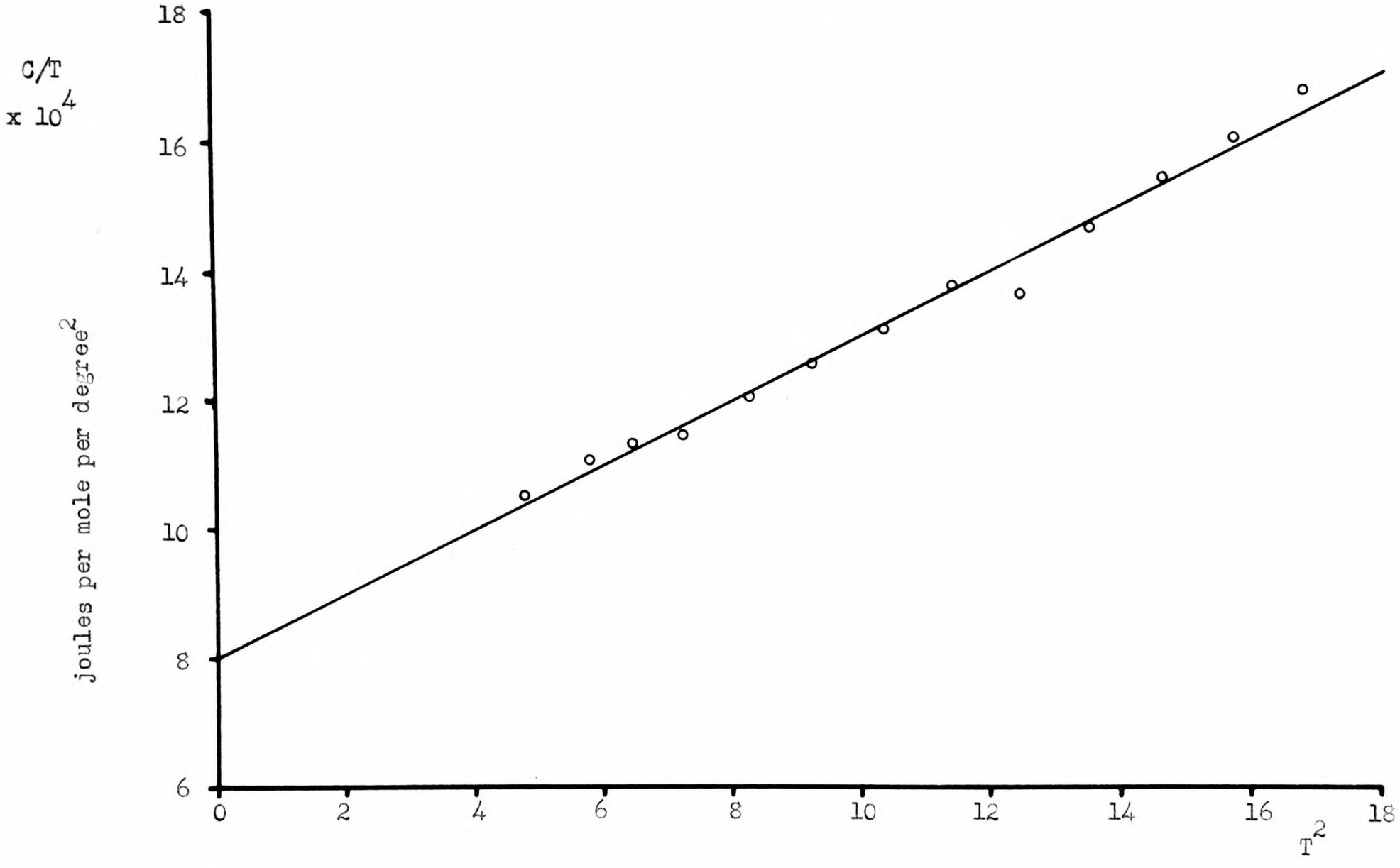
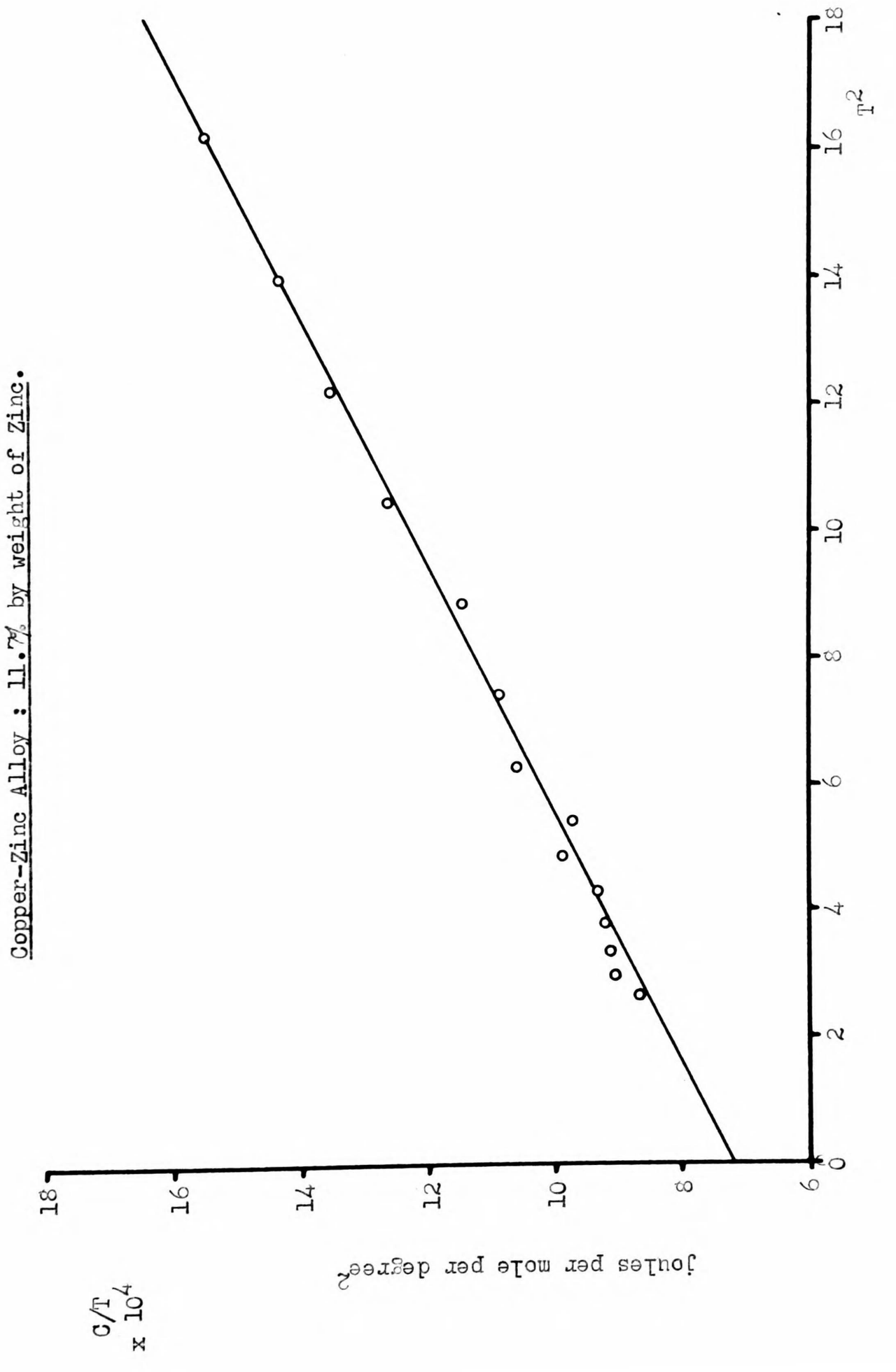


Fig. 5.5

Fig. 5.6


Copper-Zinc Alloy : 11.7% by weight of Zinc.
C/T x 10^4
joules per mole per degree
T^2
0
2
4
6
8
10
12
14
16
18

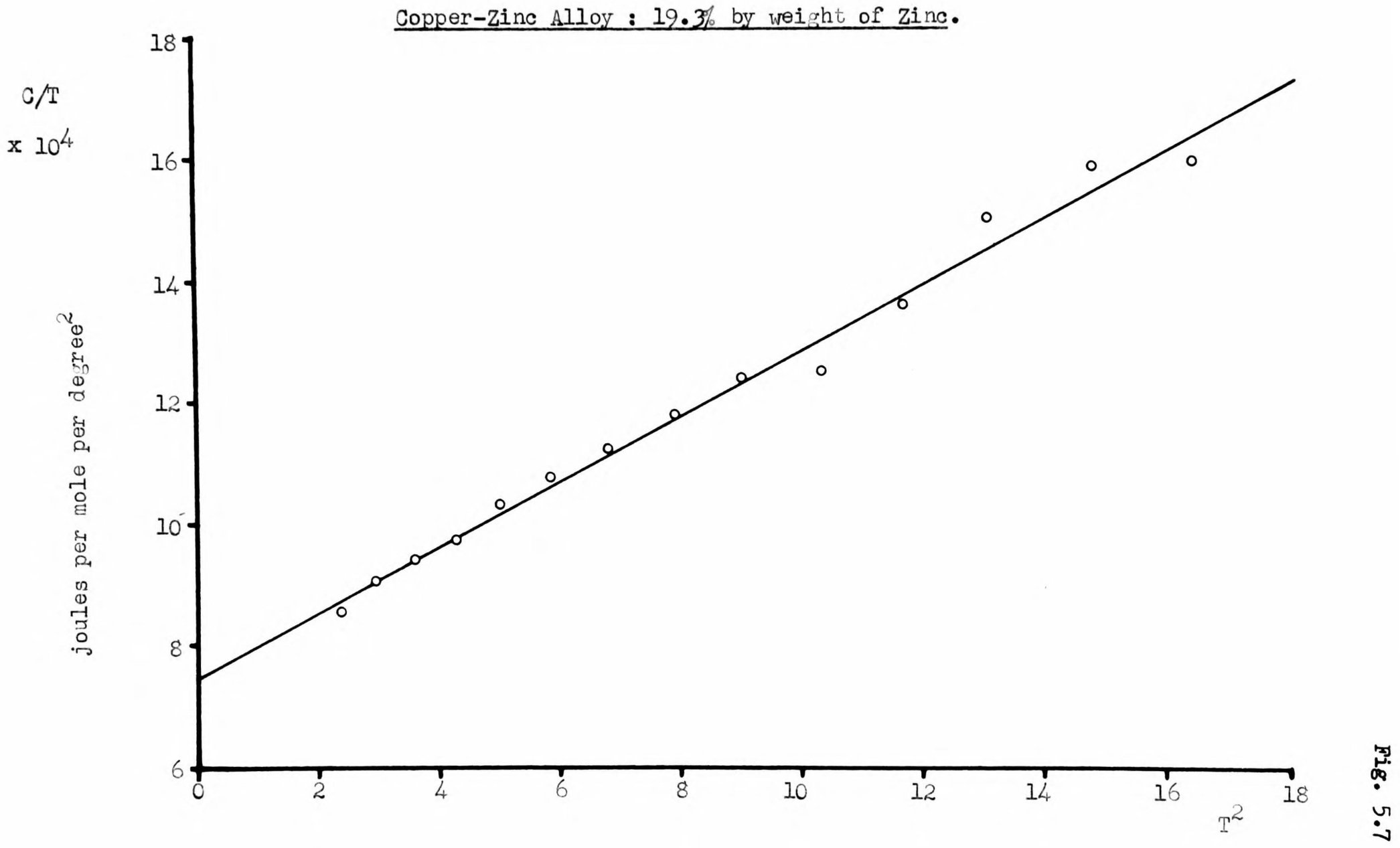

Copper-Zinc Alloy : 19.3% by weight of Zinc.
C/T
x 10^4
joules per mole per degree^2
18
16
14
12
10
8
6
0
2
4
6
8
10
12
14
16
18
T^2

Fig. 5.7

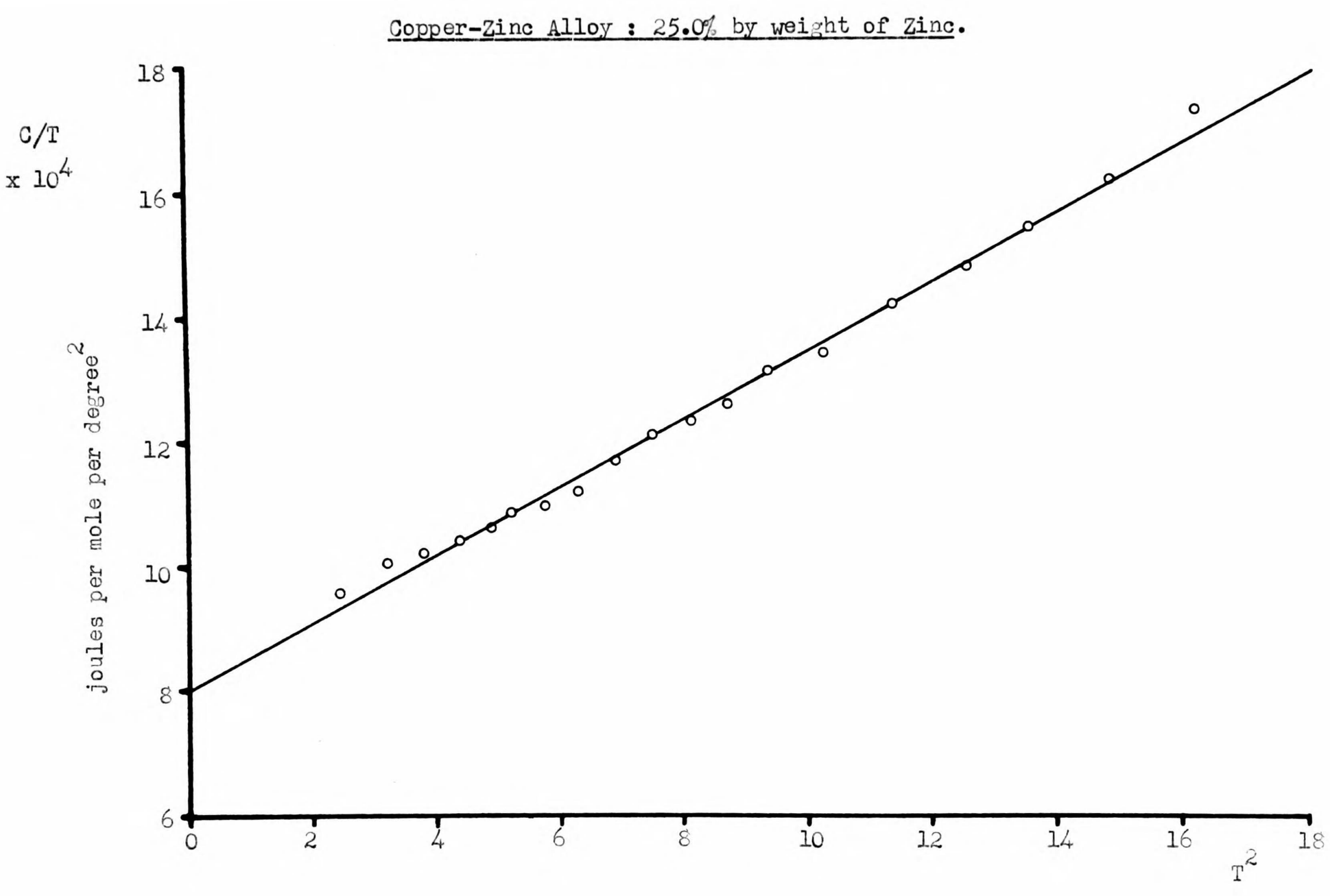

Copper-Zinc Alloy : 25.0% by weight of Zinc.
C/T
x 10^4
joules per mole per degree^2
18
16
14
12
10
8
6
0
2
4
6
8
10
12
14
16
18
T^2

Fig. 5.8

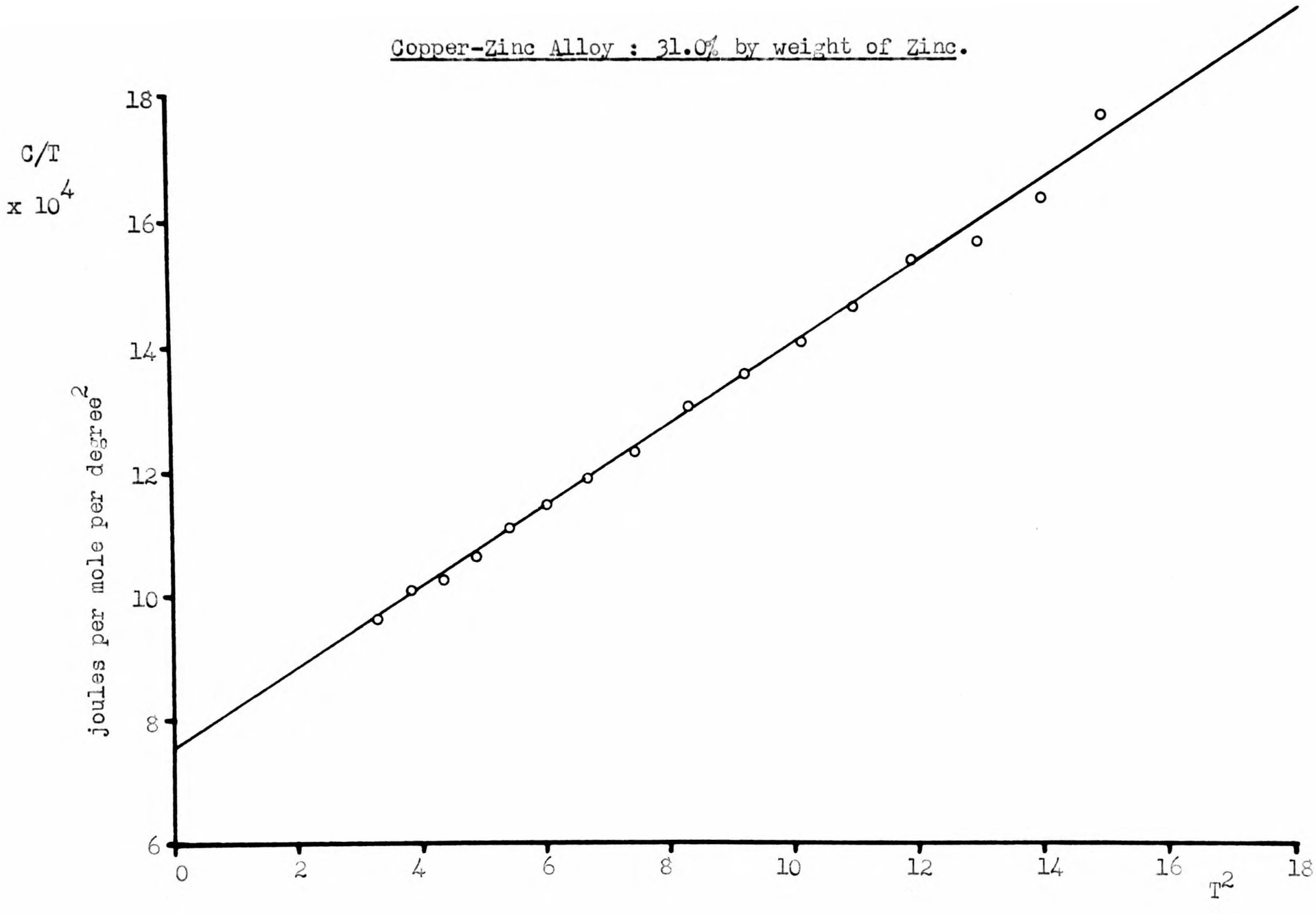

Copper-Zinc Alloy : 31.0% by weight of Zinc.
C/T
x 10^4
joules per mole per degree^2
18
16
14
12
10
8
6
0
2
4
6
8
10
12
14
16
18
T^2

Fig. 5.9

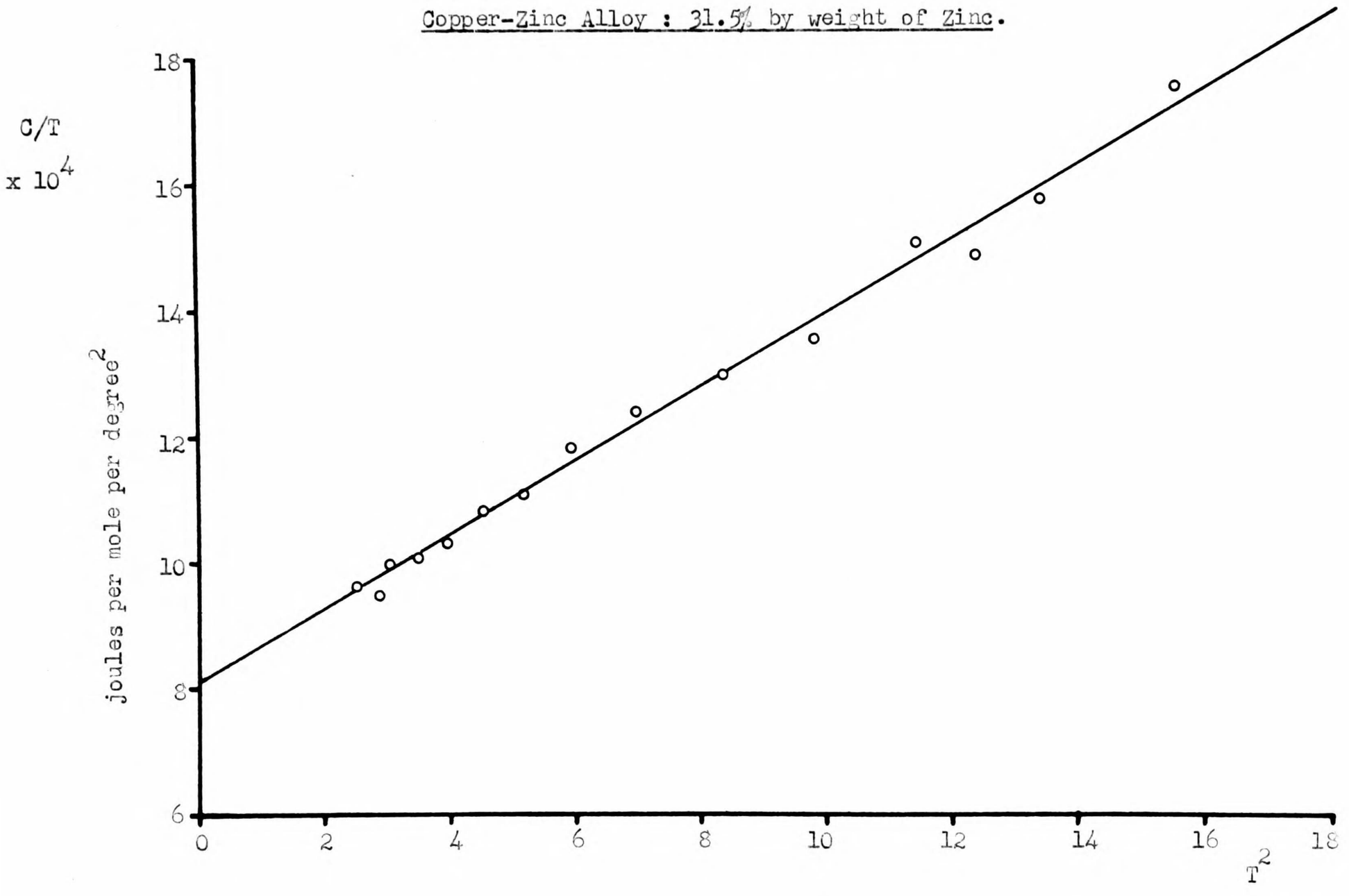

Copper-Zinc Alloy : 31.5% by weight of Zinc.
C/T
x 10^4
joules per mole per degree^2
18
16
14
12
10
8
6
0
2
4
6
8
10
12
14
16
18
T^2

Fig. 5.10

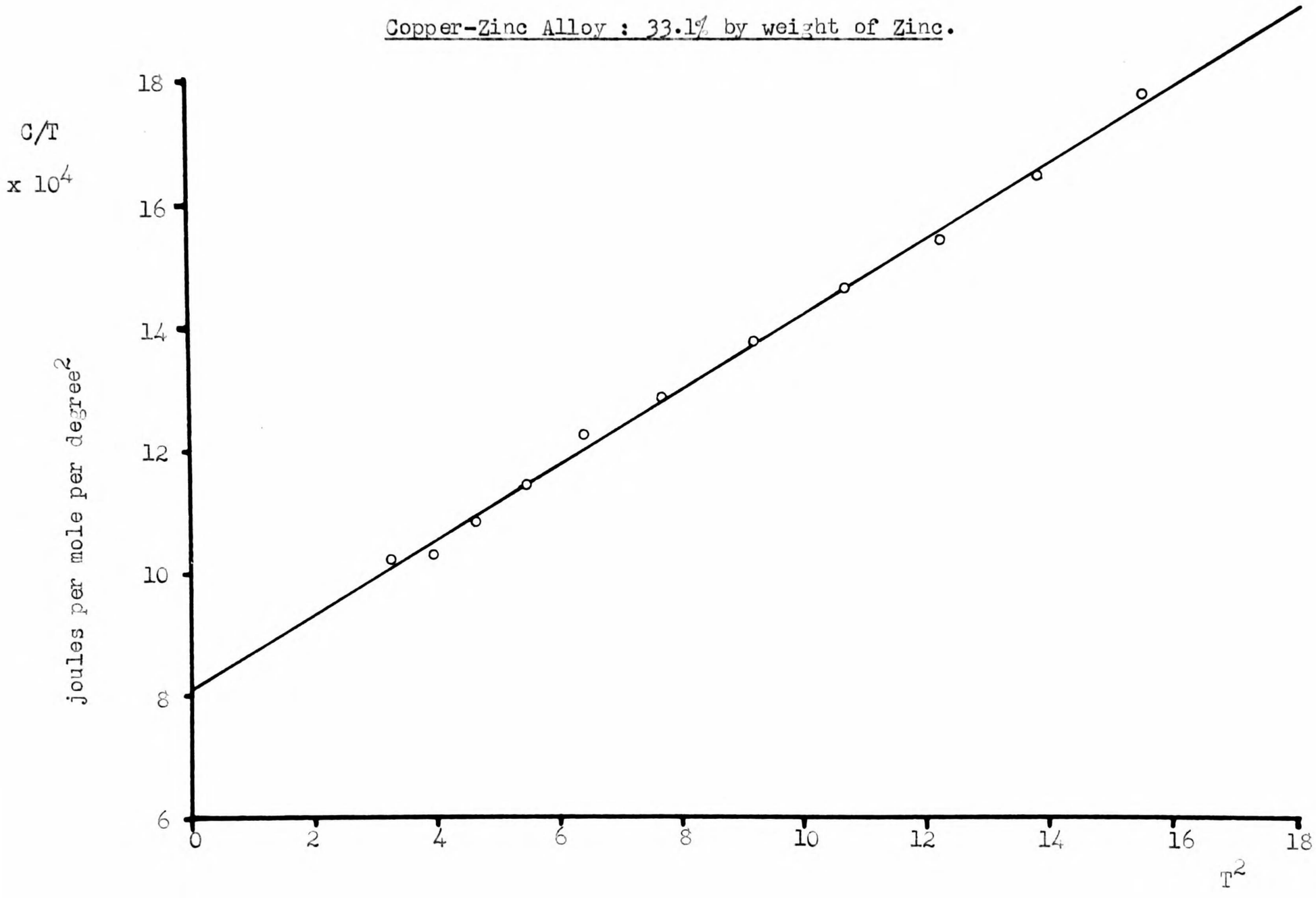

Copper-Zinc Alloy : 33.1% by weight of Zinc.
C/T
x 10^4
joules per mole per degree^2
18
16
14
12
10
8
6
0
2
4
6
8
10
12
14
16
18
T^2

Fig. 5.11

Copper-Zinc Alloy : 48.3% by weight of Zinc.

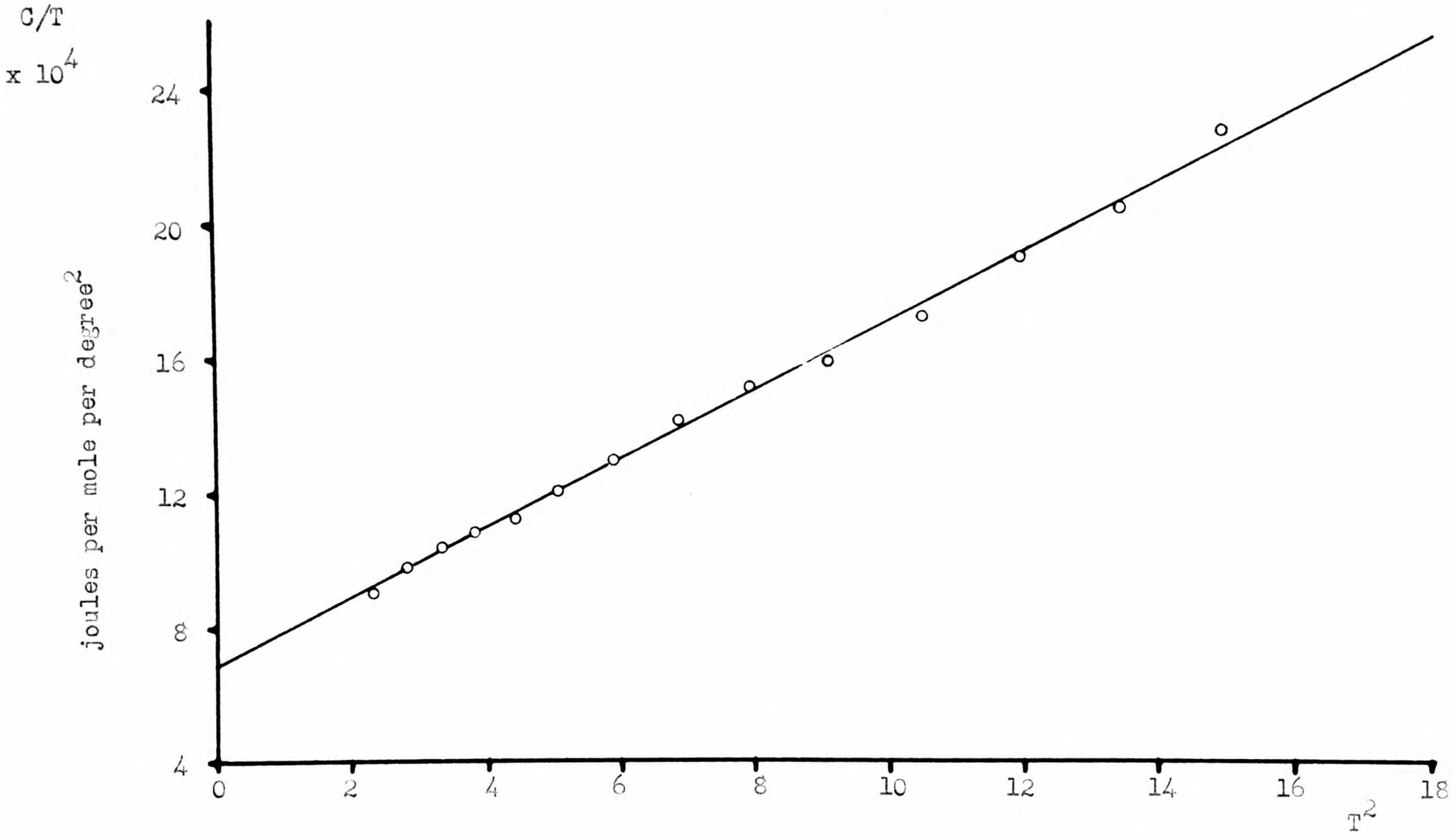


Fig. 5.12

Copper-Zinc Alloy : 49.0% by weight of Zinc.

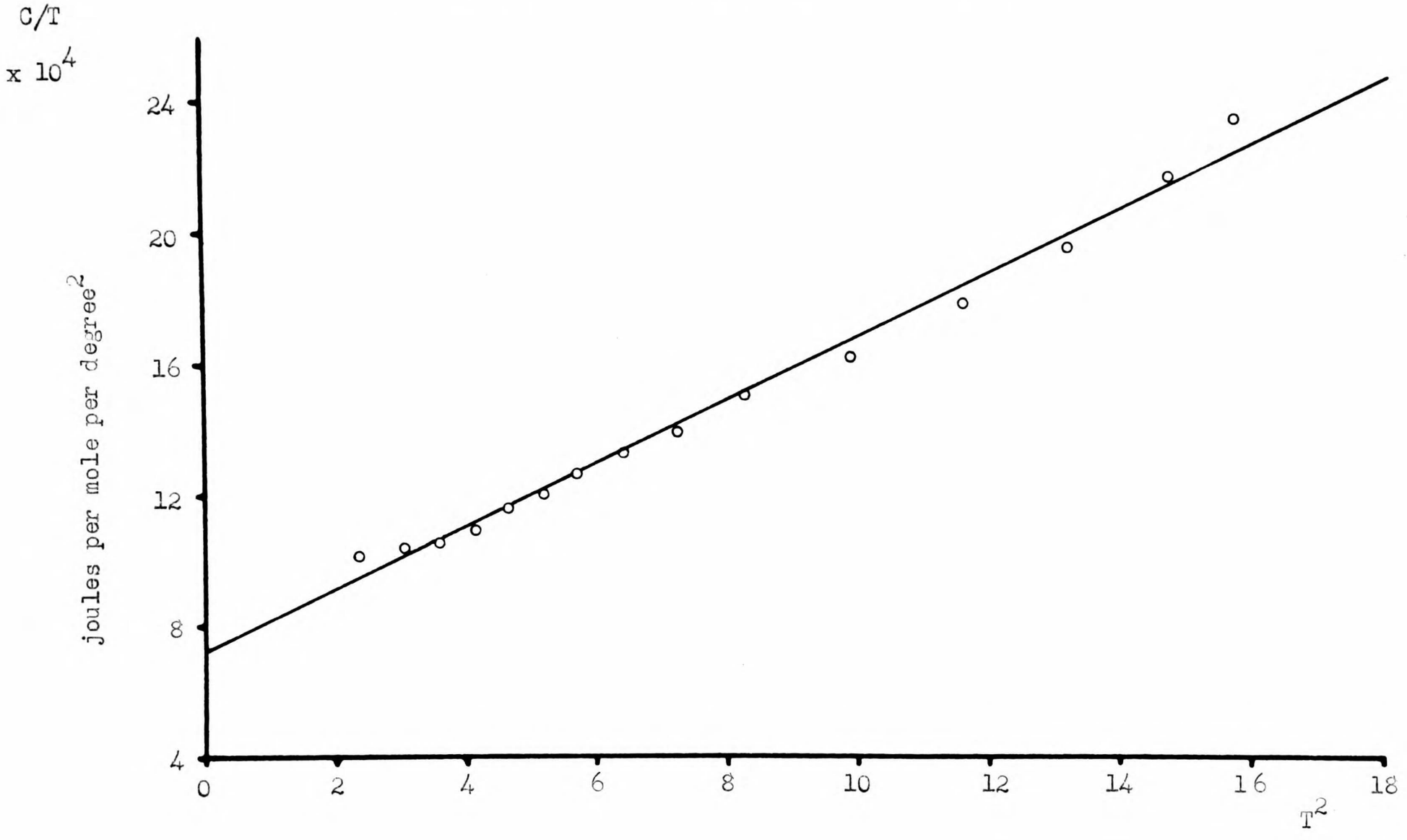


Fig. 5.13

Copper-Zinc Alloy : 60.1% by weight of Zinc.

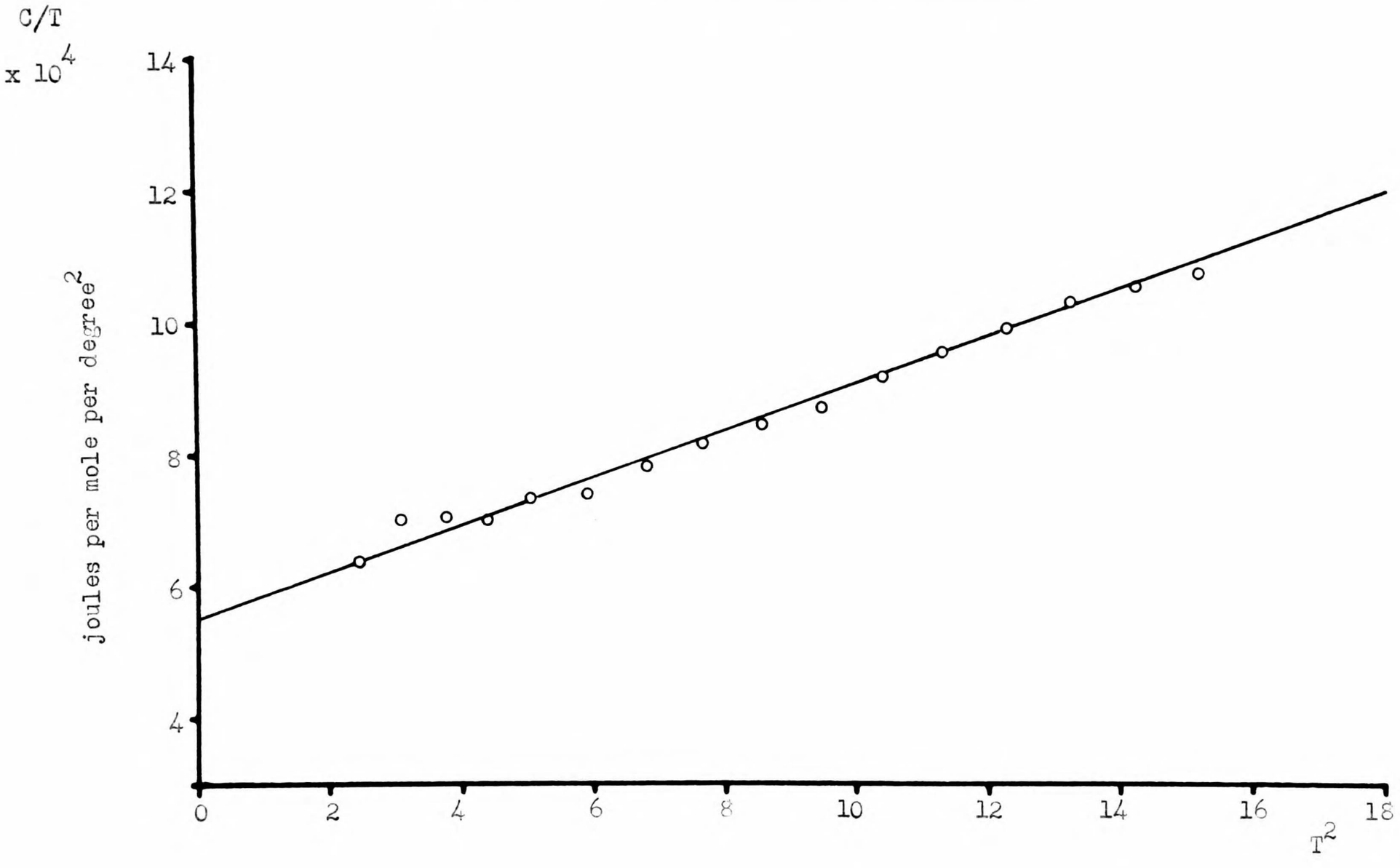


Fig. 5.14

Copper-Zinc Alloy : 62.6% by weight of Zinc.

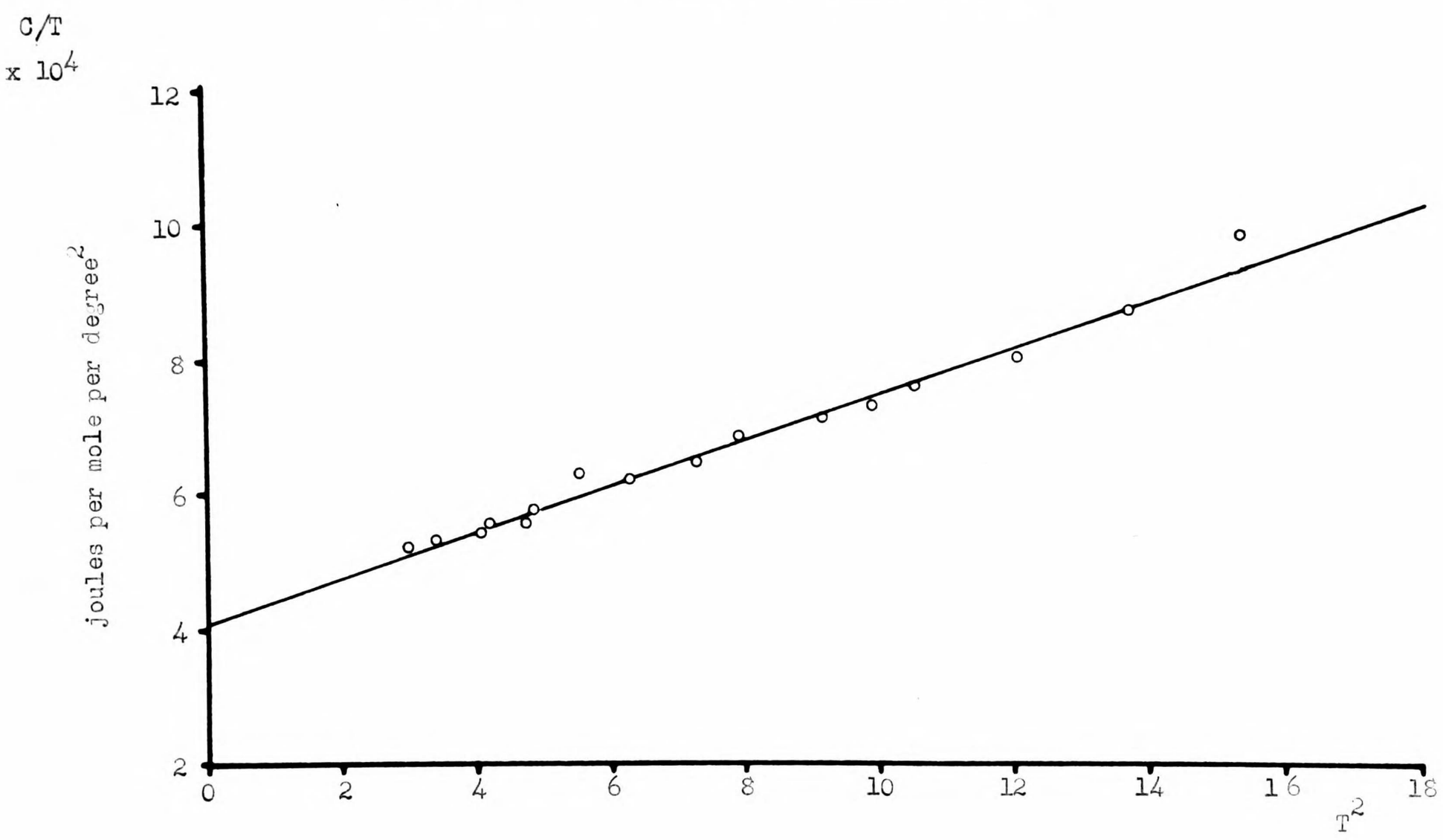


Fig. 5.15

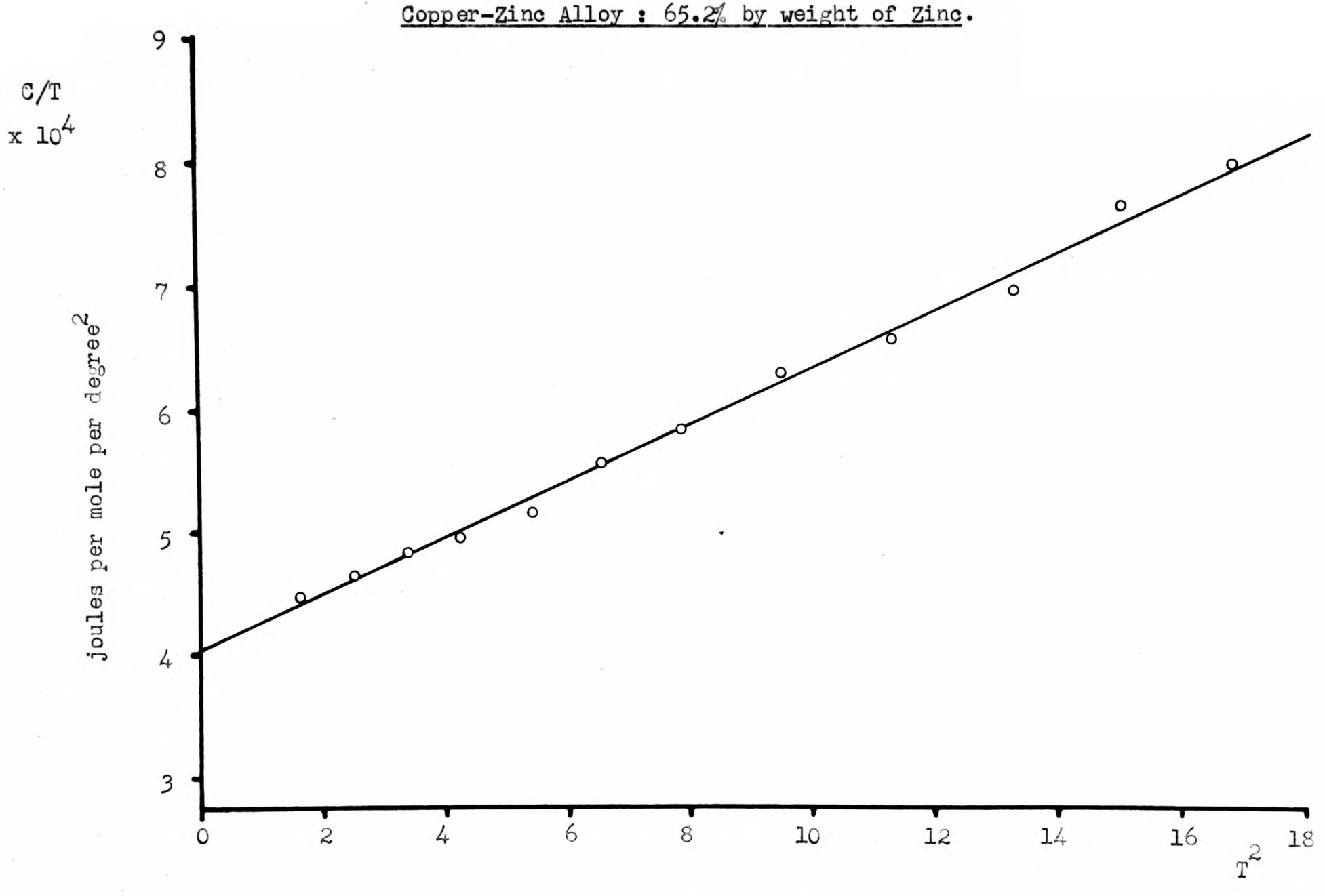

Copper-Zinc Alloy : 65.2% by weight of Zinc.
C/T
x 10^4
joules per mole per degree^2
9
8
7
6
5
4
3
0
2
4
6
8
10
12
14
16
18
T^2

Fig. 5.16

Variation of the Electronic Heat Capacity of Brasses with Zinc Concentration.

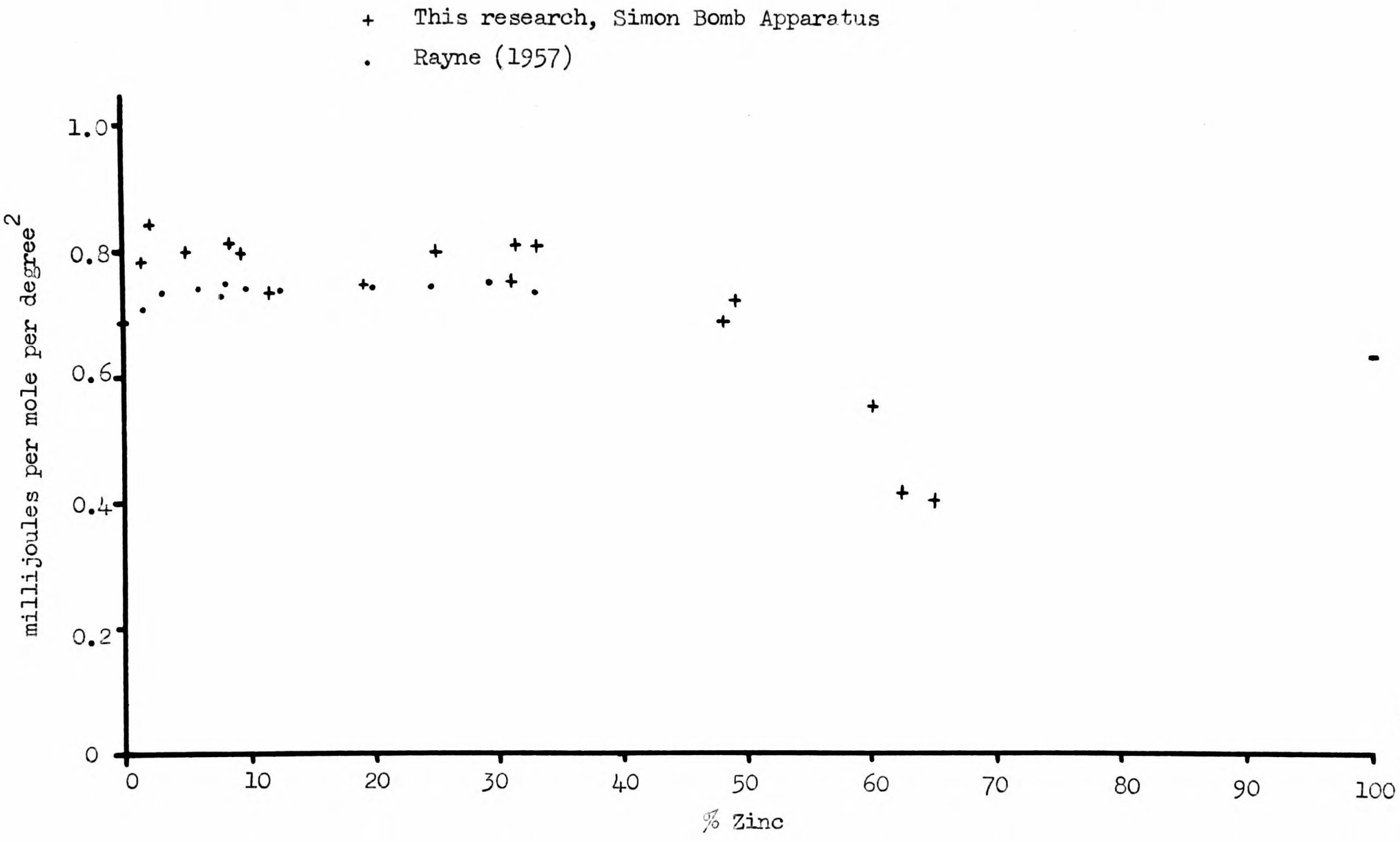


Fig. 5.17

Variation of the Debye θ of Brasses with Zinc Concentration.

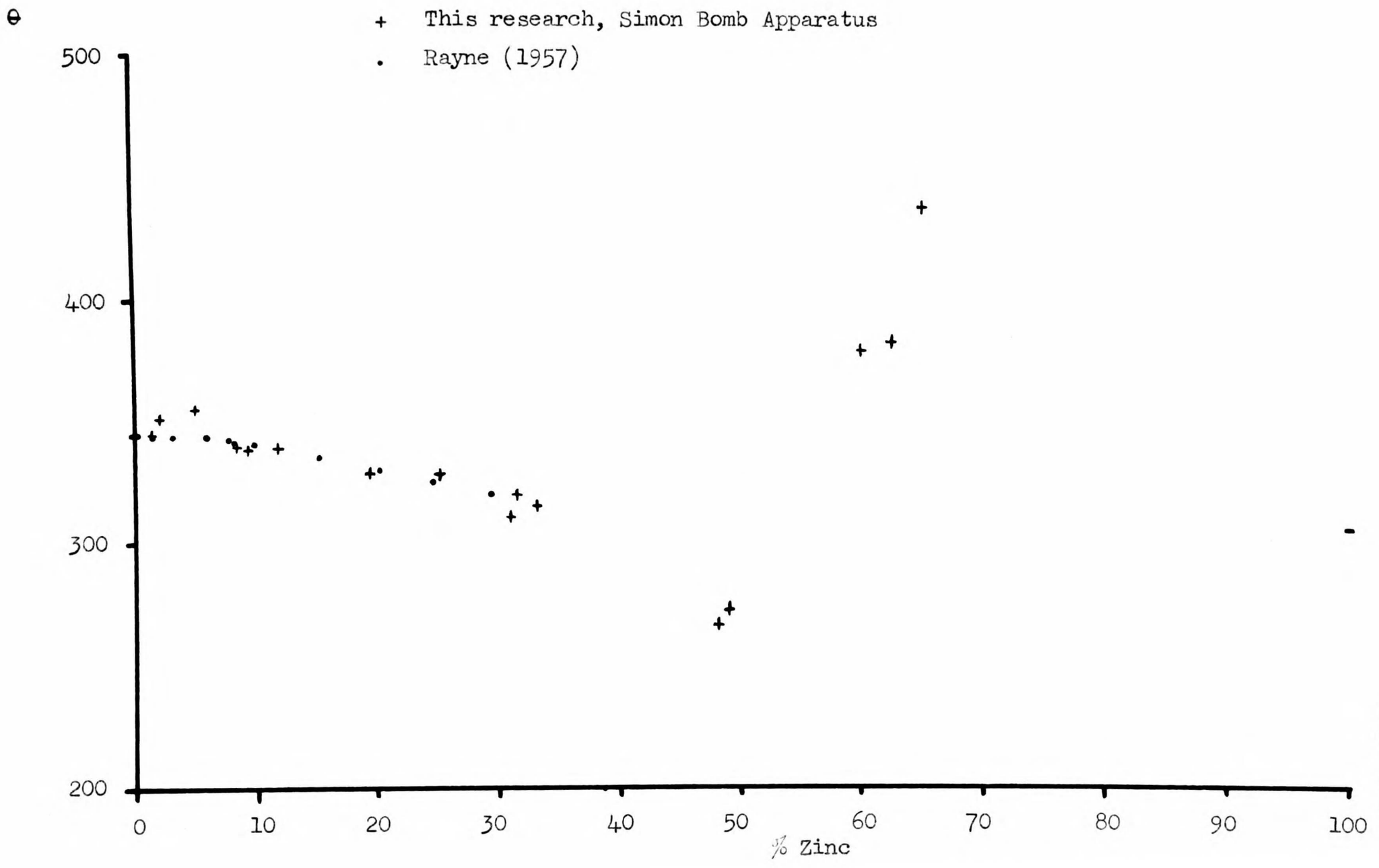


Fig. 5.18

about the line of least squares is 2% for γ and 1% for θ, and agrees with the experimental error of about 2%.

4. Discussion.

The results for the α brasses show an initial increase in θ over the value for pure copper and then monotonic decrease with increasing zinc concentration. The θ values for the two β brasses appear to continue the curve initiated by the α brasses which is not surprising when the similarity between the frequency spectra of the face centred cubic and the body centred cubic lattices is considered. The γ phase specimens with their complicated cubic structure yield a very different θ, about 50% higher than that of the β phase.

The α brasses show a rapid initial rise in γ to a value 12% higher than that for pure copper, the γ then drops slightly and increases again towards the end of the phase. The two specimens of β brass indicated that the β phase which extends over a very limited range of zinc concentration has a γ only slightly greater than that for pure copper but still higher than the free electron value predicted on the basis of the rigid band theory. The γ phase shows a rapidly decreasing value for γ.

The most interesting feature of the results was the rapid initial rise in γ for dilute α brasses with the indication of a slight maximum at about 2 1/2% zinc concentration. The increase in γ is over

ten times greater than that which would be expected from free electron theory but can be explained if it is assumed that the Fermi surface departs appreciably from sphericity. Now the density of states, $N(E_o)$ is given by

$$N(E_o) = 2V\iint \frac{dS}{|\text{grad}_k E|}$$

the integral being taken over the Fermi surface. If the Fermi surface is distorted so that $|\text{grad}_k E|$ is smaller than ~~the~~ for the free electron case then $N(E_o)$ will be larger. Thus the initial rise in γ could be explained by the Fermi surface being pulled out towards the nearest faces of the first Brillouin zone with added zinc concentration up to 2.2%. At about this concentration of zinc the Fermi surface may be supposed to make contact with the Brillouin zone, with further increase of zinc content the density of states will decrease giving the observed decrease in γ. However it was seen in the previous Chapter that the bulk of the evidence pointed to an almost spherical Fermi surface distorted in the (111) directions and almost certainly making contact with the first Brillouin zone even in pure copper.

Jones (1957) offered an explanation of the observed electronic specific heat by considering a form of electron-lattice interaction which is appreciable only when the electronic energy, as a function of momentum, differs considerably from the free electron case. This explanation therefore also requires the Fermi surface to approach

very close to the first Brillouin zone but not to have made contact in either pure copper or in the most dilute α brasses. In such a case the elastic shear constants of the metal are sensitive to changes in the electronic distribution in momentum space resulting from thermal excitation. The magnitude of the resulting additional term in the specific heat is large when the Fermi surface lies close to the zone boundaries, but falls to negligible values when the electron concentration is increased to the point at which the Fermi surface touches these boundaries. This term could therefore explain the observed peak in the γ versus zinc concentration curve and would once again require contact between the Fermi surface and the zone boundaries at a concentration of about 2.2%.

It was at this juncture that Rayne (1957) published the results of his measurements of the heat capacities of α brasses below $4.2^{\circ}K$. Rayne estimated the overall accuracy of his measurements to be a little better than 1%. The Θ values agree with the present research to within the combined limits of accuracy but some of the γ values differed by up to 6%, in particular there was no evidence of a maximum in γ for low zinc concentrations. Thus the difference was completely outside the limits of accuracy and some other source of error than those listed in Chapter II had to be looked for. Repeated measurements of the heat capacity of a pure copper specimen showed that results obtained with the Simon bomb apparatus were not always

reproducible. On plotting the results on a graph of C/T versus T^2, although the scatter of points about the line of least squares was within the limits of accuracy of the apparatus for any particular experiment the lines obtained for different experiments gave values for γ which differed by up to three times the calculated error. The only factor which could not be accurately controlled in the experiments was the amount of helium absorbed by both the specimen and the calorimeter. Roberts (1957) had shown that the use of small amounts of helium as exchange gas could cause interference in the temperature range 1° - 2°K and besides this source the condensation chamber on the lid of the calorimeter may retain large quantities of adsorbed helium on its inner surface.

It was therefore decided to construct a new apparatus in which the use of exchange gas would be avoided and cooling would not be carried out by direct contact with liquid helium. Also, in order to imporve the accuracy of measurements, especially below 3°K, the heat leak to the specimen must be considerably reduced. Since the latter was due mainly to the heat conducted down the German silver tubes leading to the calorimeter and condensation chamber an apparatus employing a mechanical heat switch was an obvious choice. The elimination of a separate calorimeter enclosing the specimen would also ensure that the observed heat capacity was in fact the true heat capacity (Parkinson and Quarrington, 1954).

The heat-switch apparatus will be described in the following chapter and further discussion of the specific heats of the α-brasses will be deferred until Chapter VII.

REFERENCES : Chapter V.

Friedel, J., 1953, J. Phys. Radium, 14, 561.

1954, Advances in Physics, London, 3, 465.

Jones, H., 1934, Helv. Phys. Acta., 7, Suppl. 2, 84.

1957, Proc. Roy. Soc. A, 240, 321.

Mott, N.F., 1936, Proc. Cambridge Phil. Soc., 32, 281.

Parkinson, D.H. and Quarrington, J.E., 1954, Proc. Phys. Soc. A, 57, 569.

Rayne, J.A., 1957, Phys. Rev., 108, 22.

Roberts, L.M., 1957, Proc. Phys. Soc. B, 70, 738.

CHAPTER VI.

The Heat-Switch Apparatus.

1. Introduction.

The new apparatus may be briefly described as a free helium cryostat containing a vacuum calorimeter which embodies a mechanical heat switch.

Measurements of specific heats at liquid helium temperatures have almost entirely been made with the vacuum calorimeter method originated by Nernst and Euken. The vacuum calorimeter is basically a metal can in contact with a liquid helium reservoir and connected to a high vacuum system. The specimen together with its heater and thermometer is suspended by threads within this can but out of thermal contact with it. A mechanical heat switch for use at very low temperatures was first described by Keesom and Kok (1933), and more recently by Webb and Wilks (1955), Ramanathan and Srinivasan (1955) and Rayne (1956).

2. The Apparatus.

The general outline of the apparatus follows closely the, by now, well known system of vacuum jackets which can be clearly seen

in Fig. 6.1. The only slightly unusual feature is the 10 mm. German Silver tube which proceeds direct from room temperature to the innermost part of the cryostat without any diminution in size.

The main helium vessel has a capacity of approximately half a litre and contains the fixed metal siphon, the outer vacuum jacket of the siphon being an integral part of the outer vacuum space. Under normal experimental conditions the volume of liquid contained by this vessel is sufficient to last ten hours.

The experimental cryostat, shown in detail in Fig. 6.2, is suspended on thin-walled German Silver tubes below the main helium vessel. It consists of a small helium vessel, about 20 ccs., which forms the top of the vacuum calorimeter. Liquid helium is condensed in this vessel by applying an over-pressure of between 1/4 and 1/2 an atmosphere in a tube which passes through the main helium vessel. This tube has a coiled copper section in the liquid hydrogen and there is a heat exchanger above the main helium vessel in order to increase the speed and efficiency of the condensation. The heat exchanger consists of 6 mm. outside diameter cupronickel tube, which carries away the helium evaporating from the main helium vessel, with the high pressure line inside it. It takes half an hour to condense 20 ccs. of liquid helium.

The vacuum system consists of a high vacuum pumping system, with its associated measuring gauges, to evacuate the outer, inner and

The Heat-switch Apparatus.

A Fixed Helium Siphon

B Glass Dewar Vessel

C Outer Vacuum Space

D Main Helium Vessel

E Inner Vacuum Space

F Small Helium Vessel

G Experimental Chamber

H Radiation Shield

I Heat Exchanger

J Gas Thermometer

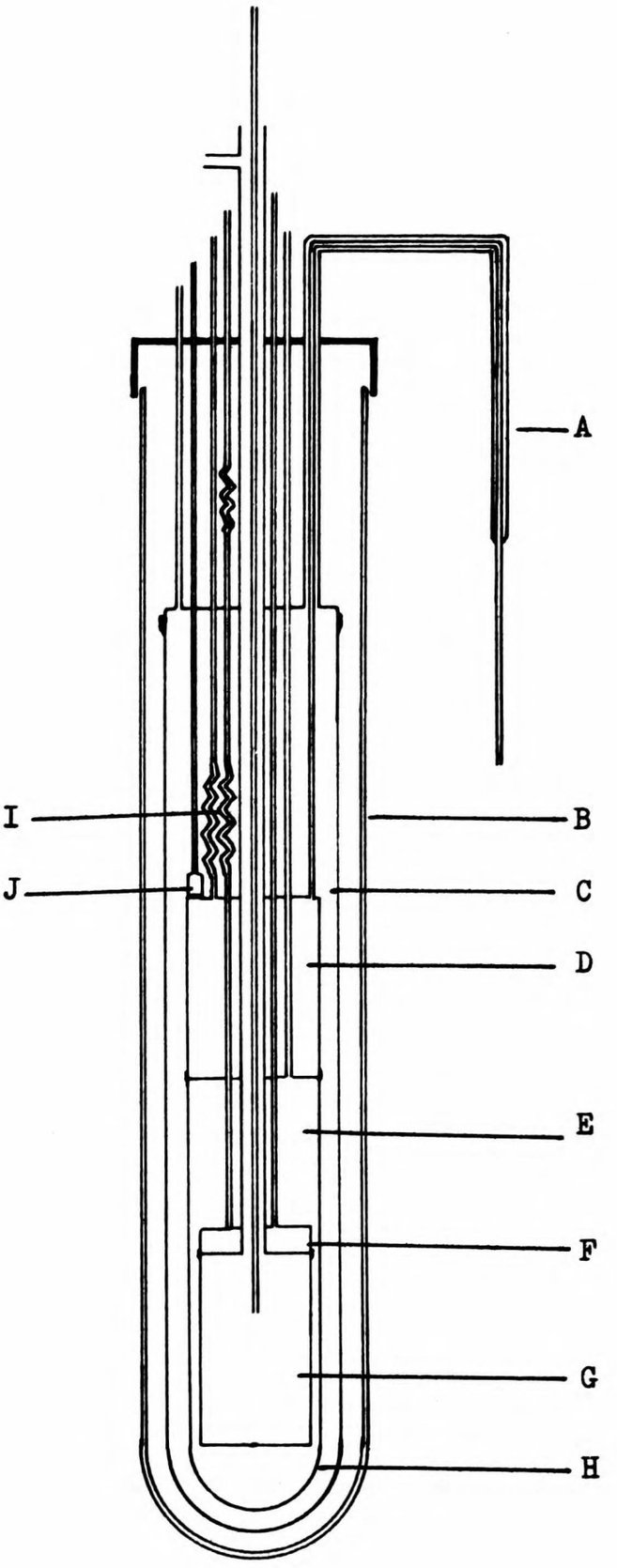
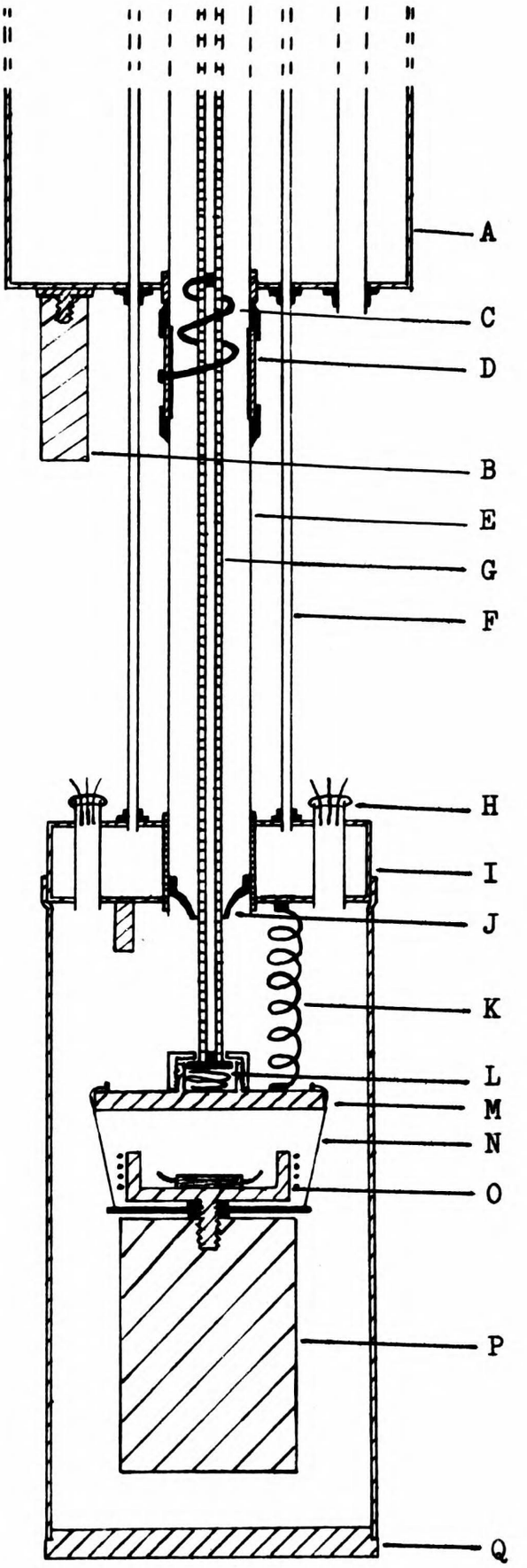


Fig. 6.2

The Vacuum Calorimeter.

A Main Helium Vessel
B Thermal Anchor for Electrical leads
C Copper spiral
D Copper sleeve
E 10 mm German Silver tube
F 3 mm German Silver tube
G 5 mm Stainless steel tube
H Platinum-glass seal
I Small Helium Vessel
J Copper 'cart-wheel'
K Copper braid
L Spring
M Copper disc
N Cotton thread
O Thermometer and Heater Assembly
P Specimen
Q Copper baseplate



vacuum calorimeter spaces and an almost separate system for pumping away the helium vapour from the small helium vessel. The temperature of the small helium vessel and consequently the vacuum calorimeter could be reduced to 1.2°K by this means. The small helium vessel can also be connected to a manometer system for thermometer calibration purposes.

Provision is also made for the admission of either helium or hydrogen gas to any part of the system.

3. The Heat Switch.

(a) Construction.

The top end of the 10 mm. German Silver tube is attached to the open end of a metal bellows. The other end of the bellows is connected externally to a screw mechanism, which allows vertical motion only, and internally to a 'push-rod'. (The material of which the push-rod is made will be discussed in section (b) below).

The 10 mm. tube is broken and replaced by 1/2 inch copper sections at the cap of the outer can, on entering and leaving the main helium vessel and where it passes through the small helium vessel. These copper sections each contain two copper cart wheels, the 'axle' of all of them being the central push-rod. The spokes of the cart wheels are staggered so that there is no direct path for radiation from the bellows to the experimental chamber. The cart wheels act as supports for the push-rod and also help as thermal anchors for

the rod.

A copper disc 4 cm. in diameter is attached to the lower end of the push-rod. The attachment is not rigid, but by means of a spring-loaded bush, so that when pressure is applied through the push-rod the disc will take up the position, not necessarily horizontal, in which the greatest area of contact is made between it and the heater assembly. This also allows the specimen to settle onto the baseplate of the experimental chamber with the greatest possible area in contact. The upper surface of the disc carries three equidistant screws near its rim which are connected by one inch lengths of cotton to a thin plate sandwiched between the heater assembly and the specimen.

(b) Experimental Operation.

An approximate order of magnitude calculation using published data by Berman (1955) indicated that loads of only a few pounds would have to be applied by the push-rod. These small loads could be applied using a push-rod of 1 mm. German Silver tube and thus keeping the heat conducted down the apparatus extremely small.

Initial experiments with the heat switch showed that with the maximum load that could be applied through the German Silver tubing the specimen took 8 hours to cool from 20°K to 4°K. As the main helium only lasts for ten hours a second transfer of helium would be necessary before any experimental readings could be taken and the

total time for each experiment would be over 18 hours. The cooling from 20°K to 4°K could be speeded up by the admission of helium exchange gas, but, the whole idea of the apparatus was to exclude helium from the experimental chamber until the calibration of the thermometer was carried out.

In order to apply greater loads the 1 mm. German Silver tube was replaced by a 5 mm. stainless steel tube. With the maximum load that could now be applied the cooling rate was considerably improved, the specimen now took only half an hour to cool from 20°K to 4°K. However, it was found that the lowest temperature that could be reached was 2.0°K, whereas the baseplate with which the specimen was in contact was at a much lower temperature. The stainless steel tube was conducting a large amount of heat to the plate at its lower end and so a more efficient means of thermally 'anchoring' the plate and the stainless steel tube had to be sought.

First the plate was connected to the small helium vessel by a coil of thick copper braid so that the necessary movements of the plate were unrestricted.

Second, the 10 mm. German Silver tube was cut below the main helium vessel and a copper section inserted which was in direct thermal contact with the vessel. One end of a spiral of thick copper wire was soldered to the central stainless steel tube and the other end passed through a hole in the copper tube which was

then sealed with solder. Thus the vertical movement of the push-rod was unrestricted. Both these modifications can be seen quite clearly in Fig. 6.2.

The specimen could now be cooled to 1.5°K and the drift rate on isolating the specimen was considerably improved as shown in the following table. A figure is given for the Simon Bomb apparatus as well.

APPARATUS	HEAT LEAK at 2°K
Simon Bomb Apparatus	29 ergs/second
Heat Switch Apparatus	6 ergs/second
Heat Switch Apparatus with plate anchored	4 ergs/second
Heat Switch Apparatus with plate anchored and copper spiral	3/2 ergs/second

Of this heat leak about 1/2 erg per second is the energy dissipated by the thermometer current so that the heat leak due to conduction down the threads, stray radiation, vibration, electrical pick-up being dissipated in the heater and thermometer and the dissipation of eddy currents induced in the specimen by local magnetic fields is only one erg per second. However, the threads should

conduct heat away from the specimen if the plate to which their upper ends are attached is efficiently anchored to the small helium vessel by its copper braid. Neglecting vibrational heating, electrical pick-up and eddy currents, the heat leak must be due to radiation reaching the experimental chamber by way of the 10 mm. German silver tubing. Thus the staggered copper cartwheels which were inserted in this tube to prevent radiation reaching the experimental chamber were not sufficient for the task. The lowest cartweel was removed and a conical copper collar was introduced which could be locked onto the central push-rod at any desired height above the copper baseplate. The position of this collar is adjusted for each specimen so that when the specimen is raised above the base of the experimental chamber the cone fits tightly into the 10 mm German silver tube.

Therefore the experimental chamber is effectively sealed off from all external sources of radiation during an experiment. By this means the heat leak at $2^{\circ}K$ is reduced to 1/2 erg per second, the whole of which can be accounted for by the energy dissipated by the thermometer. With a specimen of reasonably large thermal capacity the temperature drift rate is at all times less than 1% of the heating rate compared with the figure of 10% for the lowest temperatures in the Simon bomb apparatus.

4. The Heater and Thermometer Assembly.

The heater is wound on the outside of the cylindrical portion of the assembly (see Fig. 6.2). 45 S.W.G. minalpha wire is used as its resistance varies very little in the range $4^{o}K$ to $1.5^{o}K$. The total resistance of the heater is about 500 ohms.

Since no better thermometer was available a carbon resistance thermometer was again used. Several radio resistors were prepared and a 47 ohm L.A.B. resistor selected which showed the most useful variation of resistance with temperature. Instead of winding a spiral of enamelled copper wire around it, the resistor was turned down slightly on a lathe and then fixed into a thin copper sleeve with araldite. The copper sleeve had a flat face filed on it which was tinned and then soldered onto the inside of the cylindrical portion of the assembly. The leads from the thermometer were taken out through two small holes drilled in the base of the cylinder to prevent them from being damaged when pressure was applied by the baseplate on the centre push-rod to the top surface of the heater assembly.

The thermometer was calibrated at the end of each experiment and Figs. 6.3 and 6.4 show a typical calibration curve and its derived sensitivity curve respectively.

From the base of the cylindrical portion of the assembly protrudes a 2 B.A. thread for the attachment of specimens.

Typical Thermometer Calibration.

47 ohm L.A.B. Resistor.

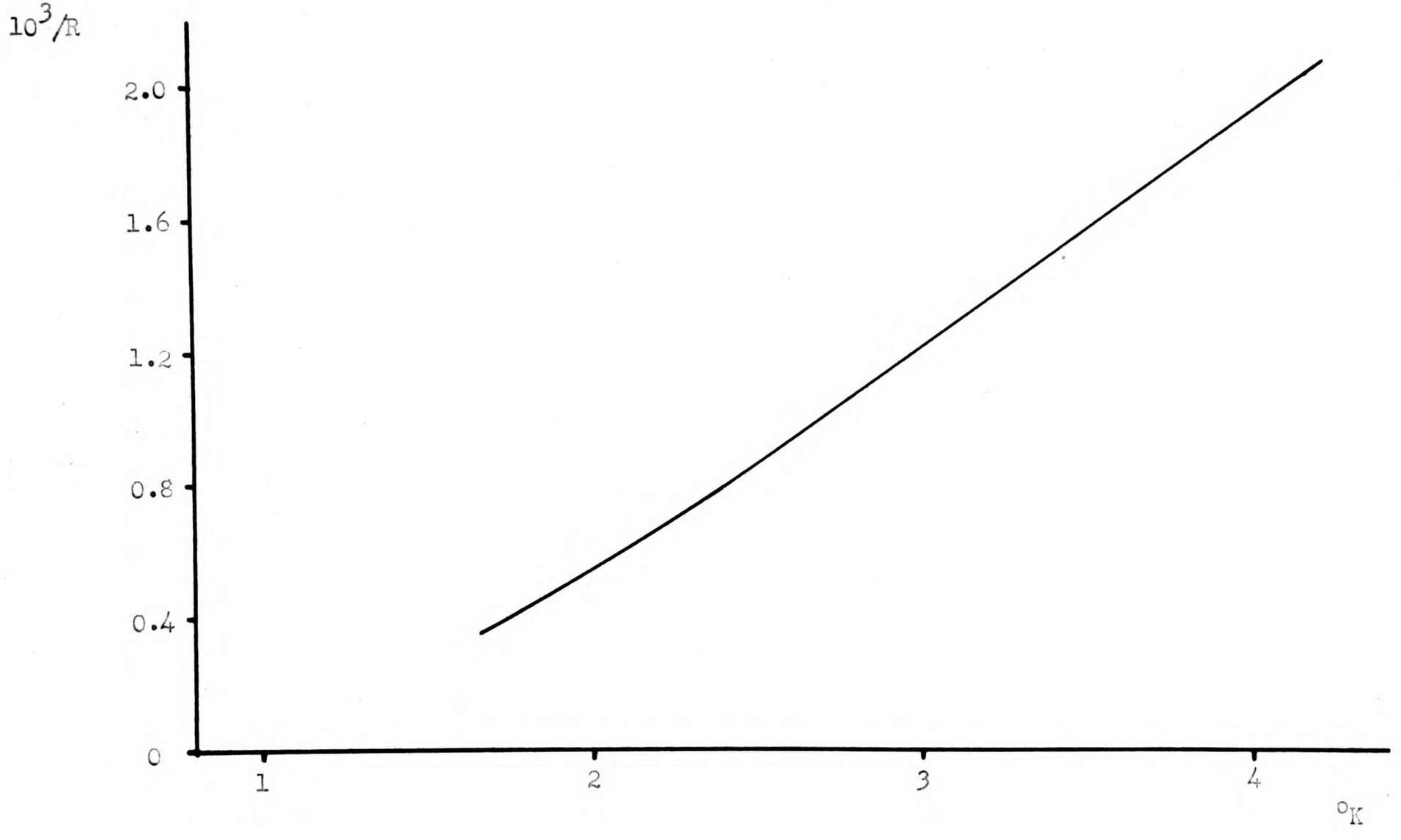
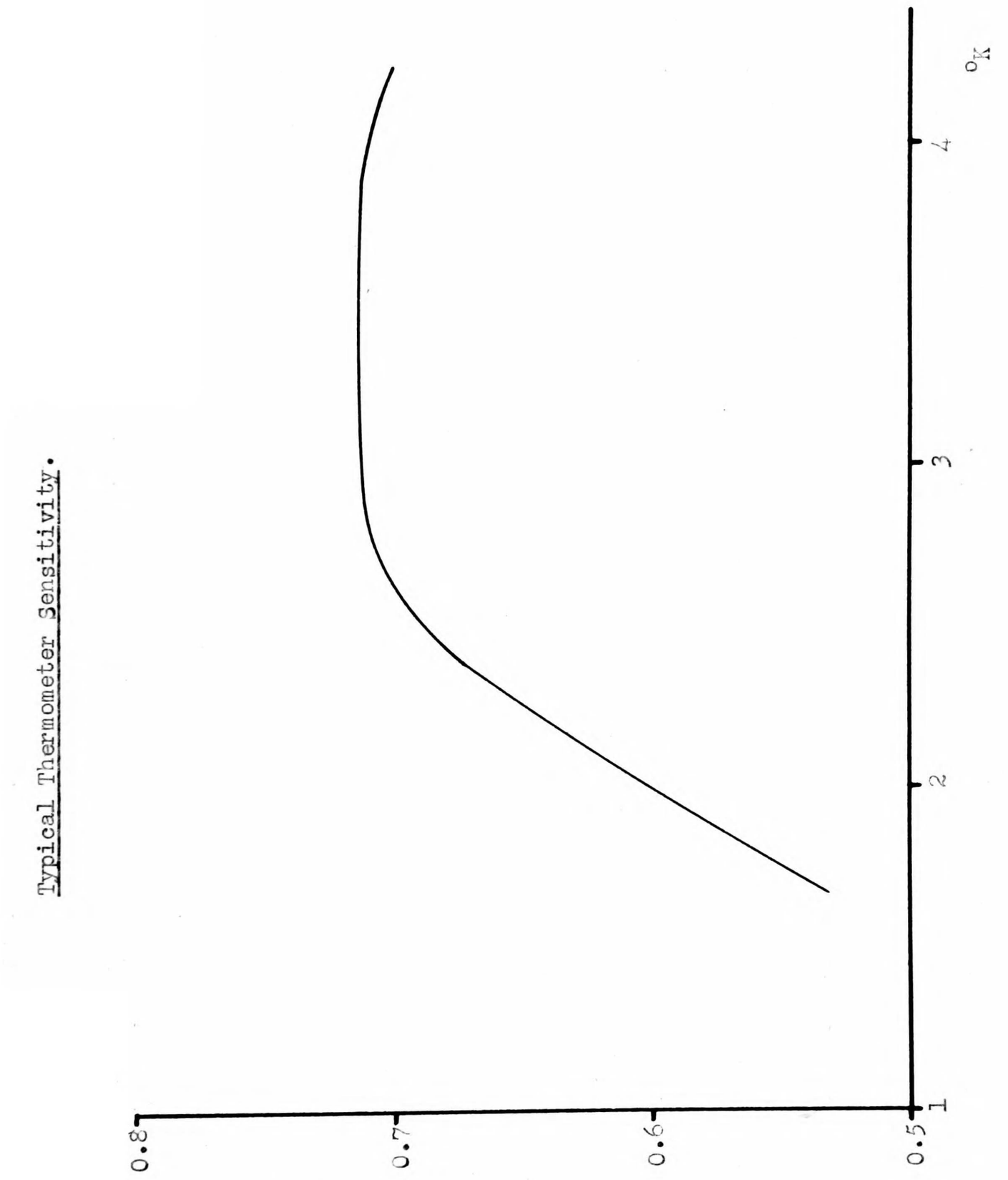


Fig. 6.3

Fig. 6.4


Typical Thermometer Sensitivity.
dρ/dT
(ρ = 10³/R)
0.8
0.7
0.6
0.5
1
2
3
4
°K

5. Electrical Circuits.

(a) General Wiring.

The pumping line for the inner vacuum space contained ten lengths of 34 S.W.G. enamelled and cotton covered constantan wire. The junctions at room temperature were made in an oil bath and the wires were thermally anchored at the base of the main helium vessel. Using the maximum value for the thermal conductivity of constantan between room temperature and $4^{o}K$ the boil-off rate of helium due to conduction down the leads would be 3 ccs. an hour.

The electrical leads were introduced into the experimental chamber by means of two sets of platinum-glass seals. The final leads to the heater and thermometer assembly were of 42 S.W.G. enamelled and cotton covered constantan wire and were thermally anchored to the small helium vessel.

(b) Thermometer and Heater.

The resistance of the thermometer was measured with a three lead system using a Wheatstone bridge in conjunction with a galvanometer amplifier. The resistance could be determined to within 1 part in 10,000.

The current passing through the heater was determined using a Tinsley potentiometer and a standard 100 ohm resistance. The resistance of the heater as a function of temperature was measured

with a Wheatstone bridge using a three lead system and to this was added the resistance of one lead which approximately corrects for the heat generated in the two heater leads. In order to determine the heat supplied the micro-switch for the current use was mechanically coupled to a stop-watch which could be read to 1/10 second.

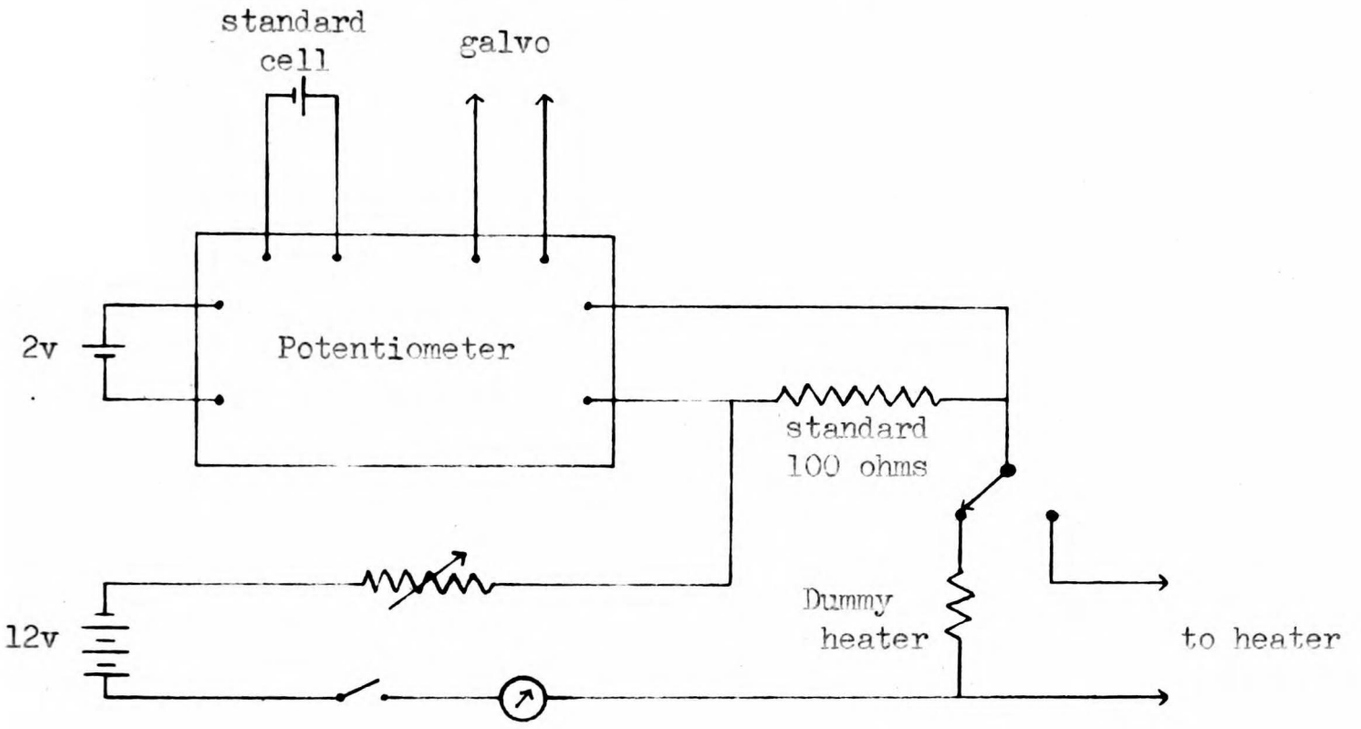
To avoid any errors due to the build up of current when the heater was switched on it was arranged that the accumulators should supply current continuously. The micro-switch did not switch the current on and off but merely switched the current from a dummy heater to the actual heater. The resistance of the dummy heater was made approximately equal to the resistance of the real heater at $4^{\circ}K$. This also allowed the potentiometer to be roughly balanced before a heating period commenced.

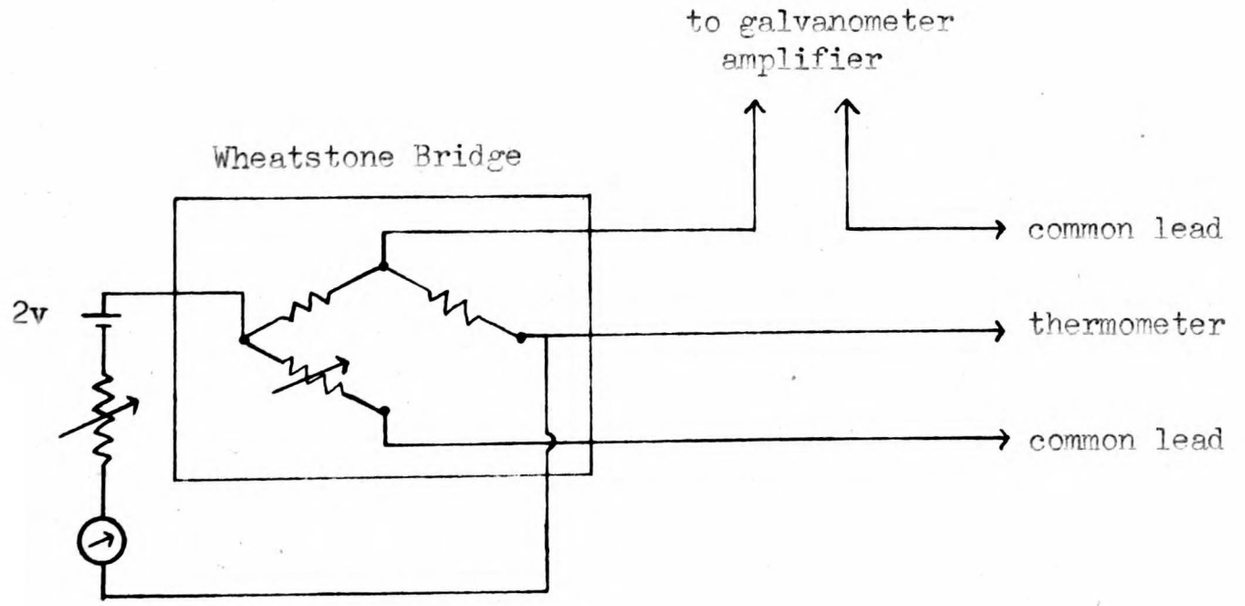
The thermometer and heater measuring circuits are shown in Fig. 6.5.

6. Experimental Procedure.

At first helium exchange gas was used in the outer and inner vacuum spaces to bring the temperature of the main helium vessel and the experimental chamber to that of the liquid hydrogen bath. The experimental chamber was continuously evacuated and the temperature of the specimen was lowered by means of the mechanical heat switch. The exchange gas was then removed from the outer and

Electrical Measuring Circuits.





inner vacuum spaces by pumping for about an hour. Liquid helium was then drawn over from a liquid helium transfer vessel into the main helium vessel by means of the fixed siphon. A quantity of helium was then condensed in the small helium vessel and its temperature was reduced to about 1.2°K by pumping away the helium vapour above the liquid.

When the temperature of the specimen had reached a steady value (about 1.5°K), the disc was raised so that the specimen was hanging freely. This position was determined by the conical radiation shield locking into the central German silver tube. The isolated specimen was then heated for timed intervals of approximately 60 seconds with a measured current, the temperature being recorded at regular intervals before and after heating. A timing device governed by a 1 second pulse gave audible warning of the end of every 15 second interval and a counter recorded the total time in minutes. Due to unavoidable heat transfer between the specimen and its surroundings the temperatures recorded showed a steady small drift which became negative at higher temperatures. Allowing for these drifts the specific heat of the specimen could be calculated at the mean temperature of the heating interval. It was aimed to make each heating interval approximately 1/10 of a degree and of 60 seconds duration.

In later experiments hydrogen exchange gas was used instead of helium in the outer and inner vacuum spaces and also some hydrogen

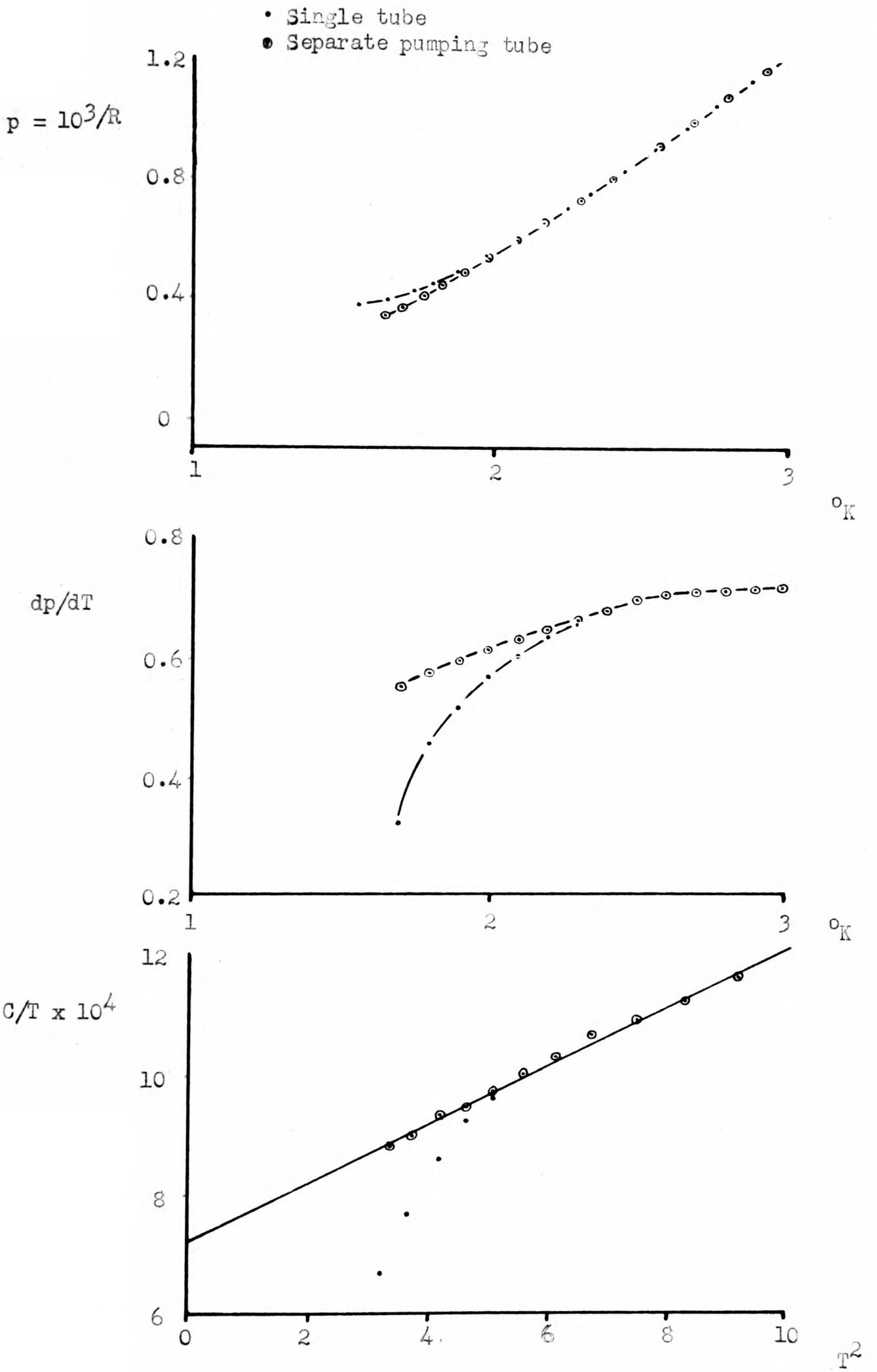
exchange gas was introduced into the experimental chamber. It was found that this improved the vacuum that could be obtained in the outer and inner vacuum spaces and had no detrimental effect on the vacuum in the experimental chamber below $4^{\circ}K$. The exchange gas in the experimental chamber had the advantage of considerably speeding up the cooling of the specimen from room temperature to $20^{\circ}K$.

The carbon thermometer had to be carefully calibrated against the vapour pressure of the liquid helium in the small helium vessel at the end of each experiment. In order to carry out this calibration a small amount of helium exchange gas was admitted to the experimental chamber.

Below the lambda point the liquid helium has to be continuously pumped to maintain a constant temperature. In the Simon bomb apparatus the same tube was used for both pumping away the helium vapour and for measuring the pressure of the vapour. Although the tube to be installed in the new apparatus was to be never less than 3 mm. in diameter it was decided to instal separate pumping and measuring tubes. Calibrations were carried out using separate and combined pumping and measuring tubes and the results showed an increasing divergence below $2.2^{\circ}K$. The error in the value of the sensitivity and therefore in the calculated specific heat points became very noticeable (see Fig. 6.6). Thus in all experiments the separate pumping and measuring tubes were used.

In order to facilitate calibration of the thermometer, especially

Error due to Single Pumping and Measuring Tube. **Fig. 6.6**



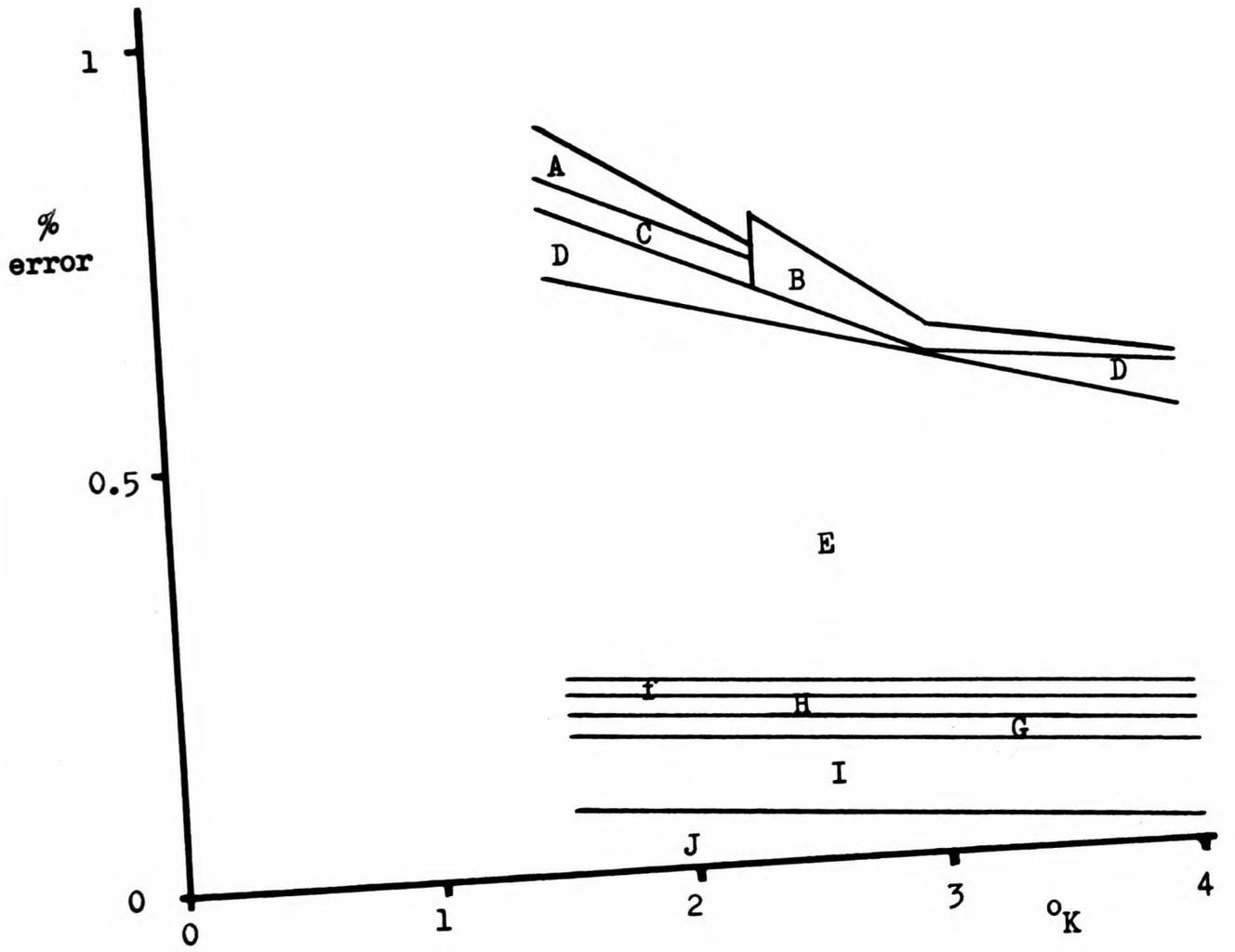
below the lambda point a manostat (Sommers, 1954) was employed to maintain the small helium vessel at a constant temperature. The desired temperature was selected on a second manometer system and the manostat enabled the temperature of the small helium vessel to be kept constant to within 1/1000 of a degree while the resistance of the thermometer was being measured and the pressure of the helium vapour in the small helium vessel was being recorded. This is a vast improvement over the needle valve adjusted by hand which was used to control pumping in the Simon bomb apparatus and greatly improves the accuracy with which the thermometer may be calibrated. The helium vapour pressures recorded were converted into temperatures on the T_{55E} scale (Clement, Logan and Gaffney, 1955).

7. Experimental Accuracy.

A detailed account of the errors involved in the heat capacity measurements will not be given here as a similar account was given in Chapter II. Fig. 6.7 shows the error versus temperature for the new apparatus, the improved accuracy over the Simon bomb apparatus is due to:

a. Temperature drifts reduced to 1/10 thus removing most of the uncertainty in the temperature heating intervals.
b. Heating periods twice as long thus halving the error.
c. Using the Tinsley potentiometer heating currents could be measured to within ± 0.01%.

Error graph for New Apparatus.



A Temperature calibration error (oil)

B Temperature calibration error (mercury)

C Oil density error

D Drift error in $\Delta(1/R)$

E Thermometer sensitivity error

F Thermometer resistance error

G Heater resistance error

H Heater lead resistance error

I Heating period error

J $(\text{current})^2$ error

d. Manostat enabled the thermometer calibration and hence the thermometer sensitivity to be known more accurately.

Also the use of a dummy heater removed any error which was introduced by the current being switched on and off and prevented any error due to the potentiometer out of balance current. Any error due to same pumping and measuring tube for the thermometer calibration had been eliminated and there could not be any exchange gas effects.

The total error throughout the range of temperatures used for measurements is about ± 0.8%.

8. Experimental Technique.

On the subject of experimental technique two points are worthy of note:

(a) It was found that prolonged pumping of the small helium vessel for about three days at room temperature before commencing an experiment considerably lengthened the life of the helium condensed into it and pumped during an experiment. Therefore there was no danger of all the helium evaporating while the specific heat measurements were being taken with consequent irregular drifts in the temperature of the specimen.

Since the pumped liquid helium is at a temperature below its λ point the bulk of the evaporation is associated with the presence of the helium film. It seems likely that the prolonged pumping at

room temperature 'cleans up' the small helium vessel so that the effective circumference as far as the helium film is concerned is greatly decreased.

(b) It was found that the temperature drift rates of the specimen were greatly improved if it was ensured that the cryostat was really 'cold' before measurements were commenced. The apparatus was left overnight with liquid air in the glass dewar, for an hour with liquid hydrogen in the dewar even though both the gas thermometer and the carbon thermometer registered 20°K after less than half that time and for an hour after both the transfer of liquid helium into the main helium vessel and the condensing of helium into the small helium vessel. A further half an hour was allowed after the lowest temperature recorded by the carbon thermometer had been reached on pumping away the vapour over the liquid helium in the small vessel.

It is thought that certain parts of the vacuum calorimeter and its contents, e.g. the cotton threads supporting the specimen, take a long time to cool and if measurements are commenced without adequate cooling radiation from these parts increases the observed temperature drifts.

REFERENCES : Chapter VI.

Berman, R., 1956, J. Appl. Phys., 27, 318.

Clement, J.R., Logan, J.K. and Gaffney, J., 1955, Phys. Rev., 100, 743.

Keesom, W.H. and Kok, J.A., 1934, Physica, 1, 770.

Ramanathan, K.G. and Srinivasan, T.M., 1955, Phil. Mag., 46, 338.

Rayne, J.A., 1956, Aust. J. Phys., 9, 189.

Sommers, H., 1954, Rev. Sci. Inst., 25, 793.

Webb, F.J. and Wilks, J., 1955, Proc. Roy. Soc. A., 230, 549.

CHAPTER VII.

Experimental Results with Heat Switch Apparatus.

1. Heat Capacity of Thermometer and Heater Assembly.

The heat capacity of the thermometer and heater assembly must be measured and subtracted from the heat capacities measured in any experiment in order to calculate the specific heat of the specimen used in that experiment.

Because of the shape of the assembly and the slightly delicate nature of the 2 B.A. thread to which the specimens are attached the assembly could not be forced into contact with the base of the experimental chamber in the same way as a specimen even if the push rod had the necessary amount of vertical travel. Therefore another experimental chamber was constructed to fit onto the small helium vessel. This chamber was shorter in length and had a specially shaped base. When the assembly was lowered the 2 B.A. thread fitted loosely into a recess in the baseplate of the chamber and the large disc which carried the cotton threads could be pressed firmly against the baseplate.

Although contact with the baseplate allowed the temperature of the assembly to be reduced to $1.7^{\circ}K$, on raising the assembly

frictional heating caused an immediate rise in temperature. Since the thermal capacity of the assembly was small, the assembly reached a temperature of 2.0°K before any experimental values of its heat capacity could be obtained. With a specimen in position the total heat capacity was much greater and so the frictional heating caused a smaller rise in temperature. Thus with the assembly, as with the calorimeter in the Simon bomb apparatus, values of the heat capacity were required at temperatures where they could not be measured experimentally. Again, on analysis of the available data on a C/T against T^2 plot showed that the heat capacity could be separated into a cubic and a linear term. Thus, values for the heat capacity of the thermometer and heater assembly below 2.0°K could be predicted with reasonable confidence.

The heat capacity of the thermometer and heater assembly was found to be given by:

$$C = 0.0000272T^3 + 0.000278T \text{ joules per degree.}$$

2. Heat Capacities of Copper-Zinc Alloys.

(a) The Specimens.

Measurements were carried out on fairly large specimens weighing up to 200 gms. as these could be easily accommodated in the cryostat. The specimens were prepared by Dr. H. Montgomery in the Metallurgy

Division of the Atomic Energy Research Establishment at Harwell. The pure metal components were sealed off in vacuo in a silica tube which was then placed in a rotating furnace. After the melt had been shaken vigorously it was quenched into water as rapidly as possible to avoid segregation. The ingots produced in this manner had a very fine dendrite size.

The ingots containing 1%, 2%, 4% and 5% nominal weights of Zinc were then machined to size, drilled and tapped to take the 2 B.A. thread on the heater assembly and their heat capacities measured. During the machining the swarf from 'top', 'bottom' and 'sides' of the ingots was collected and analysed separately to check the homogeneity of the specimen.

The 4% Zinc specimen was subsequently further homogenised by cold working in a hydraulic press. It was then sealed off in a silica tube with an atmosphere of carbon dioxide and annealed for five days at a temperature close to the solidus. No sign of the dendrite structure could be detected after this treatment and samples were removed from each end of the specimen for analysis. The specimen was again drilled and tapped and its heat capacity re-determined giving essentially the same result as before within the limits of the experimental accuracy. Despite this rather pleasing result it was decided to cold work and anneal all other specimens before measuring their heat capacities.

The pure copper was supplied by the Metals Division of Imperial Chemical Industries Ltd. A pure copper specimen was cast in a similar manner to the other specimens and its heat capacity was determined with the dual purpose of testing the apparatus and acting as a reference from which the changes in γ and θ for the alloys could be evaluated. Unfortunately the original supply of copper was used up before all the alloy specimens had been prepared and therefore a second batch of copper was required. A second pure copper specimen was prepared from this batch and its heat capacity was measured.

The analyses sent with the two batches of copper were as follows:

Tin	Trace - less than 0.0005%
Lead	Not detected - less than 0.0003%
Iron	Trace - less than 0.002%
Nickel	Not detected - less than 0.0003%
Silver	Trace - less than 0.001%
Antimony	Not detected - less than 0.002%
Bismuth	Trace - less than 0.0002%
Arsenic	0.002%
Other Elements	Not looked for, but likely to be not detectable if present, and would be less than any of the figures quoted above.

Thus the copper should be at least 99.99% pure.

After the heat capacity determinations had been carried out both of the copper specimens and all the alloy specimens were returned to I.C.I. for further analysis. Spectrographic analysis showed that the first batch of copper was rather less pure than quoted. All specimens prepared from it contained 0.001% lead, 0.0003% nickel and 0.001% silver in addition to elements reported previously, but even so its purity was still at least 99.99%. The second batch of copper agreed with the original analysis. As the specimens were melted in silica tubes silicon contamination was specifically looked for but only slight traces were found. Thus it is unlikely that the specimens contained any metallic impurities which could affect the results obtained. The only properties that could possibly affect the results are grain size and dislocation density. However the grain sizes were all of the order of 2 mm. and it is difficult to imagine that such large grains could affect the specific heat. The specimens were all annealed apart from superficial work caused by machining and as Rayne (1956) found that strain relief in pure copper had no effect upon the specific heat it is thought unlikely that there would be any effect in alloys with very low zinc content.

(b) Experimental Results.

1. Pure Copper.

The results of the two experiments on the specimen of pure copper

prepared from the first batch of copper are given in Table 7.1 and are displayed as a graph of C/T versus T^2 in Fig. 7.1. The maximum deviation of any point from the resulting straight line is less than 1 1/2%. The values for γ and θ obtained by the method of least squares were as follows:

1st Experiment $\gamma = 0.698 \times 10^{-3}$ joules/mole/deg^2, $\theta = 341.6^{\circ}K$

2nd Experiment $\gamma = 0.698 \times 10^{-3}$ joules/per /deg^2, $\theta = 341.0^{\circ}K$

Combined Result $\gamma = (0.698 \pm 0.002) \times 10^{-3}$ joules/mole/degree^2

$\theta = 341.3 \pm 1.1^{\circ}K$

The limits quoted are the probable errors calculated from the scatter of the points about the least squares line.

The results of one experiment on the specimen of pure copper from the second batch are given in Table 7.2 and are displayed as a graph of C/T versus T^2 in Fig. 7.2. The values for γ and θ for copper from the second batch were:

$\gamma = 0.699 \times 10^{-3}$ joules per mole per degree^2

$\theta = 341.7^{\circ}K$

which are in excellent agreement with the values obtained with the first batch of copper.

For comparison published results of other authors are given below in chronological order; γ is given in joules per mole per degree^2.

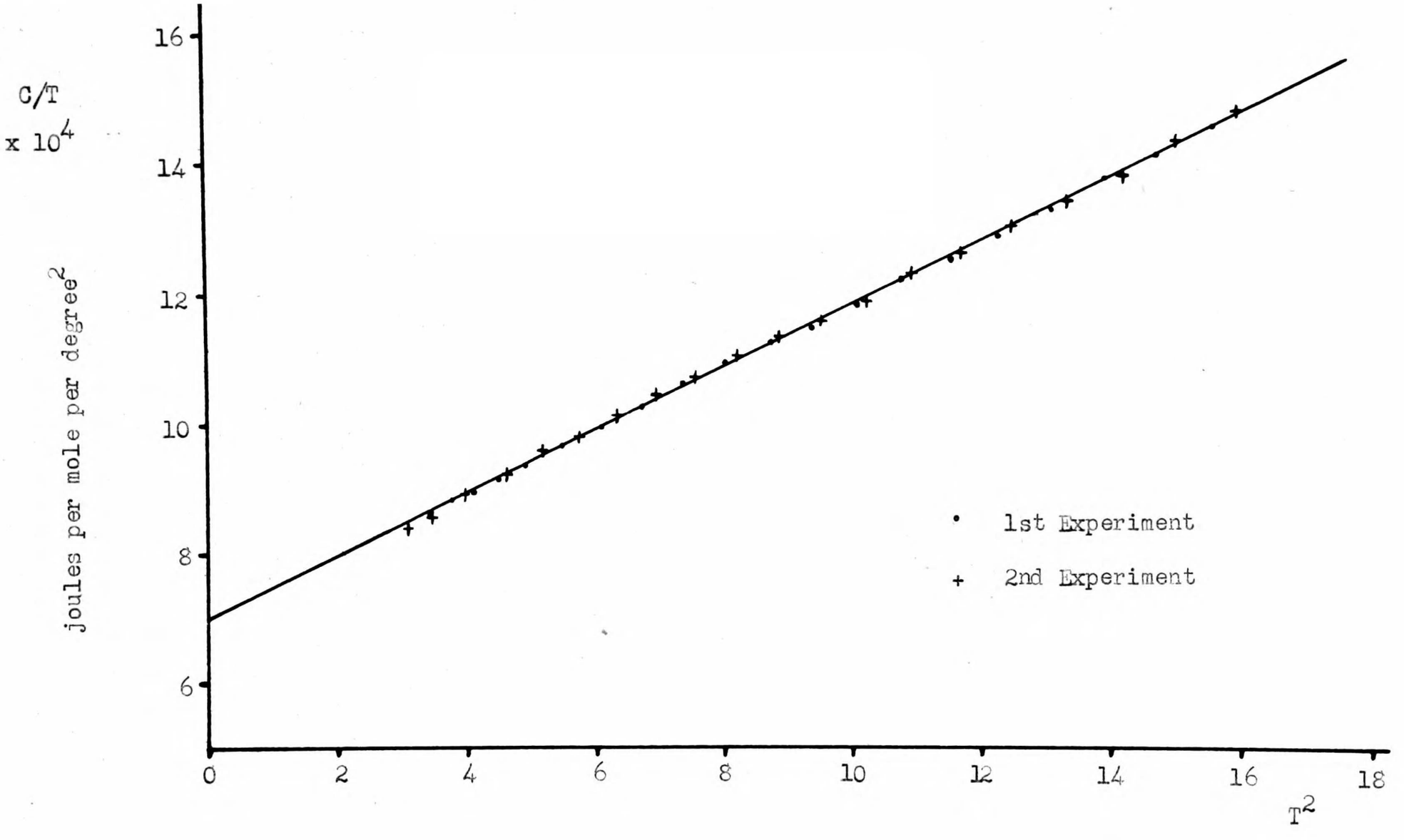

Pure Copper : 1st Batch.
C/T
x 10^4
joules per mole per degree^2
16
14
12
10
8
6
0
2
4
6
8
10
12
14
16
18
T^2
• 1st Experiment
+ 2nd Experiment

Fig. 7.1

Pure Copper : 2nd Batch.

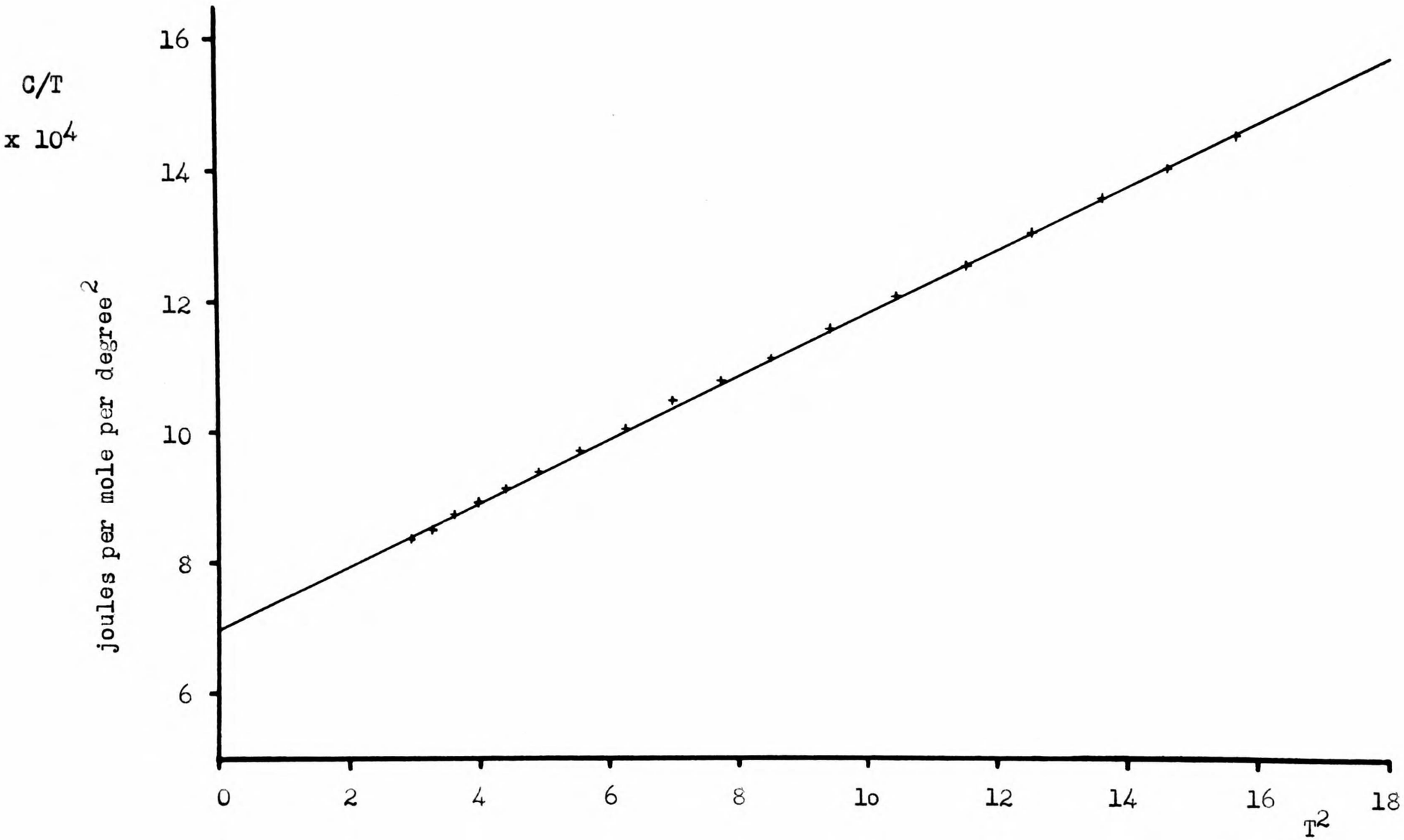


Fig. 7.2

	Purity	$\gamma \times 10^3$	θ °K
Kok and Keesom (1936)	99.9	0.74	335
Estermann, Friedberg and Goldman (1952)	99.6	0.75	315
Rayne (1954)		0.72 ± 0.03	-
Corak et al. (1955)	99.999	0.688 ± 0.004	343.2 ± 1.3
Rayne (1956)	99.999	0.686 ± 0.005	345.1 ± 0.9
	99.9	0.670 ± 0.005	338.9 ± 0.9
	99.0	0.799 ± 0.005	344.7 ± 0.9
Ramanathan and Srinivasan (1957)	99.95	0.722 ± 0.028	334.0 ± 1.8
Griffel, Vest and Smith (1957)		0.691 ± 0.006	342.0 ± 2.0
This research	99.99	0.698 ± 0.002	341.3 ± 1.1

Both Kok and Keesom, and Estermann, Friedberg and Goldman used helium exchange gas in their experiments and therefore their results are probably subject to an unassessable error. Ramanathan and Srinivasan used a mechanical heat switch but the accuracy of their experiments does not justify much weight being put on their results. The work of Corak et al was carried out with extreme care but one point is worthy of note. When the experimental points obtained below 2.1°K are plotted on a graph of C/T versus T^2 three points lie on the line obtained by a least squares analysis, eleven points lie below the line and only one point lies above it. Thus the low

temperature results where the experimental accuracy is lowest have a considerable effect on the line of least squares, without these results the value for γ would be larger, approximately 0.700×10^{-3} joules per mole per degree in much better agreement with this research. It is much more difficult to reconcile the present results with those of Rayne whose undoubtedly accurate work gives a γ 1 1/2% lower. In his paper Rayne also reports results on a specimen of 99.9% purity for which he obtained the lowest γ measured for a copper specimen, no comment is made on the 2 1/2% discrepancy between this and his 99.999% pure specimen. The measurements of Griffel, Vest and Smith were carried out as a check on their apparatus before commencing measurements on Calcium. Their results agree with the present work to within the combined probable errors calculated from the scatter of points about the respective least square lines but unfortunately no analysis of their specimen is available though it is probably at least 99.99% pure copper.

For comparison with the experimental values, θ_o values calculated from the elastic constants are given below:

Quimby and Sutton (1953)	θ =	344.4°K
De Launay (1956)		344.5°K
Betts et al (1956)		345.4°K
Alers and Neighbours (1959)		344.4°K

It will be seen that except for Rayne's value all experimental values for θ are lower than the calculated values. Thus no support

is given to the prediction of Warren and Ferrell (1958) that the calorimetric θ should be larger than the elastic θ_o because the measured elastic constants include a contribution due to a relaxation mechanism of the electrons. The available low temperature elastic constant data also does not indicate any such relaxation mechanism.

If dislocations contribute to the measured elastic constants the resulting value of θ_o would be lower than the calorimetric value, so that the present experimental results are in favour of no such contribution.

Jones (1937) obtained a value for copper of $\gamma = 0.69 \times 10^{-3}$ joules per mole per degree^2 from a density of states calculation. From this research the ratio of the observed electronic specific heat to the free electron value is $m^*/m = 1.39$. Schultz (1954) gives a value for the effective mass derived from room temperature absorptivity of copper which corresponds to a ratio of 1.44. From observations of the anomalous skin effect in copper Pippard (1957) has been able to deduce the shape of the Fermi surface, and estimates that the ratio m^*/m lies between 1.7 and 1.9. Shoenberg (1959) has recently observed the De Haas-Van Alphen effect in copper and from the temperature variation of the effect estimates that m^*/m is about 1.3. The effect was observed for one orientation of the specimen only, and was consistent with the proposed Fermi surface of Pippard.

2. Copper-Zinc Alloys.

The results of experiments on a series of α brasses are given in Tables 7.3 - 7.8 and are displayed as graphs of C/T versus T^2 in Figs. 7.3 - 7.8. Two experiments were carried out on each specimen and values for γ and θ were obtained individually and collectively from the results by the method of least squares. As a result of previous work and the published results of Rayne (1957) it was decided to investigate the form of the initial rise in γ from its value for pure copper and therefore no specimen contained more than 5% of zinc by weight. The values obtained for γ and θ are summarised below, the deviations quoted being the probable errors calculated from the scatter of points about the least square line.

wt. % of zinc	$\gamma \times 10^3$ joules/mole/degree^2	θ °K
0	0.698 ± 0.002	341.3 ± 1.1
0.10	0.714 ± 0.002	344.0 ± 1.4
0.45	0.728 ± 0.001	345.5 ± 1.1
1.03	0.735 ± 0.002	345.0 ± 1.6
1.30	0.735 ± 0.002	344.5 ± 1.4
4.13	0.732 ± 0.002	343.0 ± 1.2
4.70	0.734 ± 0.002	343.0 ± 1.2

The above results are displayed in Fig. 7.9 together with those of Rayne (1957, 1958a) on both the copper zinc alloys and copper germanium alloys. It is assumed that zinc contributes one electron

Copper-Zinc Alloy : 0.10% by weight of Zinc.

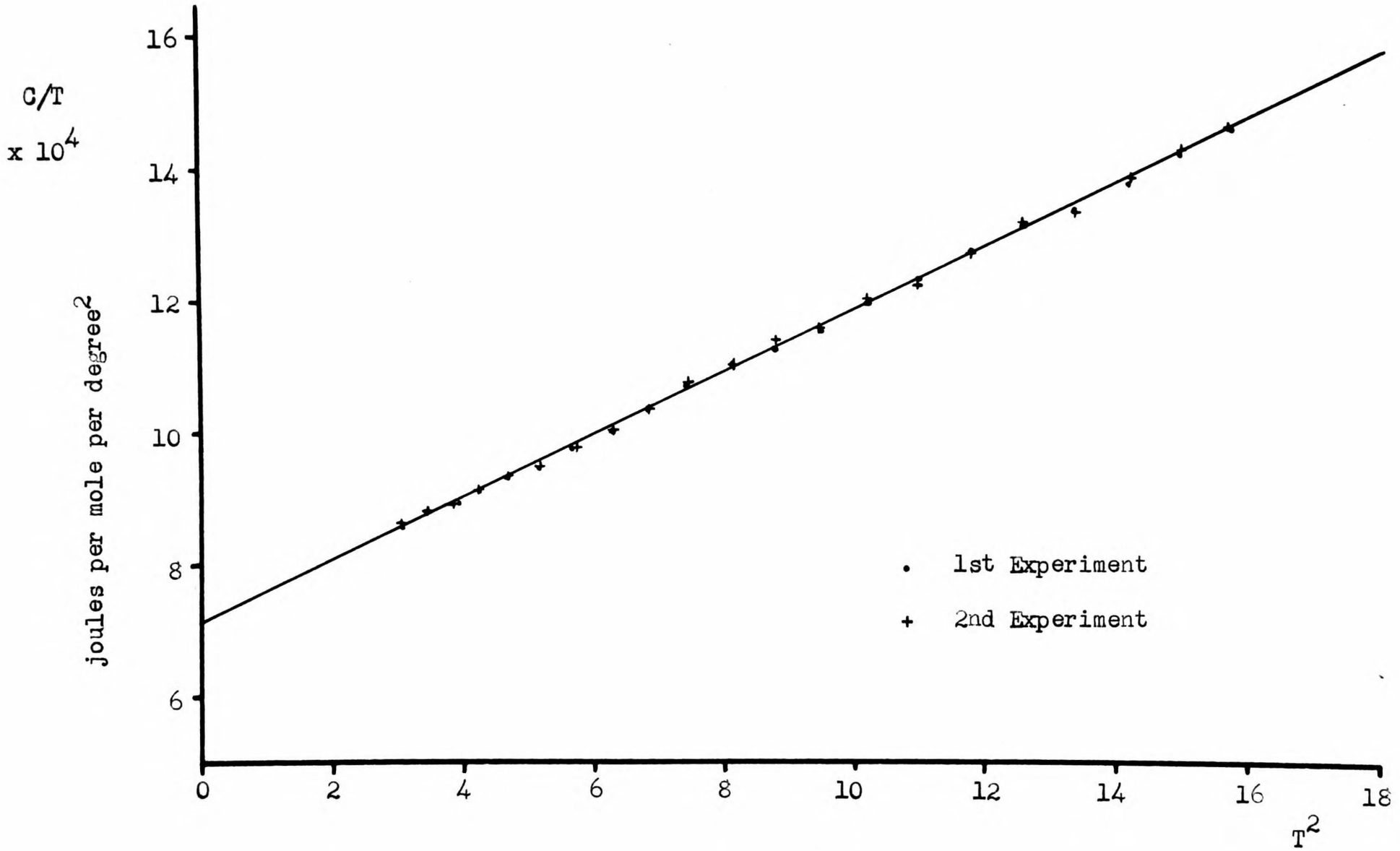


Fig. 7.3

Copper-Zinc Alloy : 0.45% by weight of Zinc.

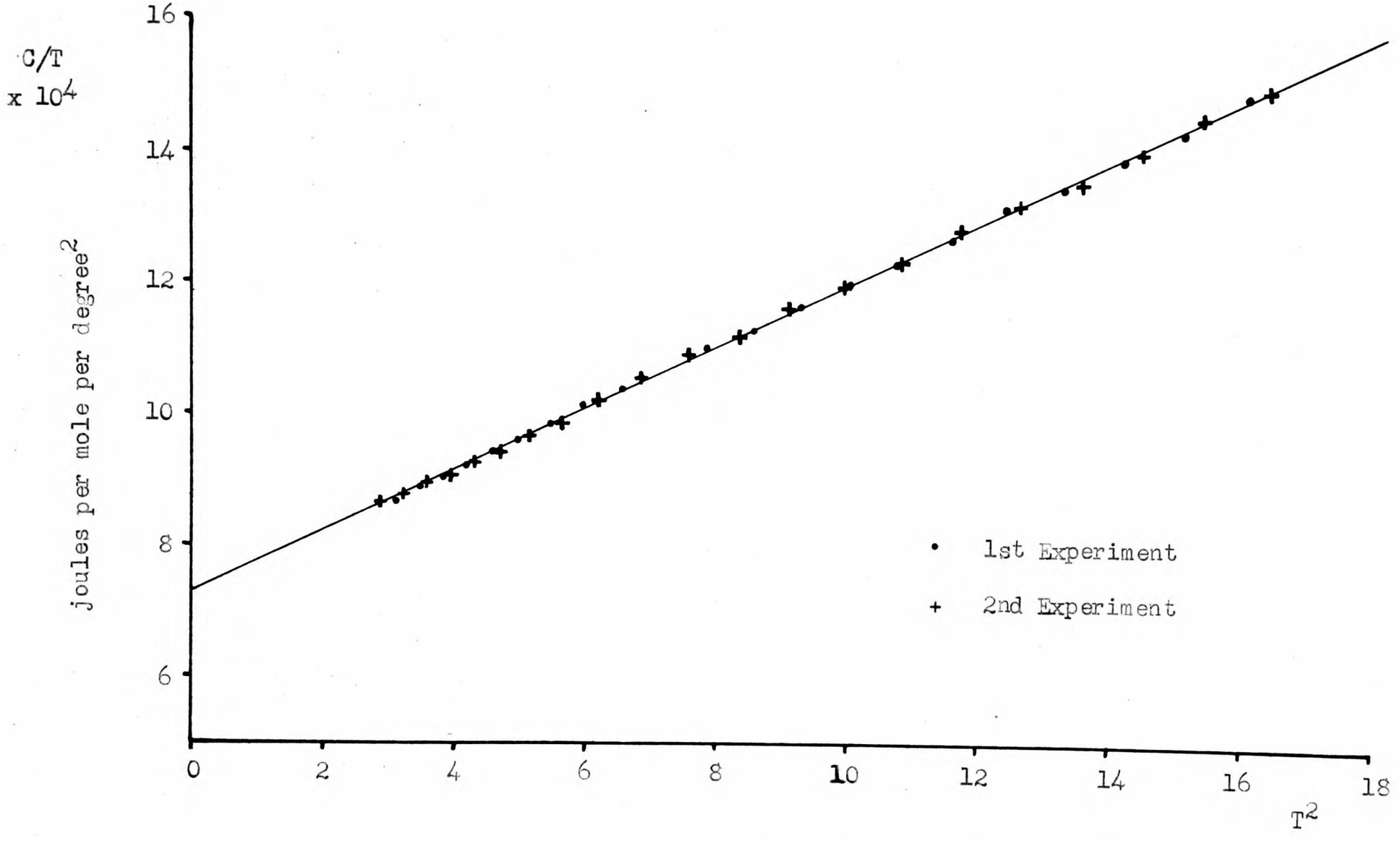


Fig. 7.4

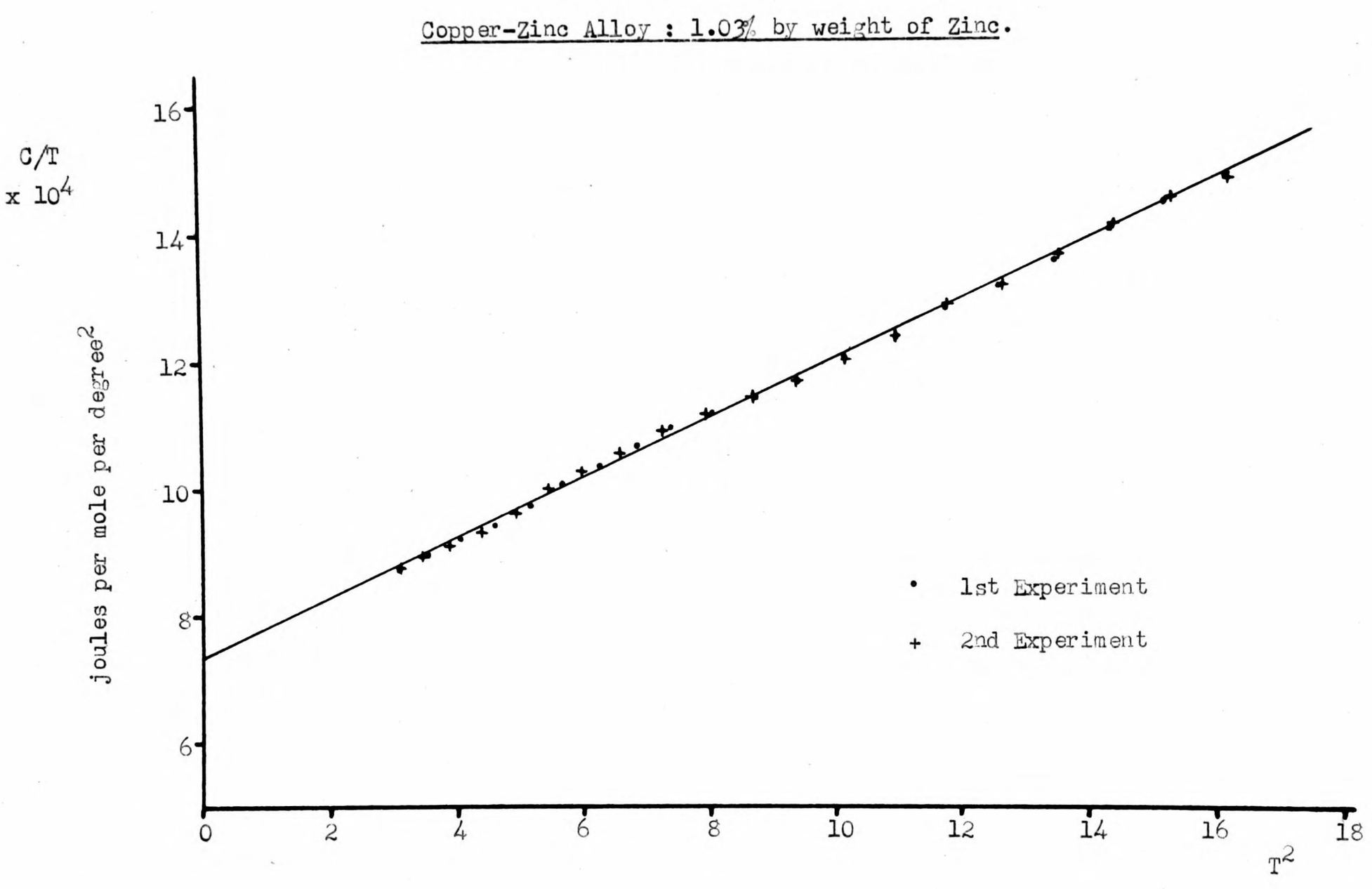

Copper-Zinc Alloy : 1.03% by weight of Zinc.
C/T
x 10^4
joules per mole per degree^2
16
14
12
10
8
6
0
2
4
6
8
10
12
14
16
18
T^2
• 1st Experiment
+ 2nd Experiment

Fig. 7.5

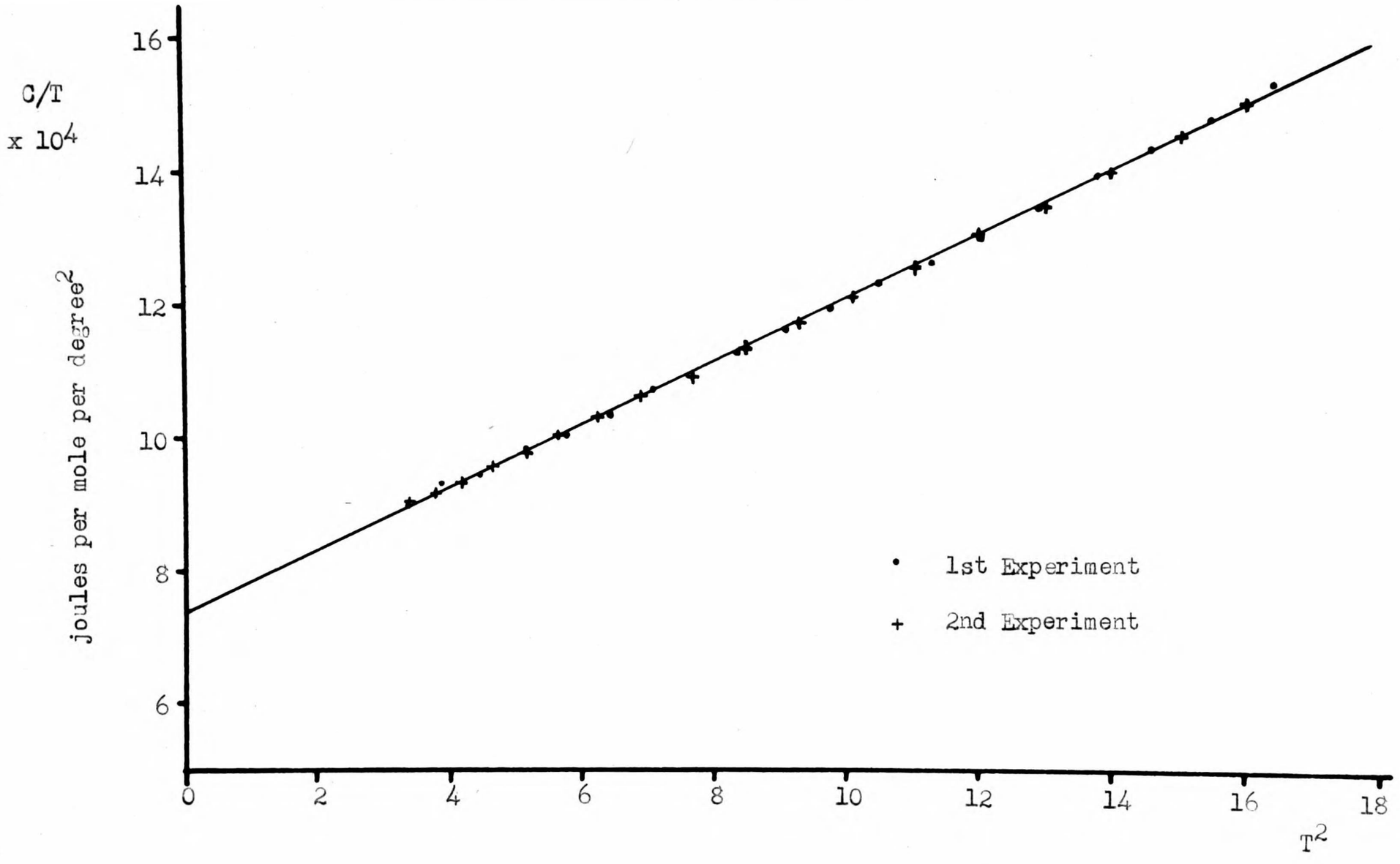

Copper-Zinc Alloy : 1.30% by weight of Zinc.
C/T
x 10^4
joules per mole per degree^2
16
14
12
10
8
6
0
2
4
6
8
10
12
14
16
18
T^2
• 1st Experiment
+ 2nd Experiment

Fig. 7.6

Copper-Zinc Alloy : 4.13% by weight of Zinc.

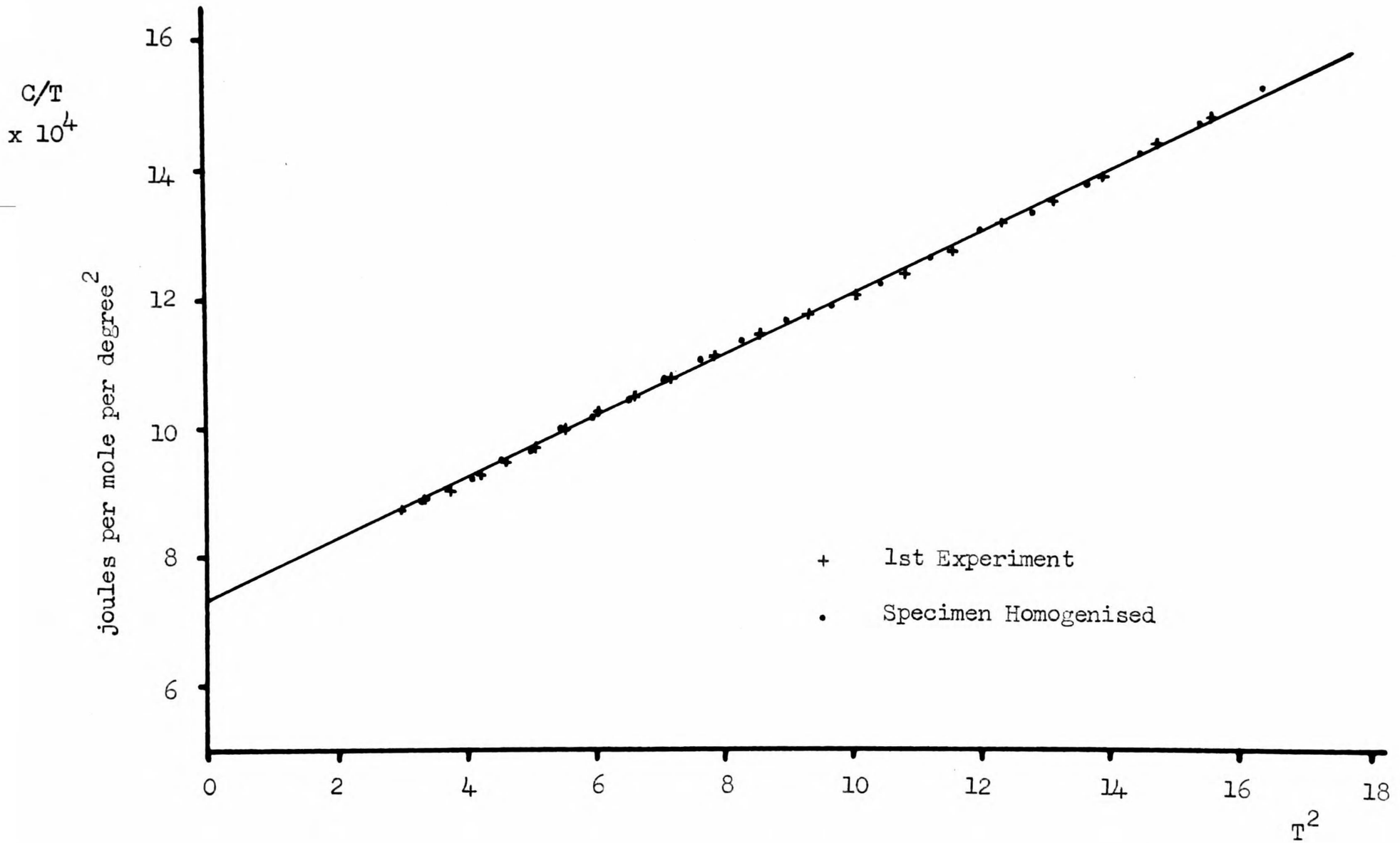


Fig. 7.7

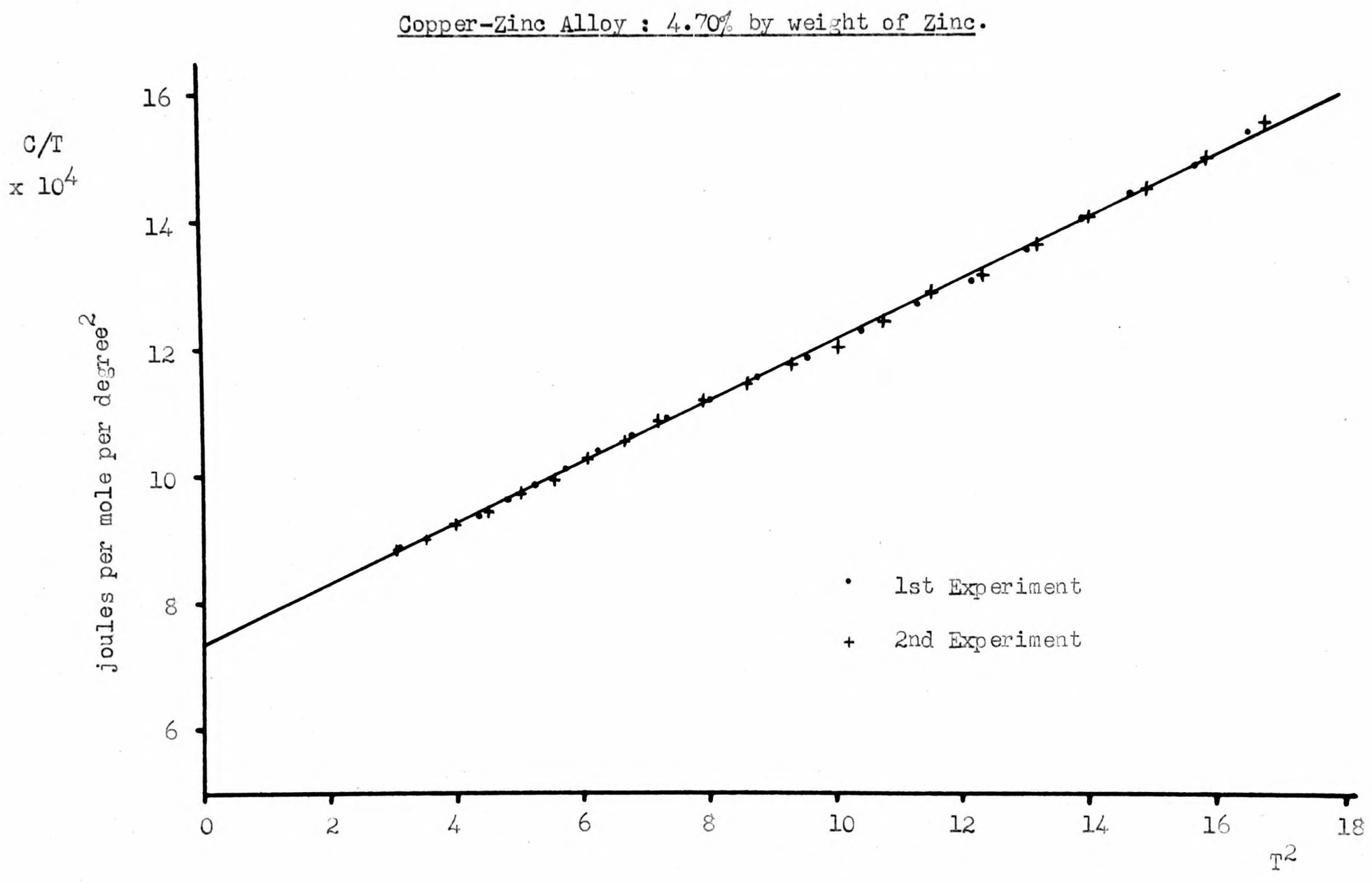

Copper-Zinc Alloy : 4.70% by weight of Zinc.
C/T
x 10^4
joules per mole per degree^2
16
14
12
10
8
6
0
2
4
6
8
10
12
14
16
18
T^2
• 1st Experiment
+ 2nd Experiment

Fig. 7.8

Variation of the Electronic Heat Capacity of α Brasses with Zinc Concentration.

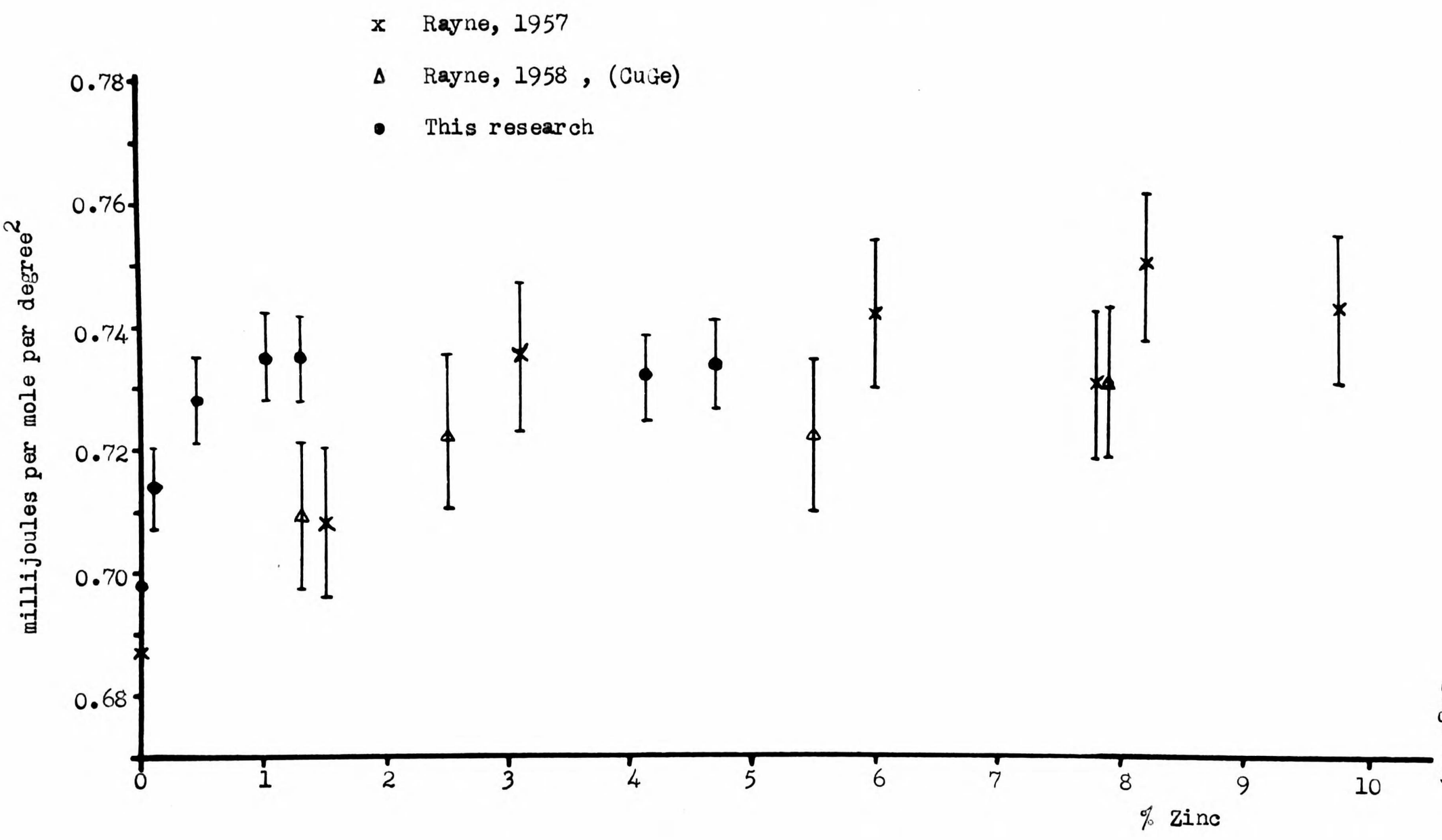


Fig. 7.9

per atom and germanium three electrons per atom. The specimens with 4.13% and 4.70% zinc have γ's which are in excellent agreement with Rayne's values but the remaining specimens with lower zinc content are not in agreement with his specimen containing 1.49% by weight of zinc. The resulting picture is of a γ which rises much more steeply with small zinc concentrations from its value for pure copper.

As far as the Θ values are concerned there is excellent agreement for all the alloys (see Fig. 7.10), Θ decreasing very slowly with increasing zinc content. In addition the results of this research give evidence of an initial 1% increase in Θ on the introduction of zinc atoms into pure copper. Guthrie (1959) also found a 1% initial increase in Θ for the pseudo coppers, $Cu_{1-2x}\ Ni_x\ Zn_x$.

(c) Discussion.

i. The Lattice Specific Heat.

No solution to the problem of the dynamics of a disordered cubic lattice has been published but for dilute alloys of zinc in copper it can be reasonably supposed that the long wavelength phonons see effectively the same lattice structure as in pure copper. The problem of the vibrational spectrum of cubic metals has been reviewed by de Launay (1956). Considering only central forces but allowing for the volume force due to the presence of electrons he obtains the following

Variation of the Debye Θ of α Brasses with Zinc Concentration.

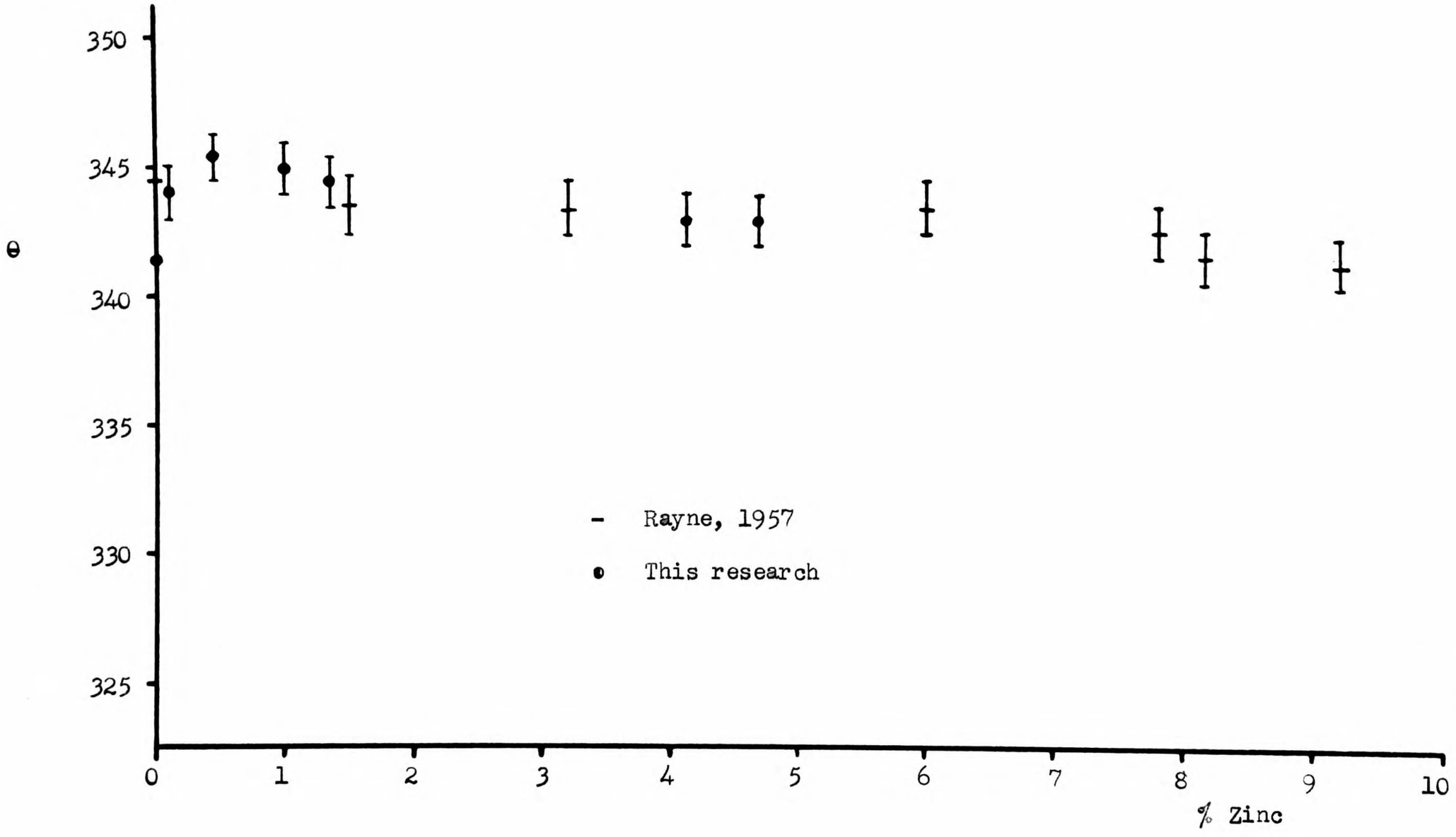


Fig. 7.10

general expression for the Debye θ at low temperatures:

$$\theta^3 = \frac{9n}{4\pi V}(h/k)^3(c_{44}/p)^{3/2}\frac{9}{18+\sqrt{3}} \cdot f(s,t)$$

where s and t are related to the elastic constants as follows

$$s = (c_{11} - c_{44})/(c_{12} - c_{44}) \quad , \quad t = (c_{12} - c_{44})/c_{44}$$

If the metal satisfies Cauchy's relation, $c_{12} = c_{44}$, then $t = 0$ and $s = (c_{11} - c_{12})/2c_{44}$.

If the dilute alloys can be assumed to behave like cubic metals then the variation of θ with zinc concentration can be related to the variations in the elastic constants of the alloys. For by rearranging the above equation for θ:

$$\theta^3(M^3/V)^{1/2} \propto c_{44}^{3/2} f(s,t)$$

Now the measurable shear constants are defined as

$$C = c_{44} \quad \text{and} \quad C' = (c_{11} - c_{12})/2$$

so that

$$\theta^3 \propto C^{3/2} f(C'/C)$$

It would seem reasonable to assume that the R.H.S. of this equation, which is a function of the elastic constants only, would depend on both the lattice spacing and the electron concentration of the alloy. However, Rayne (1958a) found that if he plotted the reduced θ values for his copper-zinc alloys and for a similar series of copper-germanium

against electron concentration they defined the same curve. This suggests that the variation of the elastic constants depends only on the electron concentration since the lattice expansion is not the same in both cases. If this is the case the variation of the shear constants is directly related to the changing shape of the Fermi surface. Jones (1952) found that for the β brasses, in which the Fermi surface makes contact with the zone boundaries, there is an appreciable electronic contribution to both the shear constants. In α brasses if the Fermi surface overlaps the first Brillouin zone in the (111) directions only there should be a marked difference in the behaviour of C and C' as a function of solute concentration. This is due to the fact that C corresponds to strains along and perpendicular to the (111) direction and C' corresponds to strains along and perpendicular to the (100) direction. If a crystal is subjected to an appropriate shear strain which leaves the volume unaltered this shear will alter the shape of the Brillouin zone. When the Fermi surface lies entirely within the zone there will be no change in the electronic energy but when there is overlap the energy will generally be altered with a consequent contribution to the shear constant. Rayne (1958b) has made room temperature ultrasonic pulse measurements of the shear constants of a series of α brasses and found that C and C' did in fact behave differently. From the nature of the variation of C with zinc concentration it seems there is an additional contribution which

increases with zinc content. Rayne assumes this contribution to be small in pure copper and become appreciable at 10% zinc, the concentration at which his experimental density of states curve shows a maximum. The concentration at which the additional contribution becomes appreciable could equally well be at 1% zinc, the value found for the maximum in the density of states curve in this research. The possibility must also not be ruled out that there is an appreciable contribution even in pure copper so that the above evidence cannot really say at what zinc concentration contact occurs between the Fermi surface and the zone boundaries.

Thus only the electronic energy need be considered when deriving the shear constants from the total energy, U

$$C = \frac{1}{2V}\frac{\partial^2 U}{\partial \alpha^2} \qquad \text{and} \qquad C' = \frac{1}{2V}\frac{\partial^2 U}{\partial \beta^2}$$

the differentiations being carried out with respect to the appropriate shears.

By differentiating the expression for θ and using the results of Overton, Jr. and Gaffney (1955) for the elastic constants of copper at $4^{\circ}K$ and the results of Neighbours and Smith (1954) for the room temperature variation of C and C' with solute concentration Rayne (1958b) was able to plot the variation of θ against the number of electrons per atom. Agreement with direct experiment is not very good and use of the results of this research would not materially affect the result. Obviously not

much can be said about the disagreement until the result of using low temperature data on the variation of C and C' with solute concentration can be investigated. Rayne is at present carrying out the necessary measurements.

ii. The Electronic Specific Heat.

The initial rise in γ for low concentrations of zinc is in much better agreement with the theoretical density of states curve for copper derived by Jones (1937) than the results of Rayne (1957). The shallow maximum occurs at about 1% zinc compared with 2 1/2% zinc calculated by Jones and 10% zinc found by Rayne. There is no evidence for the additional linear term of Jones (1957) unless it occupies a very small range of concentration of zinc. It seems likely that the relevant phonon electron interaction is not as large as anticipated. The initial rise is again inexplicable from the free electron point of view and it must be assumed that the Fermi surface departs appreciably from sphericity. It would appear that the Fermi surface makes contact with the zone boundaries at a zinc concentration of about 1%. This is still in conflict with much of the evidence given in Chapter IV which favoured contact even in pure copper.

In order to reconcile the specific heat measurements with the results of Pippard, Cohen and Heine (1958) have suggested that the rigid band hypothesis should be dispensed with completely. They suggest that the addition of impurities distorts the Fermi surface causing it to pull

away from the zone boundaries and tend to become more spherical. Only when many more electrons have been added is the sphere forced back into contact with the zone boundary. Thus the zone boundary effect which from the present research occurs at about 1% zinc in copper is not the Fermi surface making contact with the zone boundaries but pulling away from them.

In reaching this conclusion, Cohen and Heine first found a model of the band structure applicable to pure monovalent metals. Their model assigned a dominant role to the magnitude and sign of the energy gap between the purely s like and purely p like states at the centres of the Brillouin zone faces nearest to the origin in k space. By relating the energy gap, $E_s - E_p$, to the s-p excitation energy Δsp of the free atom they are able to estimate the energy gap for the pure metals and construct the band structure they suggest. They then show that these structures, with a few minor alterations, are consistent with relevant experimental data. For alloys they start with the model for the pure metal and assume that adding solute not only fills up the band but at the same time alters the shape of the band because of the change in the average Δsp. The latter fact was neglected by the rigid band model. Since the solute atoms have always a larger Δsp than the solvent atoms in the α phase alloys of the noble metals the energy E_p must be raised relative to E_s as the solute concentration is increased. Now the distortion of the Fermi surface from the spherical depends on the

magnitude of $1/2(E_s - E_p)$ that the energy at the zone boundary is depressed below the mean parabola, so that there are now two factors affecting its shape. For copper their model assigns $E_p < E_s$ in complete disagreement with the band structure calculations by Howarth (1953, 1955). However Mott (1953) has already suggested that the x-ray spectrum of copper indicates that E_p may lie below E_s and observations of the Knight shift in copper alloys add weight to this idea. Therefore on alloying the change in E_p tends to make the Fermi surface in copper more spherical. If it is assumed that the Fermi surface touches the zone boundaries in pure copper then on alloying the change in E_p will tend to make the Fermi surface pull away but the filling up of the band structure with electrons from the solute will have the opposite effect. Only by considering experimental evidence can it be decided which is the dominant factor and hence whether there is initial contact with the Fermi surface pulling away from the zone boundaries or whether there is no contact initially with the Fermi surface approaching the zone boundaries with increasing solute. The available evidence of the band structure of pure copper points to the first alternative being the most likely. It is impossible to say whether the Fermi surface pulls right away from the zone boundaries or remains just touching. If the Fermi surface has to remake contact with the zone boundaries then a further zone boundary effect in the specific heat at a higher concentration of

zinc would be expected. Cohen and Heine suggest that in Rayne's data there is a suspicion of a peak at the electron to atom ratio of 1.3 but without further investigation of this region it is felt that no statement can be made on this question.

Ziman (1959) argues that if contact of the Fermi surface with the zone boundaries is broken on alloying then changes would be expected in the residual resistance and other transport properties because of the topological discontinuity in the shape of the Fermi surface. He calculates that in a metal where the Fermi surface just touches the zone boundaries the residual resistance should fall slightly with increasing temperature and there should also be a positive thermopower anomaly. Pure copper shows no resistance minimum but it grows rapidly in size as impurity is added and this could be explained by assuming appreciable contact in pure copper which contracts in area as impurity is added until contact is broken. Ziman shows that the predicted size of the effect is quite comparable with the resistance changes observed in a CuSn alloy by MacDonald and Pearson (1955). The positive thermopower anomaly however does not agree with experiments which give an anomaly but negative in sign.

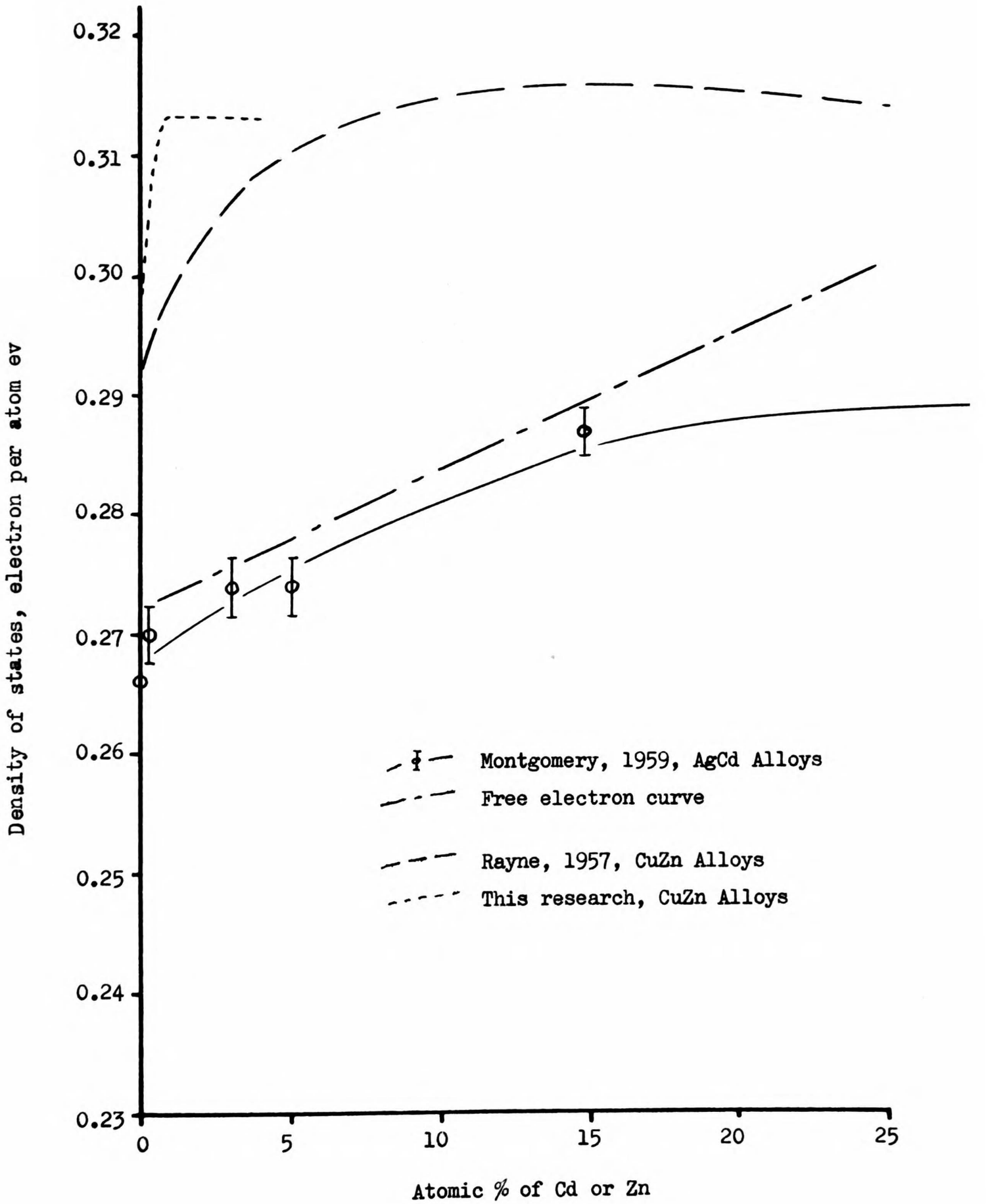
Examination of Cohen and Heine's predictions for the other noble metals is not very fruitful. No experimental data is available on alloys of gold but Montgomery (1959) has kindly made available specific heat measurements on a series of silver-cadmium

alloys and these are shown in Fig. 7.11. The variation in γ for low concentrations of cadmium is almost identical with that to be expected from the rigid band theory for a free electron gas. The results therefore indicate that the Fermi surface in silver is nearly spherical and that the effective mass approximates to the free electron value. Unfortunately Cohen and Heine are not able to make any clear predictions in the case of silver although the magnitude of $E_s - E_p$ is probably small agreeing with a nearly spherical Fermi surface. As far as the ratio of the optical and thermal masses is concerned, Cohen (1958) decides that a spherical surface or a surface making contact with the zone boundaries are equally probable. In the absence of a direct investigation of the shape of the Fermi surface by the anomalous skin effect the absence of any zone boundary effect in the specific heat of the silver-cadmium alloys suggests that there is no contact between the Fermi surface and the zone boundaries in silver. Thus the silver-cadmium alloys do not reject the rigid band model but on the other hand the model of Cohen and Heine is also applicable.

Further evidence for the breakdown of the rigid band model is given by the results of Guthrie (1959) on the heat capacity of pseudo copper. Measurements were carried out on the alloys $Cu_{1-2x}Ni_xZn_x$ which have the same ratio of electrons to atoms as pure copper and have the same lattice structure as well. Guthrie found that the Θ for the alloy with $x = 0.03$ was only 1% higher than the Θ for pure copper but that the

Fig. 7.11

Density of States for AgCd and CuZn Alloys.



γ was 20% higher than the γ for pure copper and increasing with increasing x. Here there can be no question of the filling up of the band structure with electrons and the results can only be accounted for by a change in band structure. This is contrary to the rigid band theory and the theory of Friedel (1954) but can be accounted for by Cohen and Heine's model. The larger increase in γ compared with the copper-zinc alloys can be explained by the absence of electrons to fill up the band so that there is no factor to counteract the pulling away of the Fermi surface from the zone boundaries.

The evidence against the rigid band theory is now overwhelming but whereas its abandonment a few years ago would have left an unsatisfactory vacuum, this is now filled by the model proposed by Cohen and Heine. However this model can only give a qualitative interpretation of the observed experimental results and a solution of the non periodic potential problem is still the most important requirement.

REFERENCES : Chapter VII.

Alers, G.A. and Neighbours, J.R., 1959, Rev. Mod. Phys., 31, 675.

Betts, D.D., Bhatia, A.B. and Wyman, M., 1956, Phys. Rev., 104, 37.

Cohen, M.H., 1958, Phil. Mag. Ser. 8, 3, 762.

Cohen, M.H. and Heine, V., 1958, Advances in Physics, 7, 395.

Corak, W.S., Garfunkel, M.P., Satterthwaite, C.B. and Wexler, A., 1955, Phys. Rev., 98, 1699.

Estermann, I., Friedberg, S.A. and Goldman, J.E., 1952, Phys. Rev., 87, 582.

Friedel, J., 1954, Advances in Physics, 3, 465.

Griffel, M., Vest., R.W. and Smith, J.F., 1957, J. Chem. Phys., 27, 1267.

Guthrie, G.L., 1959, Phys. Rev., 113, 793.

Howarth, D.J., 1953, Proc. Roy. Soc. A, 220, 513.

1955, Phys. Rev., 99, 469.

Jones, H., 1937, Proc. Phys. Soc., 49, 250.

1952, Phil. Mag., 43, 105.

1957, Proc. Roy. Soc. A, 240, 321.

Keesom, W.H. and Kok, J.A., 1936, Physica, 3, 1035.

de Launay, J., 1956, Solid State Physics, 2, 285.

MacDonald, D.K.C. and Pearson, W.B., 1955, Acta. Metall., 3, 392, 403.

Montgomery, H., 1959, Private communication.

Mott, N.F., 1953, Phil. Mag., 44, 187.

Neighbours, J.R. and Smith, C.S., 1954, Acta Metall., 2, 591.

Overton, W.C., Jr. and Gaffney, J., 1955, Phys. Rev., 98, 969.

Pippard, A.B., 1957, Phil. Trans. A, 250, 325.

Quimby, S.L. and Sutton, P.M., 1953, Phys. Rev., 91, 1122.

Ramanathan, K.G. and Srinivasan, T.M., 1957, J. Sci. Ind. Res., 16B, 277.

Rayne, J.A., 1954, Phys. Rev., 95, 1428.

1956, Aust. J. Phys., 9, 189.

1957, Phys. Rev., 108, 22.

1958a, Phys. Rev., 110, 606.

1958b, Phys. Rev., 112, 1125.

Schulz, L.G., 1954, Phys. Rev., 94, 1422.

Shoenberg, D., 1959, Nature (London), 183, 171.

Warren, J.L. and Ferrell, R.A., 1958, Bull. Am. Phys. Soc., Ser.II, 3, 226.

Ziman, J.M., 1959, Proc. Roy. Soc. A, 252, 63.

APPENDIX.

Specific Heat Tables.

Table 2.1.

Heat Capacity of Empty Calorimeter.

C given in units of calories per degree.

$T^{o}K$	C	$T^{o}K$	C
1.920	0.000191	7.10	0.00272
2.190	231	7.73	342
2.420	268	8.25	405
2.635	311	8.78	481
2.815	354	9.35	572
2.967	383	9.97	676
3.100	418	10.57	779
3.223	441	11.27	912
3.368	496	11.94	0.0102
3.522	535	12.65	119
3.650	573	13.38	139
3.768	614	14.20	164
3.888	657	14.97	189
3.988	698	15.69	212
4.080	727	16.43	239
4.53	942	17.17	267
5.18	0.00127	17.92	301
5.83	173	18.68	333
6.50	216	19.58	381

Table 2.2.

Experimental Specific Heat of Cerium Magnesium Nitrate.

$T^{o}K$	C_p/R	$T^{o}K$	C_p/R	$T^{o}K$	C_p/R
1.640	0.00503	3.452	0.0502	7.12	0.722
1.884	0.00773	3.680	0.0646	7.52	0.873
2.042	0.00968	3.893	0.0800	7.92	1.025
2.194	0.0118	4.16	0.112	8.30	1.17
2.333	0.0143	4.68	0.171	8.68	1.31
2.465	0.0172	5.10	0.233	9.04	1.45
2.602	0.0196	5.46	0.295	9.45	1.67
2.773	0.0240	5.78	0.371	9.92	1.89
3.002	0.0307	6.20	0.469	10.42	2.15
3.237	0.0397	6.70	0.590		

Table 2.3.

Specific Heat of Cerium Magnesium Nitrate from Smoothed Curve.

$T^{o}K$	C_p/R	$T^{o}K$	C_p/R
0.5	0.000141	4.0	0.124
1.0	0.00113	5.0	0.216
1.5	0.00380	6.0	0.416
2.0	0.00901	7.0	0.694
2.5	0.0176	8.0	1.05
3.0	0.0304	9.0	1.47
3.5	0.0533	10.0	1.93

Table 3.1.

Experimental values of the Specific Heat of Uranium Tetrafluoride.

(Powdered Specimen).

C_p given in units of calories per mole per degree

T^oK	C_p	T^oK	C_p
1.800	0.0130	3.173	0.116
1.927	0.0178	3.413	0.137
2.032	0.0231	3.650	0.156
2.127	0.0289	3.860	0.166
2.208	0.0349	4.33	0.196
2.294	0.0413	4.83	0.228
2.433	0.0532	5.38	0.249
2.766	0.0817	6.17	0.266
2.954	0.0963	7.29	0.282

Table 3.2.

Experimental Values of the Specific Heat of Ammonium Chloroiridate.

C_p given in units of calories per mole per degree.

1st Run.

T^oK	C_p	T^oK	C_p	T^oK	C_p
3.10	0.488	8.53	0.855	17.34	4.48
3.30	0.478	9.53	1.08	18.38	5.00
3.54	0.480	10.06	1.18	19.40	5.71
3.80	0.485	11.05	1.45		
4.28	0.485	11.64	1.73		
4.71	0.500	12.47	2.00		
5.41	0.526	13.42	2.47		
6.23	0.576	14.31	2.90		
6.93	0.620	15.24	3.30		
7.49	0.705	16.26	3.79		

2nd Run.

T^oK	C_p	T^oK	C_p	T^oK	C_p
1.760	0.555	1.990	1.38	2.160	3.88
1.790	0.599	2.043	2.01	2.225	1.60
1.825	0.637	2.092	4.66	2.320	0.818
1.862	0.736	2.125	6.13	2.430	0.569
1.902	0.891	2.145	12.60	2.548	0.480
1.940	0.980	2.150	8.20	2.675	0.459
				2.860	0.470

Table 3.3.

Experimental Values of the Specific Heat of Potassium Chloroiridate.

C_p given in units of calories per mole per degree.

T^oK	C_p	T^oK	C_p
1.730	0.122	5.65	0.648
1.840	0.178	6.30	0.762
1.925	0.181	7.02	0.863
2.030	0.239	7.80	1.085
2.130	0.303	8.55	1.29
2.225	0.385	9.36	1.53
2.330	0.475	10.28	1.86
2.565	0.721	11.14	2.14
2.804	1.22	11.97	2.47
2.935	1.68	12.83	2.91
3.050	2.78	13.95	3.45
3.220	1.17	15.06	3.98
3.515	0.603	15.98	4.48
3.810	0.562	16.88	5.02
4.025	0.555	17.73	5.39
4.35	0.544	18.58	6.02
4.68	0.536	19.42	6.50
5.10	0.592		

Table 3.4.

Experimental Values of the Specific Heat of Sodium Chloroiridate.

C_p given in units of calories per mole per degree.

T^oK	C_p	T^oK	C_p
1.758	0.137	4.84	0.986
1.848	0.141	5.19	1.022
1.970	0.155	5.50	1.015
2.100	0.172	5.87	1.037
2.220	0.198	6.32	0.966
2.330	0.212	6.92	1.057
2.426	0.228	7.44	1.194
2.507	0.244	7.94	1.32
2.613	0.275	8.42	1.47
2.737	0.317	8.88	1.63
2.846	0.359	9.35	1.75
2.947	0.402	9.80	1.89
3.054	0.462	10.18	2.02
3.160	0.521	10.76	2.21
3.260	0.592	11.35	2.42
3.358	0.671	11.90	2.68
3.457	0.762	12.50	2.98
3.553	0.883	13.08	3.27
3.657	1.018	14.03	3.84
3.765	1.203	14.65	4.12
3.885	1.392	15.25	4.48
4.038	1.394	15.98	4.91
4.23	1.096	17.03	5.56
4.50	1.041	18.12	6.18

Table 5.1.

Copper-Zinc Alloy.

Composition by weight : 1.5% Zinc.

C_p given in units of joules per mole per degree, T in degrees Kelvin.

T	C_p	T	C_p
1.600	0.00149	2.665	0.00297
1.840	0.00173	2.773	0.00324
1.965	0.00190	2.902	0.00332
2.064	0.00205	3.065	0.00371
2.163	0.00220	3.246	0.00411
2.252	0.00227	3.405	0.00440
2.338	0.00242	3.542	0.00485
2.420	0.00257	3.702	0.00528
2.500	0.00271	3.842	0.00578
2.582	0.00286	3.977	0.00623

$\gamma = 0.783 \times 10^{-3}$ joules per mole per degree^2, $\theta = 345^\circ K$.

Copper-Zinc Alloy.

Composition by weight : 2.2% Zinc.

T	C_p	T	C_p
1.662	0.00161	2.576	0.00294
1.760	0.00176	2.716	0.00318
1.795	0.00182	2.853	0.00342
1.928	0.00197	3.064	0.00377
2.008	0.00209	3.288	0.00418
2.086	0.00220	3.474	0.00460
2.163	0.00231	3.650	0.00533
2.240	0.00241	3.840	0.00589
2.335	0.00255	4.029	0.00665
2.446	0.00274		

$\gamma = 0.846 \times 10^{-3}$ joules per mole per degree^2, $\theta = 351^\circ K$.

Table 5.2.

Copper-Zinc Alloy.

Composition by weight : 5.0% Zinc.

C_p given in units of joules per mole per degree, T in degrees Kelvin.

T	C_p	T	C_p
1.550	0.00141	2.523	0.00265
1.643	0.00150	2.688	0.00296
1.744	0.00159	2.872	0.00334
1.825	0.00171	3.057	0.00370
1.910	0.00184	3.230	0.00403
2.018	0.00198	3.443	0.00452
2.118	0.00211	3.730	0.00527
2.250	0.00230	3.978	0.00584
2.402	0.00255	4.255	0.00675

$\gamma = 0.800 \times 10^{-3}$ joules per mole per degree^2, $\theta = 356^{\circ}K$.

Copper-Zinc Alloy.

Composition by weight : 8.4% Zinc.

T	C_p	T	C_p
1.810	0.00176	2.758	0.00334
1.990	0.00204	2.899	0.00364
2.146	0.00221	3.040	0.00385
2.274	0.00246	3.205	0.00423
2.395	0.00263	3.405	0.00468
2.514	0.00285	3.660	0.00535
2.634	0.00307	3.940	0.00640

$\gamma = 0.815 \times 10^{-3}$ joules per mole per degree^2, $\theta = 339^{\circ}K$.

Table 5.3.

Copper-Zinc Alloy.

Composition by weight : 9.3% Zinc.

C_p given in units of joules per mole per degree, T in degrees Kelvin.

T	C_p	T	C_p
2.188	0.00231	3.375	0.00464
2.406	0.00267	3.532	0.00481
2.545	0.00289	3.680	0.00539
2.695	0.00310	3.825	0.00589
2.876	0.00347	3.968	0.00635
3.041	0.00382	4.100	0.00686
3.222	0.00422		

$\gamma = 0.799 \times 10^{-3}$ joules per mole per degree^2, $\theta = 339^\circ K$.

Copper-Zinc Alloy.

Composition by weight : 11.7% Zinc.

T	C_p	T	C_p
1.623	0.00141	2.502	0.00266
1.720	0.00156	2.722	0.00297
1.827	0.00167	2.972	0.00341
1.941	0.00179	3.229	0.00408
2.069	0.00194	3.488	0.00472
2.190	0.00217	3.731	0.00535
2.329	0.00227	4.020	0.00623

$\gamma = 0.735 \times 10^{-3}$ joules per mole per degree^2, $\theta = 339^\circ K$.

Table 5.4.

Copper-Zinc Alloy.

Composition by weight : 19.3% Zinc.

C_p given in units of joules per mole per degree, T in degrees Kelvin.

T	C_p	T	C_p
1.53	0.00131	2.81	0.00333
1.71	0.00156	3.00	0.00375
1.89	0.00178	3.21	0.00404
2.06	0.00202	3.41	0.00466
2.23	0.00231	3.61	0.00545
2.41	0.00261	3.84	0.00611
2.60	0.00293	4.05	0.00648

$\gamma = 0.750 \times 10^{-3}$ joules per mole per degree^2, $\theta = 329^{\circ}K$.

Copper-Zinc Alloy.

Composition by weight : 25.0% Zinc.

T	C_p	T	C_p
1.57	0.00151	2.85	0.00353
1.79	0.00181	2.95	0.00373
1.95	0.00200	3.06	0.00403
2.09	0.00218	3.20	0.00431
2.21	0.00235	3.37	0.00479
2.28	0.00249	3.54	0.00525
2.40	0.00264	3.68	0.00569
2.51	0.00283	3.85	0.00624
2.63	0.00309	4.02	0.00697
2.74	0.00333		

$\gamma = 0.802 \times 10^{-3}$ joules per mole per degree^2, $\theta = 328^{\circ}K$.

Table 5.5.

Copper-Zinc Alloy.

Composition by weight : 31.0% Zinc.

C_p given in units of joules per mole per degree, T in degrees Kelvin.

T	C_p	T	C_p
1.810	0.00174	2.880	0.00376
1.950	0.00197	3.033	0.00412
2.078	0.00214	3.179	0.00447
2.203	0.00234	3.312	0.00485
2.324	0.00258	3.450	0.00531
2.443	0.00281	3.595	0.00564
2.582	0.00308	3.731	0.00610
2.732	0.00337	3.860	0.00681

$\gamma = 0.752 \times 10^{-3}$ joules per mole per degree^2, $\theta = 310^{\circ}K$.

Copper-Zinc Alloy.

Composition by weight : 31.5% Zinc.

T	C_p	T	C_p
1.570	0.00151	2.636	0.00328
1.685	0.00160	2.890	0.00377
1.740	0.00175	3.126	0.00425
1.860	0.00188	3.377	0.00510
1.986	0.00205	3.515	0.00523
2.120	0.00230	3.653	0.00577
2.265	0.00251	3.930	0.00690
2.430	0.00288		

$\gamma = 0.812 \times 10^{-3}$ joules per mole per degree^2, $\theta = 321^{\circ}K$.

Table 5.6.

Copper-Zinc Alloy.

Composition by weight : 33.1% Zinc.

C_p given in units of joules per mole per degree, T in degrees Kelvin.

T	C_p	T	C_p
1.811	0.00185	3.030	0.00418
1.990	0.00205	3.271	0.00479
2.156	0.00234	3.494	0.00539
2.341	0.00268	3.717	0.00610
2.535	0.00311	3.936	0.00698
2.777	0.00358		

$\gamma = 0.810 \times 10^{-3}$ joules per mole per degree^2, $\theta = 317^{\circ}K$.

Copper-Zinc Alloy.

Composition by weight : 48.3% Zinc.

T	C_p	T	C_p
1.517	0.00138	2.615	0.00372
1.664	0.00164	2.811	0.00427
1.808	0.00189	3.013	0.00482
1.952	0.00212	3.235	0.00560
2.098	0.00237	3.453	0.00656
2.248	0.00316	3.857	0.00878

$\gamma = 0.690 \times 10^{-3}$ joules per mole per degree^2, $\theta = 266^{\circ}K$.

Table 5.7.

Copper-Zinc Alloy.

Composition by weight : 49.0% Zinc.

C_p given in units of joules per mole per degree, T in degrees Kelvin.

T	C_p	T	C_p
1.535	0.00156	2.690	0.00376
1.745	0.00181	2.875	0.00434
1.890	0.00199	3.150	0.00514
2.030	0.00222	3.405	0.00610
2.155	0.00251	3.615	0.00706
2.270	0.00273	3.835	0.00832
2.380	0.00301	4.030	0.00945
2.530	0.00338		

$\gamma = 0.722 \times 10^{-3}$ joules per mole per degree^2, $\theta = 272^{\circ}K$.

Copper-Zinc Alloy.

Composition by weight : 60.1% Zinc.

T	C_p	T	C_p
1.560	0.00100	2.925	0.00249
1.754	0.00124	3.080	0.00269
1.933	0.00137	3.222	0.00296
2.096	0.00147	3.364	0.00321
2.252	0.00166	3.505	0.00349
2.427	0.00180	3.644	0.00376
2.607	0.00204	3.776	0.00399
2.770	0.00228	3.902	0.00440

$\gamma = 0.555 \times 10^{-3}$ joules per mole per degree^2, $\theta = 379^{\circ}K$.

Table 5.8.

Copper-Zinc Alloy.

Composition by weight : 62.6% Zinc.

C_p given in units of joules per mole per degree, T in degrees Kelvin.

T	C_p	T	C_p
1.725	0.00091	2.687	0.00175
1.830	0.00097	2.800	0.00193
2.010	0.00109	3.020	0.00216
2.043	0.00114	3.140	0.00234
2.172	0.00121	3.235	0.00247
2.195	0.00127	3.465	0.00278
2.350	0.00149	3.690	0.00322
2.507	0.00157	3.912	0.00387

$\gamma = 0.409 \times 10^{-3}$ joules per mole per degree^2, $\theta = 382^{\circ}K$.

Copper-Zinc Alloy.

Composition by weight : 65.2% Zinc.

T	C_p	T	C_p
1.26	0.00056	2.80	0.00164
1.58	0.00074	3.08	0.00195
1.84	0.00089	3.36	0.00222
2.06	0.00101	3.64	0.00255
2.30	0.00123	3.87	0.00297
2.56	0.00143	4.10	0.00328

$\gamma = 0.405 \times 10^{-3}$ joules per mole per degree^2, $\theta = 437^{\circ}K$.

Table 7.1.

Pure Copper - 1st Batch.

C_p given in units of joules per mole per degree, T in degrees Kelvin.

1st Experiment.

T	C_p	T	C_p
1.853	0.001590	2.948	0.003326
1.939	0.001716	3.062	0.003512
2.026	0.001819	3.171	0.003764
2.114	0.001934	3.281	0.004016
2.214	0.002068	3.392	0.004251
2.338	0.002256	3.500	0.004516
2.464	0.002458	3.610	0.004804
2.588	0.002656	3.721	0.005138
2.710	0.002881	3.829	0.005416
2.830	0.003114	3.938	0.005730

$\gamma = 0.6983 \times 10^{-3}$ joules per mole per degree^2, $\theta = 341.6^{\circ}K$.

2nd Experiment.

T	C_p	T	C_p
1.750	0.001468	2.974	0.003379
1.858	0.001591	3.082	0.003575
1.995	0.001778	3.192	0.003800
2.142	0.001980	3.302	0.004070
2.273	0.002180	3.412	0.004314
2.396	0.002349	3.523	0.004614
2.514	0.002551	3.643	0.004893
2.633	0.002758	3.758	0.005190
2.749	0.002950	3.868	0.005554
2.862	0.003165	3.983	0.005894

$\gamma = 0.6978 \times 10^{-3}$ joules per mole per degree^2, $\theta = 341.0^{\circ}K$.

Combined Result.

$\gamma = (0.698 \pm 0.002) \times 10^{-3}$ joules per mole per degree^2.

$\theta = (341.3 \pm 1.1)^{\circ}K$.

Table 7.2.

Pure Copper - 2nd Batch.

C_p given in units of joules per mole per degree, T in degrees Kelvin.

T	C_p	T	C_p
1.730	0.001450	2.783	0.003008
1.820	0.001550	2.920	0.003252
1.908	0.001672	3.072	0.003567
2.000	0.001785	3.233	0.003915
2.104	0.001923	3.392	0.004268
2.223	0.002091	3.540	0.004636
2.360	0.002294	3.687	0.005025
2.505	0.002532	3.825	0.005383
2.648	0.002783	3.953	0.005757

$\gamma = 0.699 \times 10^{-3}$ joules per mole per degree^2.

$\theta = 341.7^{\circ}K.$

Table 7.3.

Copper-Zinc Alloy.

Composition by weight : Nominal 0.1% Zinc, Actual 0.10 ± 0.03% Zinc

C_p given in units of joules per mole per degree, T in degrees Kelvin.

1st Experiment.

T	C_p	T	C_p
1.741	0.001496	2.960	0.003344
1.847	0.001628	3.072	0.003564
1.948	0.001749	3.190	0.003835
2.050	0.001880	3.310	0.004109
2.156	0.002014	3.427	0.004399
2.267	0.002153	3.543	0.004673
2.381	0.002334	3.653	0.004909
2.497	0.002516	3.760	0.005195
2.613	0.002725	3.863	0.005505
2.728	0.002937	3.961	0.005798
2.845	0.003146		

$\gamma = 0.7148 \times 10^{-3}$ joules per mole per degree^2, $\theta = 344.2^{\circ}K$.

2nd Experiment.

T	C_p	T	C_p
1.743	0.001514	2.963	0.003394
1.852	0.001626	3.073	0.003573
1.955	0.001748	3.190	0.003857
2.057	0.001879	3.308	0.004059
2.167	0.002020	3.425	0.004377
2.276	0.002168	3.542	0.004685
2.392	0.002343	3.655	0.004880
2.502	0.002516	3.761	0.005226
2.614	0.002718	3.863	0.005536
2.731	0.002947	3.958	0.005789
2.849	0.003148		

$\gamma = 0.7126 \times 10^{-3}$ joules per mole per degree^2, $\theta = 343.8^{\circ}K$.

Combined Result.

$\gamma = (0.714 \pm 0.002) \times 10^{-3}$ joules per mole per degree^2.

$\theta = 344.0 \pm 1.4^{\circ}K$.

Table 7.4.

Copper-Zinc Alloy.

Composition by weight : Nominal 1/2% zinc, Actual 0.45 ± 0.03%.

1st Experiment.

C_p given in units of joules per mole per degree, T. in degrees Kelvin.

T	C_p	T	C_p
1.760	0.001525	2.922	0.003302
1.855	0.001651	3.044	0.003557
1.950	0.001759	3.160	0.003797
2.037	0.001876	3.280	0.004046
2.132	0.002016	3.400	0.004314
2.230	0.002141	3.638	0.004906
2.438	0.002473	3.758	0.005225
2.553	0.002653	3.880	0.005557
2.796	0.003088	4.000	0.005950

$\gamma = 0.7277 \times 10^{-3}$ joules per mole per degree^2, $\theta = 345.3^\circ K$.

2nd Experiment.

T	C_p	T	C_p
1.697	0.001472	2.746	0.003000
1.792	0.001573	2.885	0.003222
1.890	0.001696	3.015	0.003508
1.981	0.001800	3.149	0.003771
2.071	0.001916	3.287	0.004070
2.165	0.002039	3.420	0.004396
2.264	0.002187	3.550	0.004692
2.371	0.002342	3.682	0.004989
2.490	0.002547	3.801	0.005329
2.615	0.002769	3.920	0.005695

$\gamma = 0.7284 \times 10^{-3}$ joules per mole per degree^2, $\theta = 345.6^\circ K$.

Combined Result.

$\gamma = (0.728 \pm 0.001) \times 10^{-3}$ joules per mole per degree^2.

$\theta = (345.5 \pm 1.1)^\circ K$.

Table 7.5.

Copper-Zinc Alloy.

Composition by weight : Nominal 1% zinc, Actual 1.03 ± 0.03%.

1st Experiment.

C_p given in units of joules per mole per degree, T in degrees Kelvin.

T	C_p	T	C_p
1.755	0.001536	2.954	0.003387
1.878	0.001687	3.068	0.003604
2.012	0.001854	3.185	0.003857
2.148	0.002028	3.307	0.004119
2.272	0.002217	3.422	0.004411
2.380	0.002404	3.544	0.004684
2.502	0.002602	3.665	0.005008
2.618	0.002802	3.782	0.005347
2.723	0.002998	3.893	0.005669
2.838	0.003184	4.010	0.006012

$\gamma = 0.7343 \times 10^{-3}$ joules per mole per degree^2, $\theta = 344.9^\circ K$.

2nd Experiment.

T	C_p	T	C_p
1.763	0.001543	2.948	0.003387
1.864	0.001675	3.068	0.003597
1.972	0.001798	3.190	0.003846
2.100	0.001956	3.312	0.004118
2.222	0.002139	3.430	0.004435
2.336	0.002342	3.552	0.004715
2.448	0.002526	3.674	0.005041
2.568	0.002723	3.790	0.005387
2.694	0.002949	3.905	0.005703
2.823	0.003164	4.015	0.005982

$\gamma = 0.7357 \times 10^{-3}$ joules per mole per degree^2, $\theta = 345.3^\circ K$.

Combined Result.

$\gamma = (0.735 \pm 0.002) \times 10^{-3}$ joules per mole per degree^2.

$\theta = (345.0 \pm 1.6)^\circ K$.

Table 7.6.

Copper-Zinc Alloy.

Composition by weight : Nominal 2% Zinc, Actual 1.30 ± 0.03% Zinc.

1st Experiment.

C_p given in units of joules per mole per degree, T in degrees Kelvin.

T	C_p	T	C_p
1.833	0.001649	3.125	0.003724
1.968	0.001838	3.241	0.003984
2.112	0.002006	3.357	0.004228
2.264	0.002233	3.470	0.004511
2.403	0.002419	3.592	0.004836
2.534	0.002629	3.708	0.005188
2.658	0.002856	3.814	0.005470
2.892	0.003269	3.928	0.005800
3.008	0.003513	4.046	0.006187

$\gamma = 0.7357 \times 10^{-3}$ joules per mole per degree^2, $\theta = 344.2^\circ K$.

2nd Experiment.

T	C_p	T	C_p
1.843	0.001667	2.914	0.003302
1.950	0.001785	3.048	0.003576
2.049	0.001906	3.183	0.003860
2.159	0.002060	3.324	0.004176
2.270	0.002217	3.468	0.004536
2.380	0.002396	3.609	0.004876
2.495	0.002576	3.746	0.005225
2.628	0.002791	3.880	0.005623
2.773	0.003030	4.007	0.005993

$\gamma = 0.7357 \times 10^{-3}$ joules per mole per degree^2, $\theta = 345.3^\circ K$.

Combined Result.

$\gamma = (0.735 \pm 0.002) \times 10^{-3}$ joules per mole per degree^2.

$\theta = (344.5 \pm 1.4)^\circ K$.

Table 7.7.

Copper-Zinc Alloy.

Composition by weight : Nominal 4% zinc, Actual 4.13 ± 0.03%.

1st Experiment.

C_p given in units of joules per mole per degree, T in degrees Kelvin.

T	C_p	T	C_p
1.722	0.001513	2.930	0.003378
1.823	0.001625	3.053	0.003632
1.937	0.001743	3.172	0.003869
2.047	0.001903	3.288	0.004111
2.148	0.002038	3.398	0.004361
2.250	0.002190	3.507	0.004659
2.352	0.002366	3.618	0.004919
2.455	0.002536	3.727	0.005215
2.568	0.002706	3.833	0.005555
2.682	0.002899	3.943	0.005863
2.804	0.003140		

$\gamma = 0.7309 \times 10^{-3}$ joules per mole per degree^2, $\theta = 342.2^{\circ}K$.

2nd Experiment.

Specimen homogenised by hot working and annealing. Composition by weight now : 3.84 ± 0.03% zinc.

T	C_p	T	C_p
1.813	0.001606	2.996	0.003492
1.922	0.001746	3.115	0.003711
2.023	0.001863	3.233	0.003958
2.130	0.002025	3.348	0.004240
2.237	0.002161	3.462	0.004531
2.340	0.002340	3.575	0.004768
2.444	0.002492	3.690	0.005086
2.556	0.002672	3.800	0.005409
2.660	0.002866	3.917	0.005757
2.766	0.003068	4.040	0.006146
2.879	0.003276		

$\gamma = 0.7318 \times 10^{-3}$ joules per mole per degree^2, $\theta = 343.7^{\circ}K$.

Combined Result.

$\gamma = (0.732 \pm 0.002) \times 10^{-3}$ joules per mole per degree^2.

$\theta = (343.0 \pm 1.2)^{\circ}K$.

Table 7.8.

Copper-Zinc Alloy.

Composition by weight : Nominal 5% Zinc, Actual 4.70 ± 0.03%.

1st Experiment.

C_p given in units of joules per mole per degree, T in degrees Kelvin.

T	C_p	T	C_p
1.750	0.001556	2.826	0.003162
1.866	0.001686	2.954	0.003414
1.977	0.001826	3.088	0.003662
2.083	0.001957	3.224	0.003962
2.186	0.002105	3.357	0.004264
2.282	0.002247	3.480	0.004549
2.387	0.002420	3.602	0.004891
2.488	0.002604	3.722	0.005230
2.593	0.002769	3.818	0.005526
2.703	0.002954	3.948	0.005869
		4.057	0.006231

$\gamma = 0.7364 \times 10^{-3}$ joules per mole per degree^2, $\theta = 343.2$.

2nd Experiment.

T	C_p	T	C_p
1.750	0.001548	2.933	0.003371
1.872	0.001688	3.050	0.003584
1.995	0.001840	3.165	0.003804
2.118	0.002008	3.280	0.004079
2.233	0.002174	3.390	0.004368
2.352	0.002334	3.505	0.004617
2.465	0.002535	3.622	0.004934
2.578	0.002717	3.738	0.005253
2.682	0.002923	3.852	0.005572
2.812	0.003154	3.972	0.005950
		4.086	0.006338

$\gamma = 0.7317 \times 10^{-3}$ joules per mole per degree^2, $\theta = 342.6^\circ K$.

Combined Result.

$\gamma = (0.734 \pm 0.002) \times 10^{-3}$ joules per mole per degree^2.

$\theta = (343.0 \pm 1.2)^\circ K$.